2006-12

Experimental investigation and numerical prediction of the performance of a cross-flow fan

Yu, Huai-Te.

Monterey California. Naval Postgraduate School

http://hdl.handle.net/10945/2408

NAVAL POSTGRADUATE SCHOOL

MONTEREY, CALIFORNIA

THESIS

EXPERIMENTAL INVESTIGATION AND NUMERICAL PREDICTION OF THE PERFORMANCE OF A CROSS-FLOW FAN

by

Huai-Te Yu

December 2006

Thesis Advisor:	Garth V. Hobson
Second Reader:	Raymond P. Shreeve

Approved for public release; distribution is unlimited

THIS PAGE INTENTIONALLY LEFT BLANK

REPORT DOCUMENTATION PAGE			*Form Approved OMB No. 0704-0188*
Public reporting burden for this collection of information is estimated to average 1 hour per response, including the time for reviewing instruction, searching existing data sources, gathering and maintaining the data needed, and completing and reviewing the collection of information. Send comments regarding this burden estimate or any other aspect of this collection of information, including suggestions for reducing this burden, to Washington headquarters Services, Directorate for Information Operations and Reports, 1215 Jefferson Davis Highway, Suite 1204, Arlington, VA 22202-4302, and to the Office of Management and Budget, Paperwork Reduction Project (0704-0188) Washington DC 20503.			
1. AGENCY USE ONLY *(Leave blank)*	**2. REPORT DATE** December 2006	**3. REPORT TYPE AND DATES COVERED** Master's Thesis	
4. TITLE AND SUBTITLE Experimetal Investigation and Numerical Predication of a Cross-Flow Fan			**5. FUNDING NUMBERS**
6. AUTHOR(S) Yu, Huai-Te			
7. PERFORMING ORGANIZATION NAME(S) AND ADDRESS(ES) Naval Postgraduate School Monterey, CA 93943-5000			**8. PERFORMING ORGANIZATION REPORT NUMBER**
9. SPONSORING /MONITORING AGENCY NAME(S) AND ADDRESS(ES) N/A			**10. SPONSORING/MONITORING AGENCY REPORT NUMBER**
11. SUPPLEMENTARY NOTES The views expressed in this thesis are those of the author and do not reflect the official policy or position of the Department of Defense or the U.S. Government.			
12a. DISTRIBUTION / AVAILABILITY STATEMENT Approved for public release; distribution is unlimited			**12b. DISTRIBUTION CODE**

13. ABSTRACT

The concept of a fan-wing aircraft configuration for the purpose of vertical takeoff and landing has drawn much attention. Recently, more investigations revealed that a cross-flow fan (CFF) was capable of providing the propulsion. Several characteristics of the off-design performance of a CFF were experimentally measured, but insufficient numerical predictions were obtained.

In the present study, the commercial CFD software ANSYS CFX was employed to calculate the unsteady flow through a CFF with a sliding mesh incorporated. The results of the CFD showed the necessity to re-investigate the cross-flow fan with 12-inch diameter, 1.5-inch span and 30 blades, and additional measurement locations were implemented to carry out a more accurate experiment. A new digital sensor array was used to record the pressures within the experiment, which contributed to the high fidelity of the present data. Successful comparisons were made between the predicted and measured performance at various rotational speeds from an open throttle position to a setting at stall. Visualization of the computed flow field showed where stall occurred, both within the rotor and in the exhaust duct.

14. SUBJECT TERMS Cross-Flow Fan, Computational Fluid Dynamics (CFD), vertical and short takeoff and landing (V/STOL)			**15. NUMBER OF PAGES** 131
			16. PRICE CODE
17. SECURITY CLASSIFICATION OF REPORT Unclassified	**18. SECURITY CLASSIFICATION OF THIS PAGE** Unclassified	**19. SECURITY CLASSIFICATION OF ABSTRACT** Unclassified	**20. LIMITATION OF ABSTRACT** UL

NSN 7540-01-280-5500

Standard Form 298 (Rev. 2-89)
Prescribed by ANSI Std. 239-18

THIS PAGE INTENTIONALLY LEFT BLANK

Approved for public release; distribution is unlimited

EXPERIMENTAL INVESTIGATION AND NUMERICAL PREDICTION OF THE PERFORMANCE OF A CROSS-FLOW FAN

Huai-Te Yu
Captain, Taiwan Army
B.S., Chung Cheng Institute of Technology, 2000

Submitted in partial fulfillment of the
requirements for the degree of

MASTER OF SCIENCE IN MECHANICAL ENGINEERING

from the

NAVAL POSTGRADUATE SCHOOL
December 2006

Author: Huai-Te Yu

Approved by: Garth V. Hobson
Thesis Advisor

Raymond P. Shreeve
Second Reader

Anthony J Healey
Chairman, Department of Mechanical and Astronautical Engineering

THIS PAGE INTENTIONALLY LEFT BLANK

ABSTRACT

The concept of a fan-wing aircraft configuration for the purpose of vertical takeoff and landing has drawn much attention. Recently, more investigations revealed that a cross-flow fan (CFF) was capable of providing the propulsion. Several characteristics of the off-design performance of a CFF were experimentally measured, but insufficient numerical predictions were obtained.

In the present study, the commercial CFD software ANSYS CFX was employed to calculate the unsteady flow through a CFF with a sliding mesh incorporated. The results of the CFD showed the necessity to re-investigate the cross-flow fan with 12-inch diameter, 1.5-inch span and 30 blades, and additional measurement locations were implemented to carry out a more accurate experiment. A new digital sensor array was used to record the pressures within the experiment, which contributed to the high fidelity of the present data. Successful comparisons were made between the predicted and measured performance at various rotational speeds from an open throttle position to a setting at stall. Visualization of the computed flow field showed where stall occurred, both within the rotor and in the exhaust duct.

THIS PAGE INTENTIONALLY LEFT BLANK

TABLE OF CONTENTS

THIS PAGE INTENTIONALLY LEFT BLANK

LIST OF FIGURES

LIST OF TABLES

THIS PAGE INTENTIONALLY LEFT BLANK

ACKNOWLEDGMENTS

I would like to express my appreciation to the following people whose valuable contribution to the completion of this thesis.

Professor Garth Hobson, for sparking my interest in the cross-flow fan concept, and without his patience and instruction, I would not have come this far.

Professor Max Platzer, for his enthusiasm and guidance into this topic. Without his hypercritical examination into the model, my simulation could not be run so smoothly

Professor Ray Shreeve, for his instruction in a course of compressible flow. He not only is an excellent instructor, but showed the utmost solicitude to me.

Dr. Anthony Gannon, for his assistance in programming the data acquisition system. With his understanding and explanation, the program was created in just few days.

Rick Still and John Gibson, for always making the test rig run properly. Their reliability made the experiment a success.

Finally, I would like to thank my wife, Jui-Feng Tsou, for her consideration. With her full support, I can concentrate on this study with no second thought. Meanwhile, we are glad to have my first son, Jason Yu.

THIS PAGE INTENTIONALLY LEFT BLANK

I. INTRODUCTION

Vertical and short takeoff and landing (V/STOL) vehicles have been studied for many years. Requirements for larger thrust and higher fuel efficiency were encountered. In order to meet those requirements, a device, the Cross-Flow Fan (CFF), was first introduced in 1975 by the Vought Systems Division (VSD) [Ref. 1] of LTV Aerospace Corporation. Several tests were performed on various fan and housing configurations. Also, the location of shocks and vortices within the device were investigated. The capabilities of this device to be used as a propulsion system were recommended. However, more experiments needed to be carried out to provide more understanding of the off-design performance of the cross-flow fan.

Based on the experimental data by VSD, Dean H. Gossett [Ref. 2] designed a light-weight VTOL aircraft to be used for transportation between cities. Fan number 6 with an exit duct height of 4.6-inch was selected due to its higher thrust production. Theoretically, his concept of a wing-and-canard type air vehicle sparked the possibilities of utilizing a cross-flow fan as the sole propulsive device for the aircraft.

The performance of a cross-flow fan was tested in the Turbopropulsion Laboratory of the Naval Postgraduate School by M. Scot Seaton [Ref. 3]; and a numerical model, using FLO++, was also initiated to predict the performance for further design purposes. Moreover the concept of the Fan-Wing aircraft was not only proposed but also treated numerically in a conceptual wing configuration. This work was continued by Wee Teck Cheng [Ref. 4] who measured the off-design performance of the 12-inch CFF up to 6000RPM. He also predicted the design performance of the CFF at 3000RPM using FLO++, however, his off-design prediction did not follow the experimental trends.

Using the experimental results from [Ref. 4] , a cross-flow fan embedded into an airfoil was proposed and designed by Joseph D. Kummer [Ref. 5]; an incredible enhancement of airfoil lift coefficient under specific conditions was predicted by employing the software package, FLUENT. Practically, it would be a problem to couple this device into an aircraft. It was revealed that the utilization of a cross-flow fan to achieve high lift propulsion should be given more attention.

Since the concept of a Fan-Wing aircraft with a cross-flow fan was regarded as a possible application, a smaller sized cross-flow fan was needed and its performance needed to be investigated. More recently, a 6-inch CFF was tested both with a 1-1/2-inch span and a 6-inch span rotor at low to moderate speeds [Ref. 6]. Since the simulation by FLO++ only provided results for incompressible flow, the software package, ANSYS CFX, was used in the present study. The code could more accurately model compressible flow and could also model rotating machinery. Discrepancies found in the measurement of mass flow rate in the previous data, necessitated repeating the test of the 12-inch rotor with a new pressure measuring digital sensor array. The off-design performance prediction using CFX-5 more closely followed the experimental results obtained in the present study.

II. EXPERIMENTAL SETUP

A. DESCRIPTION OF THE EXPERIMENTAL APPARATUS

1. Test Rig

The fan was tested in the Turbine Test Rig (TTR) at the Turboproplusion Laboratory of the Naval Postgraduate School. The TTR was powered by compressed air from an Allis-Chalmers compressor, which was driven by a 1,250 horsepower motor. The compressor could produce 10,000 cubic feet per minute of air at a maximum pressure of 30 psig. A schematic of TTR is shown in Figure 1.

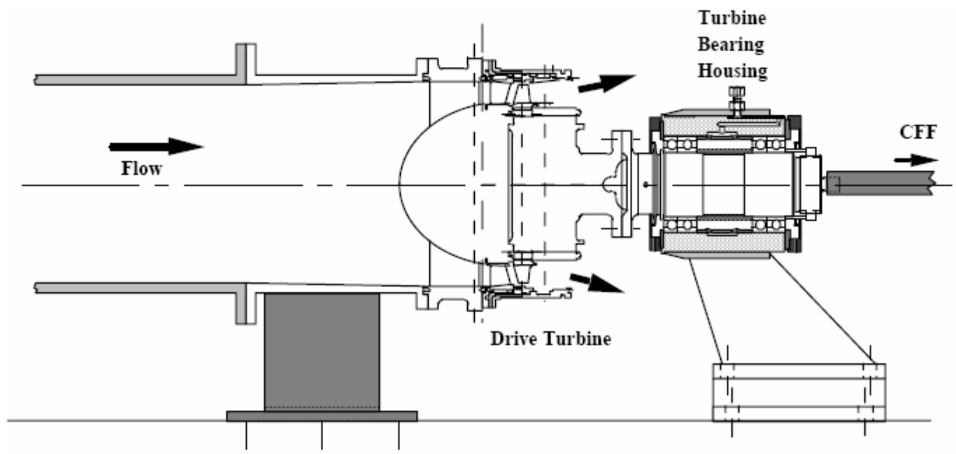

Figure 1. Schematic of the Turbine Test Rig (from Ref 5)

2. Cross-Flow Fan Test Assembly (CFFTA)

The Cross-Flow Fan Test Assembly (CFFTA) design was derived from the VSD Multi-Bypass Ratio System test assembly #6 [Ref. 1]. A schematic of it is shown in Figure 2. The configuration of the CFFTA was composed of a fan rotor (with 30 blades, 12-inch diameter and 1.5 inch span), two cavity components, an exhaust duct wall, a drive shaft, and bearing housing.

For the initial tests, unlike [Ref. 3] and [Ref. 4], an inlet bell-mouth was used to measure the mass flow rate, which was denoted Test Plan I. For the second test, an extended exhaust duct and butterfly throttle valve, were added in order to measure the performance at various mass-flow rates. This was denoted as Test Plan II.

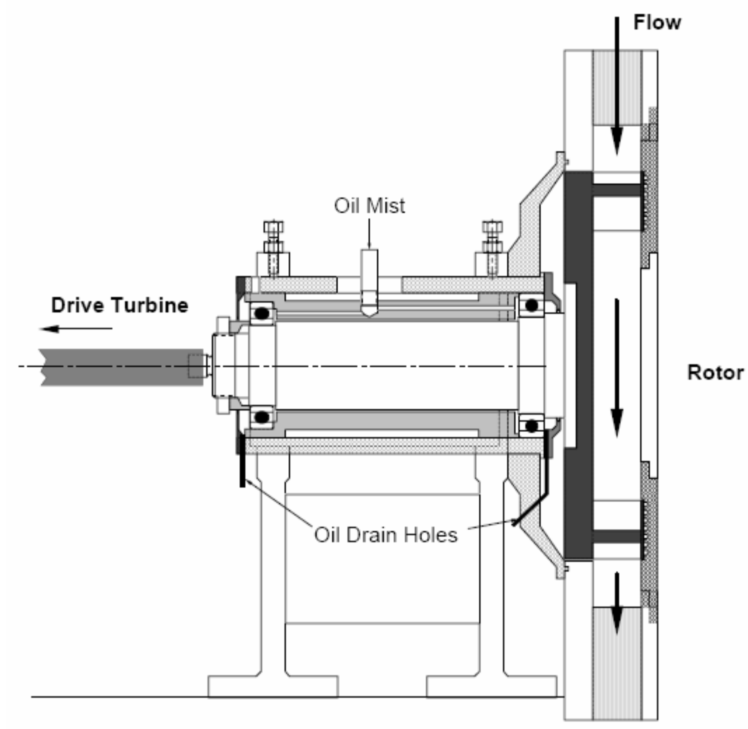

(a) Schematic


(b) Fan Rotor

(c) Partially Assembled

Figure 2. Cross-Flow Test Assembly (CFFTA, from Ref. 5)

3. Control Station

The CFFTA was controlled by adjusting a bypass dump valve, and an inlet valve to the TTR. Atmospheric pressure, rotational speed of the fan, bearing temperatures and vibrations were monitored, and were recorded in a logbook during the test, once a desired rotational speed and throttle setting was stably achieved

4. Data Acquisition and Instrumentation

Instruments employed to measure the flow properties were United Sensor Devices model USD-C-161 3 mm (1/8-inch) combination thermocouple/pressure probes, and static pressure taps. The locations of the probes, which are shown in the schematic in Figure 3, were slightly different from [Ref 3] and [Ref 4]. Two more probes were added in the exhaust duct, and one was placed in the inlet section at the 12 o'clock position. The type of measurement and labels of probes are listed in Table 1 and Table 2.

It was concluded that the variation of total pressure of the three inlet combination probes was not significant; therefore, they were averaged by introducing "tees" to combine them before being connected to the pressure transducer array. In the same manner, this averaging technique was applied to the three static pressure tapes at the throat of the bell-mouth and to the two exhaust duct static pressure taps.

Once the data were acquired, the pressures were converted from analog signals through the digital sensor array (DSA) into digital signals which were acquired by the computer via an internet cable. Temperatures were recorded by a Hewlett- Packard HP E1326B Multimeter Adapter, which was connected to computer via the VXI mainframe.

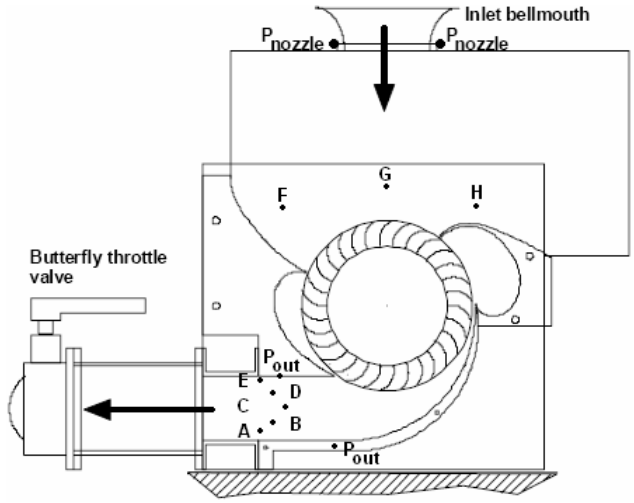

Figure 3. Combination probes and pressure tap layout

Multiplexer Channel	Probe	Nomenclature
4	A	$T_{t,out,A}$
13	B	$T_{t,out,B}$
14	C	$T_{t,out,C}$
15	D	$T_{t,out,D}$
5	E	$T_{t,out,E}$
6	F	$T_{t,in,F}$
8	G	$T_{t,in,G}$
9	H	$T_{t,in,H}$
10		$T_{t,in,TTR}$
11		$T_{t,out,TTR}$
12		$T_{t,in,orifice}$

Table 1. Thermocouple scanning multiplexer channel assignments

Port #	Probe	Nomenclature	Type
4	A	$P_{t,out,A}$	Total Pressure
5	B	$P_{t,out,B}$	Total Pressure
6	C	$P_{t,out,C}$	Total Pressure
7	D	$P_{t,out,D}$	Total Pressure
8	E	$P_{t,out,E}$	Total Pressure
3	F G H	$\overline{P}_{t,in}$	Total Pressure
2		P_{nozzle}	Static Pressure
1		$\overline{P}_{out}$ (for Test Plan II only)	Static Pressure

Table 2. Scanivalve port assignments

B. DATA ACQUISITION AND REDUCTION

The software Agilent VEE, which is a window-based data acquisition program, was used to develop a new graphical use interface (GUI), called CFF_DAQ, to acquire all temperatures, pressures and the rotational speed of the CFF. This is shown in Figure 4. All data were written to a text file, which EXCEL could read, and then data reduction procedures were performed to calculate parameters of interest. The program structure of CFF_DAQ is given in APPENDIX A.

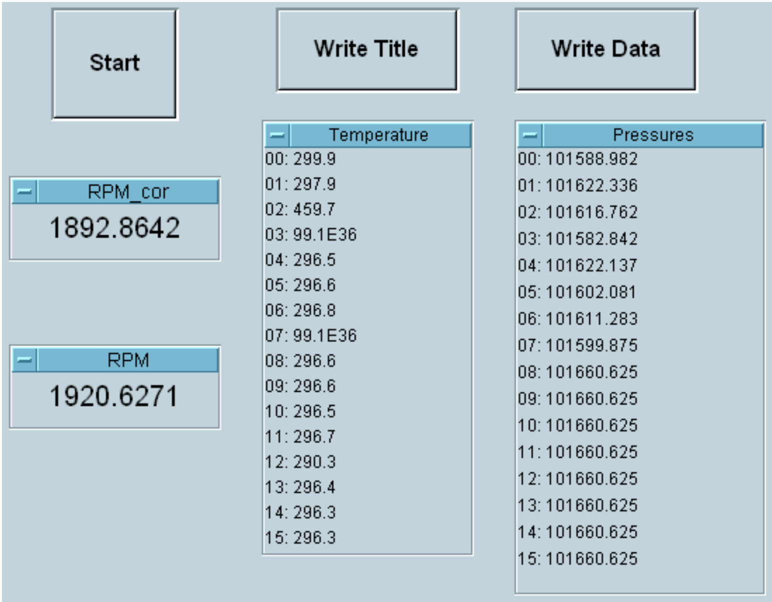

Figure 4. CFF_DAQ graphical user interface

During the post processing, several properties had to be related since mass-flow rate, total pressure ratio, total temperature ratio, efficiency, thrust, and power had to be calculated. Data reduction included referring to standard day conditions ($T_{t,std} = 288.15K$ and $P_{t,std} = 101{,}325Pa$).

The mass flow rate was obtained from the bell-mouth measurements, and the basic equations used for the calculation are presented below. For a detailed derivation, please refer to APPENDIX B.

$$\dot{m}_{in} = \frac{P_1}{RT_1} AV_{in} \quad (1)$$

$$T_1 = T_{t1} - \frac{(\gamma - 1)}{2\gamma R} V_{in}^{\ 2} \quad (2)$$

$$V_{in} = \sqrt{\frac{2RT_{t1}}{\frac{1}{\gamma} + \left(\frac{\gamma - 1}{2}\right)\left(\frac{P_{t1}}{P_1}\right)}\left(\frac{P_{t1}}{P_1} - 1\right)} \quad (3)$$

where $P_1 = P_{nozzle}$; A is the cross-area of the bell-mouth; $P_{t1} = P_{atm}$, which was read from the control station; $T_{t1} = T_{t,in}$, which was an average of $T_{t,in,F}$, $T_{t,in,G}$ and $T_{t,in,H}$. (See Figure 3)

Since there were five probes placed in the outlet section, as shown in Figure 5, five zones (from A to E) were utilized to calculate mass-averaged outlet properties of total pressure and temperature. The expressions of compressible flow were introduced from [Ref. 7] and used to evaluate the mass flow rate within each zone;

$$\dot{m}_i = X_i \left(1 - X_i^{\ 2}\right)^{\frac{1}{\gamma - 1}} \frac{P_{t,i}}{RT_{t,i}} \sqrt{2c_p T_{t,i}} A_i \quad (4)$$

where X was defined as a fraction equal to the velocity referred to the stagnation velocity. This was calculated from the following relationship between local static and stagnation pressures;

$$X_i = \sqrt{1 - \left(\frac{P}{P_{t,i}}\right)^{\frac{\gamma-1}{\gamma}}} \quad (5)$$

where

$$P = P_{atm} \text{ (for Test Plan I)}, \; P = \overline{P}_{t,out} \text{ (for Test Plan II)},$$

and i indicates each zone. $R = 287 m^2/s^2 \cdot K$; $c_p = 1004.4 J/kg \cdot K$; $\gamma = 1.402$; $P_{t,i}$ and $T_{t,i}$ were measured from the five combination probes; A_i was the area of each zone and the values provided in Table 3 were measured according to the actual locations of the probes.

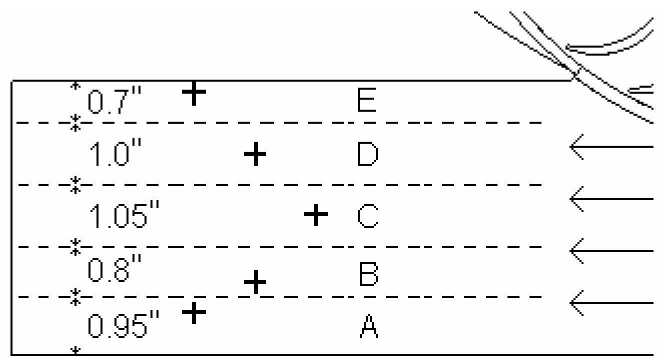

Figure 5. Schematic of the position of the combination probes in the exhaust duct

Zone	Area [m^2]
A	0.000919353
B	0.000774192
C	0.001016127
D	0.00096774
E	0.000677418

Table 3. Area values of each zone

Thus, the mass averaged total pressure and temperature in the exhaust duct were obtained from;

$$\overline{P}_{t,out} = \frac{\dot{m}_A P_{t,out,A} + \dot{m}_B P_{t,out,B} + \dot{m}_C P_{t,out,C} + \dot{m}_D P_{t,out,D} + \dot{m}_E P_{t,out,E}}{\sum_{i=A}^{E} \dot{m}_i} \quad (6)$$

$$\overline{T}_{t,out} = \frac{\dot{m}_A T_{t,out,A} + \dot{m}_B T_{t,out,B} + \dot{m}_C T_{t,out,C} + \dot{m}_D T_{t,out,D} + \dot{m}_E T_{t,out,E}}{\sum_{i=A}^{E} \dot{m}_i} \quad (7)$$

The total pressure ratio (π), total temperature ratio (τ) and efficiency (η) were then found by;

$$\pi = \frac{\overline{P}_{t,out}}{\overline{P}_{t,in}} \quad (8)$$

$$\tau = \frac{\overline{T}_{t,out}}{\overline{T}_{t,in}} \quad (9)$$

$$\eta = \frac{\pi^{\frac{\gamma-1}{\gamma}} - 1}{\tau - 1} \quad (10)$$

Next, the thrust force was obtained from;

$$F_{thrust} = \dot{m}_{in}\left(u_{out} - u_{in}\right) \quad (11)$$

where u_{in} was assumed to be zero and;

$$u_{out} = M_{out}\sqrt{\gamma R T_{out}} \quad (12)$$

$$T_{out} = \frac{\overline{T}_{t,out}}{1 + \frac{\gamma - 1}{2} M_{out}^{\ 2}} \quad (13)$$

$$M_{out} = \left\{ \frac{2}{\gamma - 1}\left[\left(\frac{\overline{P}_{t,out}}{P_{atm}}\right)^{\frac{\gamma-1}{\gamma}} - 1\right]\right\}^{\frac{1}{2}} \quad (14)$$

Finally, the power absorbed by the CFF was calculated from;

$$P_{ower} = \dot{m}_{in} c_p \left(\overline{T}_{t,out} - \overline{T}_{t,in}\right) \quad (15)$$

After all the parameters were calculated, the correction to standard day conditions was accomplished as follows;

$$\delta = \frac{P_{t,in}}{P_{t,std}};\ \theta = \frac{T_{t,in}}{T_{t,std}} \quad (16)$$

$$\dot{m}_{corr} = \dot{m}\frac{\sqrt{\theta}}{\delta};\ N_{corr} = \frac{N}{\sqrt{\theta}};\ F_{corr} = \frac{F}{\delta};\ P_{corr} = \frac{P}{\delta\sqrt{\theta}} \quad (17)$$

C. TEST PLANS

Two test plans were performed with both cavities opened; these were, Test Plan I - the Baseline Configuration, which was run from 1000RPM up to 5000RPM, and Test Plan II - the Throttling Investigation, where throttle settings were employed to control the mass flow rate at particular rotational speeds. The complete assemblies of both configurations are shown in Figure 6.

(a)

(b)

Figure 6. CFFTA for (a) Test Plan I and (b) Test Plan II

III. DESCRIPTION OF THE NUMERICAL MODEL

A. OVERVIEW

In order to study characteristics of a flow in a cross-flow fan, the commercial computational fluid dynamics (CFD) package, CFX-5, which was developed by ANSYS Inc, was used to more accurately model the compressible flow through the CFF. Three modules were included; CFX-Pre, CFX-Solver and CFX-Post. In CFX-Pre, a simulation type was defined; rotating or stationary domain, boundary conditions and the interface surfaces were defined; initial values, solver controls and output controls were set. After initializing the information required by CFX-Pre, the simulation was started by writing files to the CFX-Solver. Convergence histories were monitored while running with the solver, which also wrote out result files (*.res and *.out). By using CFX-Post, the results could be read and plotted for visualization and further post processing.

B. GEOMETRY AND GRID GENERATION

The geometry for the 12 inch diameter rotor with 30 blades, based on the experiment by Seaton and Cheng [Ref 5 & 1], was created by using ICEM-CFD, which was compatible with CFX-5. Since a finite-volume approach was utilized in CFX-5, a 3-dimensional geometry was required and generated with a span of 0.1 inch. It was then treated as a 2-D case, due to there being only one grid point in the span-wise direction.

There were ten volume meshes generated separately throughout the geometry. Two were in the rotational domain, which were identified as BLADES and INNERCIRCLE,and eight parts were in the stationary domain, which were identified as INLET, OUTLET, High Pressure Cavity (HPC), Low Pressure Cavity (LPC), INLET(Interface), OUTLET(Interface), HPC(Interface) and LPC(Interface). Attention needed to be paid to the last four parts in the stationary domain, since they were adjacent to the rotational domain as shown in Figure 7. A complete volume mesh was created by merging each part together, which was done by opening individual mesh files (*.uns) sequentially. Therefore, 2D planes of each part sharing a common boundary between the interfaces were generated, which are shown in Figure 8.

It was believed that the shape of the blades influenced the performance of the cross-flow fan. Thus O-grid topologies were employed for the regions around the blades in order to more accurately model the blade surface boundary layers, as shown in Figure 9. Hexahedral cells were generated for all domains. A procedure for generating this geometry and mesh are provided in APPENDIX D.

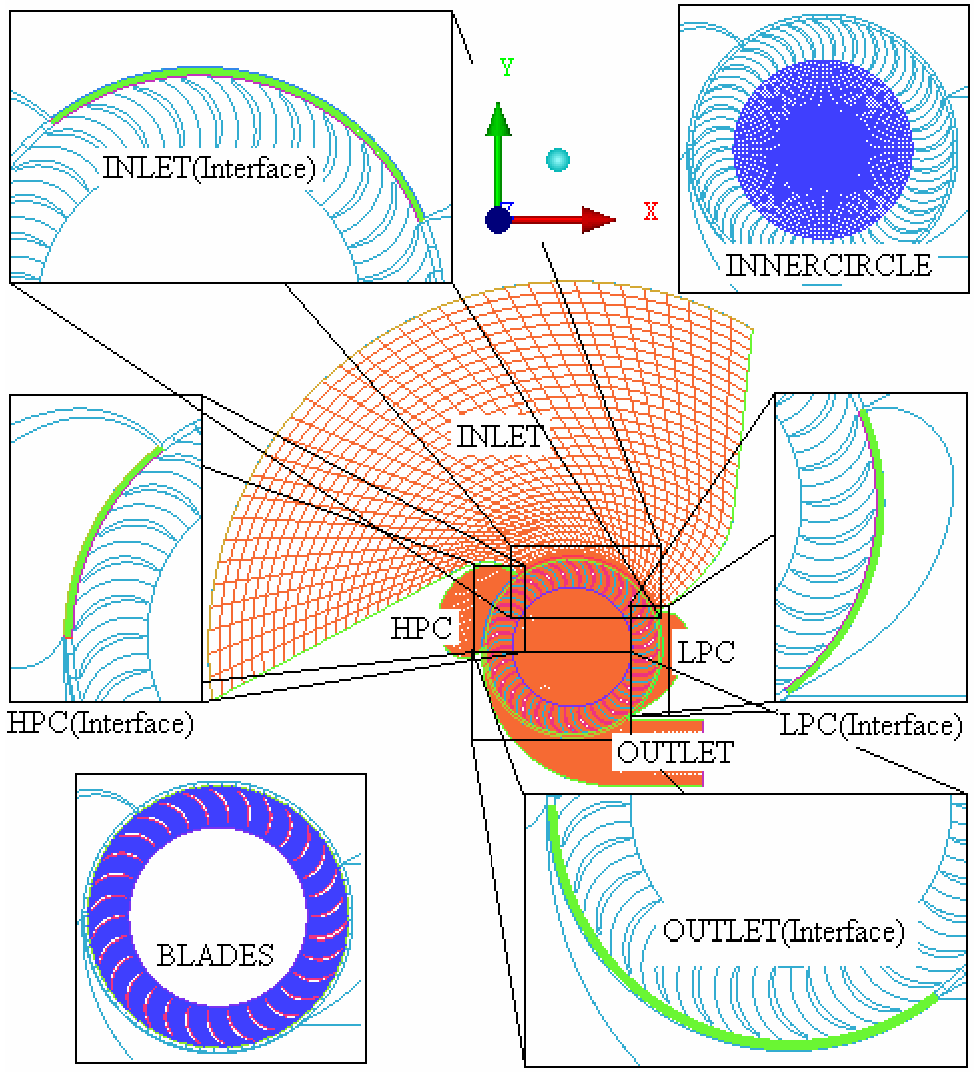

Figure 7. Identification of the ten domains of the CFF mesh

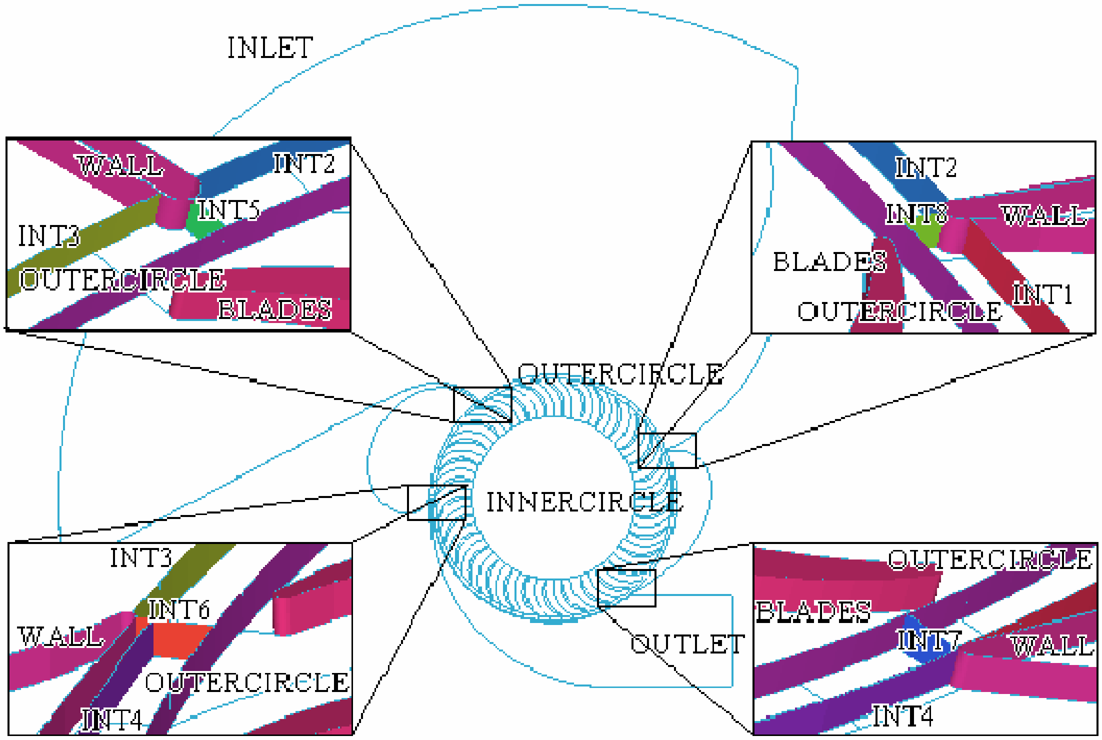

Figure 8. The planes between the interfaces

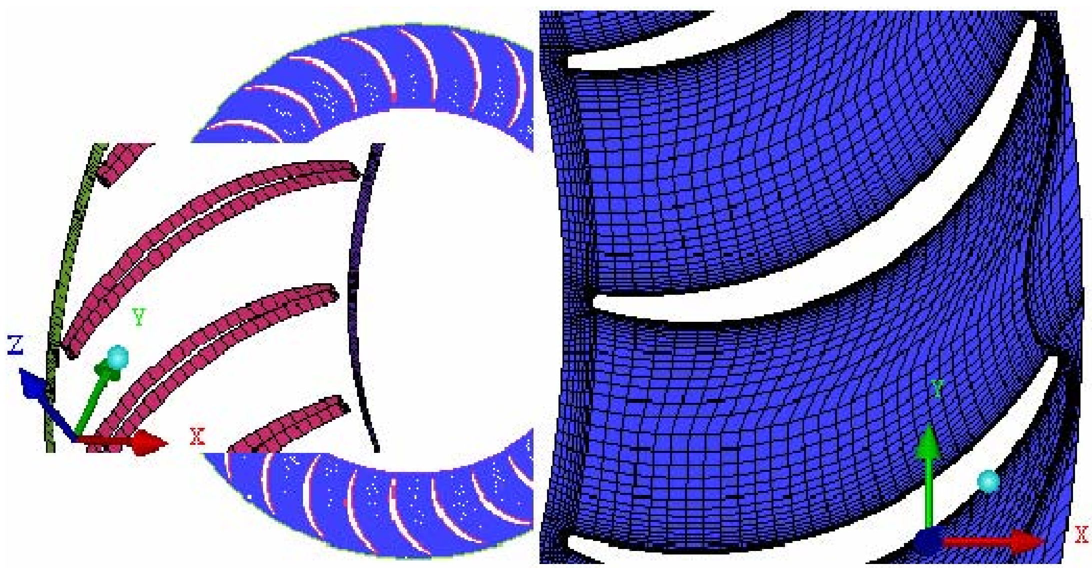

Figure 9. The meshes around blades

C. METHODOLOGY AND BOUNDARY CONDITIONS

Transient solutions were carried out by setting the interface between the rotational domains and the stationary domains within the model to “Transient Rotor-Stator”, and the sliding interfaces were then specified. The fluid was specified as an ideal gas with constant specific heat at constant pressure. With a reference pressure of 1 atm, the opening inlet and opening outlet boundary conditions were set to an average relative total pressure of 0 atm, and a relative static pressure of 0 atm, respectively. The reason for using an opening boundary condition, at both the inlet and exit, was because of uncertainty in flow recirculation at both boundaries. Static temperature of 300K, or standard day temperature, and turbulent intensity of 5% were also set for both inlet and outlet boundaries. An adiabatic smooth wall boundary with no slip was imposed, throughout on all walls.

Total energy and the k-epsilon turbulence model were used to include effects of heat transfer and turbulence, respectively. By setting a transient initialisation, the simulation could be run without initial values interpolated; the solver default values were employed at the beginning of the run. Equations involved in the solver were continuity, momentum, energy, turbulence eddy dissipation, turbulence kinetic energy, and an equation of state. The set-up procedure in CFX-Pre is also provided in APPENDIX E.

Continuity equation:

$$\frac{\partial \rho}{\partial t} + \nabla \bullet (\rho U) = 0$$

Momentum equation:

$$\frac{\partial \rho U}{\partial t} + \nabla \bullet (\rho U \otimes U) = \nabla \bullet \left(- p\delta + \mu\left(\nabla U + (\nabla U)^T\right)\right) + S_M$$

Energy equation:

$$\frac{\partial \rho h_{tot}}{\partial t} - \frac{\partial p}{\partial t} + \nabla \bullet (\rho U h_{tot}) = \nabla \bullet (\lambda \nabla T) + \nabla \bullet \left(\mu \nabla U + \nabla U^T - \frac{2}{3} \nabla \bullet U \delta U\right) + S_E$$

$$h_{tot}(p,T) = h_{stat}(p,T) + \frac{1}{2} U^2$$

Turbulent eddy viscosity

$$\mu_t = C_\mu \rho \frac{k^2}{\varepsilon}$$

Turbulent kinetic energy

$$\frac{\partial(\rho k)}{\partial t} + \nabla \bullet (\rho U k) = \nabla \bullet \left[\left(\mu + \frac{\mu_t}{\sigma_k} \right) \nabla k \right] + P_k - \rho \varepsilon$$

Turbulence Eddy Dissipation

$$\frac{\partial(\rho \varepsilon)}{\partial t} + \nabla \bullet (\rho U \varepsilon) = \nabla \bullet \left[\left(\mu + \frac{\mu_t}{\sigma_\varepsilon} \right) \nabla \varepsilon \right] + \frac{\varepsilon}{k} \left(C_{\varepsilon 1} P_k - C_{\varepsilon 2} \rho \varepsilon \right)$$

The equation of State

$$\rho(p, T) = \frac{w(p + p_{ref})}{R_0 T}$$

D. SIMULATION PLANS

Two simulation plans were embarked on to predict the performance at conditions similar to the experimental test plans. These are summarized in Table 4. The configurations of both plans are presented in Figure 10. As shown, to constrain the inlet flow into the CFF, an extending wall was added instead of the bell-mouth, the mass-flow rate was, therefore, recorded from the inlet boundary for the following analysis. More difficulties were encountered to predict the case of Test Plan II, a suitable diffuser had to be determined to carry out the expected mass flow rate variation since several effects had to be considered, such as inlet turbulence and inlet velocity profile.. From [Ref. 8], the maximum diffuser $L/W_1 = 2$ and $2\theta = 14^0$ was used. To vary the mass flow rate, the diffuser was closed gradually by 1.75 degree until stall occurred.

Case / Speed	Simulation Plan I (corresponding to Test Plan I)	Simulation Plan II (corresponding to Test Plan II)
1000RPM	V	
2000RPM	V	V
3000RPM	V	V
4000RPM	V	
5000RPM	V	V

Table 4. Summary of simulation plans

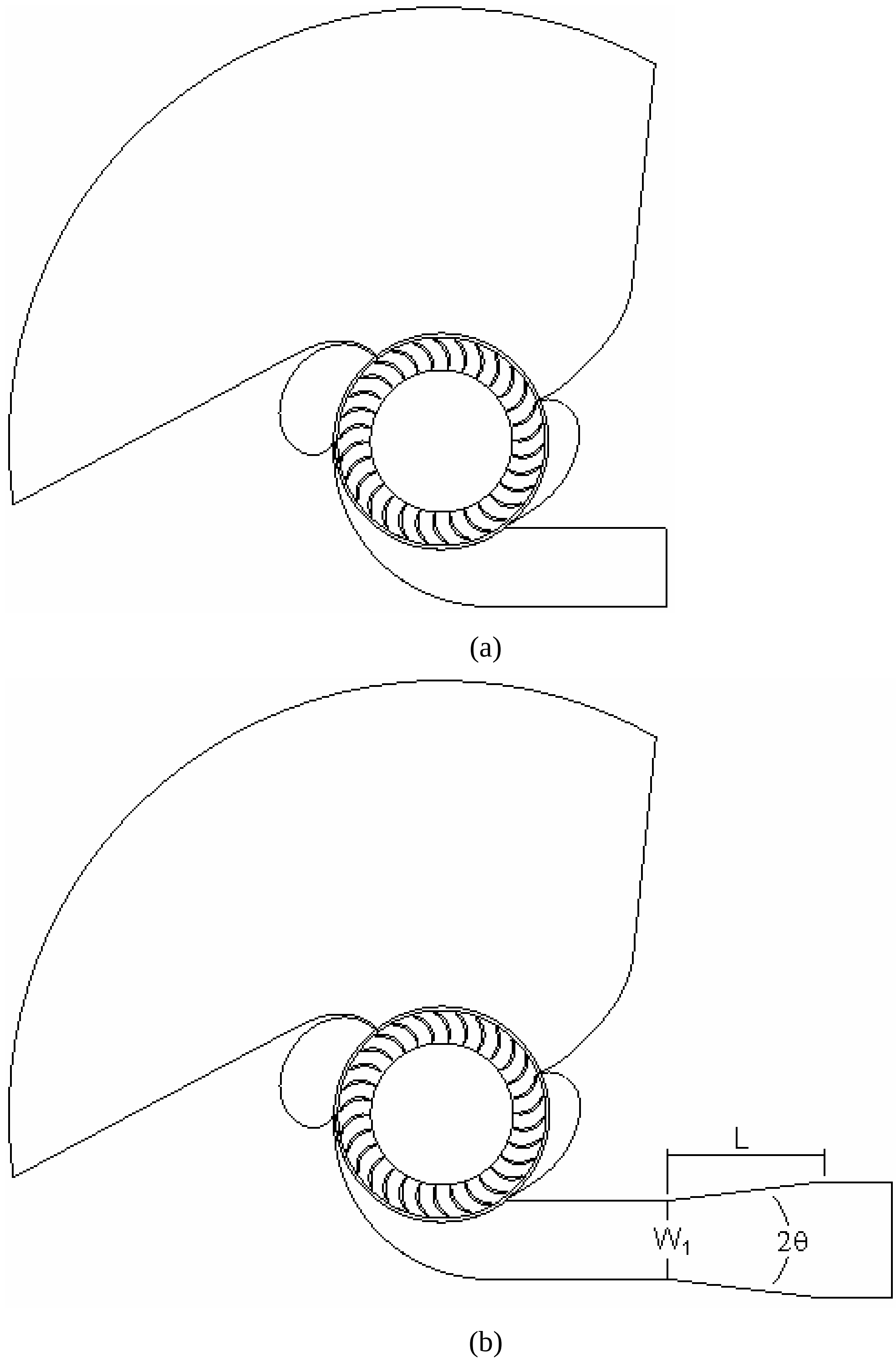

Figure 10. Geometric profile of (a) Simulation Plan I and (b) Simulation Plan II

IV. RESULTS AND DISCUSSION

A. MESH SENSITIVITY STUDY

The mesh sensitivity was studied under a rotational speed of 3000RPM with a time-step of 3.33333e-5 seconds, which corresponded to a rotation angle of 0.6 degrees per time step.

At first, with a constant number of mesh elements (62,493), the sensitivity was studied by varying the spacing of grids of specific parts, and run for 10 revolutions. Since meshes were not distributed uniformly along the interfaces, the confirmation of transferring properties between domains was required. It was required that the differences between simulated results were less than 0.06%. The best results were obtained with the most clustering of points close to the interfaces. Two more different mesh sizes were modeled, the coarse one with 13,657 elements and the finest one with 250,573 elements. Once the calculations were completed, the efficiency was used as an indicator to determine the optimum mesh size. It was found that the coarse mesh size provided an efficiency of 57.26%, and the finest one provided an efficiency of 76.16%, those were not close to the expected efficiency of 68%. The only explanation for this was that the errors accumulated in the finest meshes, which adversely effected in the transient model.

However, a medium mesh size provided the efficiency of 68.13%, which corresponded favorably with the experimental value. In addition, its corresponding corrected mass flow rate of 0.4932 kg/s was calculated, which was close to the experimental value of 0.4872 kg/s. Therefore, the mesh size of 62,493 elements was used in the subsequent simulations. All the simulations were for 10 revolutions, the reason to be discussed in the following section on convergence history.

B. TIME-STEP SELECTION

Generally, smaller time-steps need more time to calculate but provide more accurate results. The goal of the present study was to find the optimal time-step, the one that would not only take less time for the simulation, but also provide an acceptable solution. Therefore, the selection of time-step was performed based on the consequence of the mesh sensitivity study with a rotating speed of 3000RPM. A computer with Pentium@ 4 CPU with double 3.2Ghz processors and 3.25 GB RAM was used. Four cases were carried out, which were 12 degrees, 6 degrees, 1 degree and 0.6 degrees rotational angle per time step, and all cases were run for only one revolution.

It was found that all residuals (momentum and mass, turbulence, and heat transfer) were converged and fluctuated along 10^{-3}, $10^{-3} \sim 10^{-4}$, and 10^{-4} for the first three cases, and computational times were 1 hours, 2 hours and 13 hours, respectively. For the last case, the residuals were just slightly lower than 10^{-4} but required 30 hours. Hence, 1 degree angle per time step was selected for further simulations.

C. INITIAL SIMULATION RESULTS

A baseline model at 3000RPM was first simulated for 10 revolutions to see if the converged solutions could be calculated. To compare with the results of experiments, the same locations of probes were used in the computational model. For each revolution, the parameters, such as mass-flow rate, total pressure ratio, total temperature ratio and efficiency, were calculated and monitored in order to check whether steady solutions were achieved.

1. Convergence History

The calculated parameters which were used for monitoring purposes were slightly different from those used for comparison to the experimental results. Since the expression of compressible flow (Eq. 5) may result in imaginary numbers, the mass flow rate in each zone within the exhaust duct was evaluated directly from the product of density and velocity read from probes in the model. The thrust was derived in the same manner.

The convergence histories for the baseline test case at 3000RPM are shown in Figures 11-13. Figure 11 indicates that the simulation was started from no initalized flow field and it almost reached a stable value after 5 revolutions. This was also observed for the total pressure in Figure 12, however, the total temperature ratio still increased slightly, which affected the efficiency variation until the 8^{th} revolution.

The variation of efficiency for the last three revolutions in each model was about 0.004, therefore the solution at the 10th revolution was considered to be stable. All subsequent calculations were therefore carried out until 10 revolutions had been completed. The convergence histories of all subsequent models were monitored in the same manner.

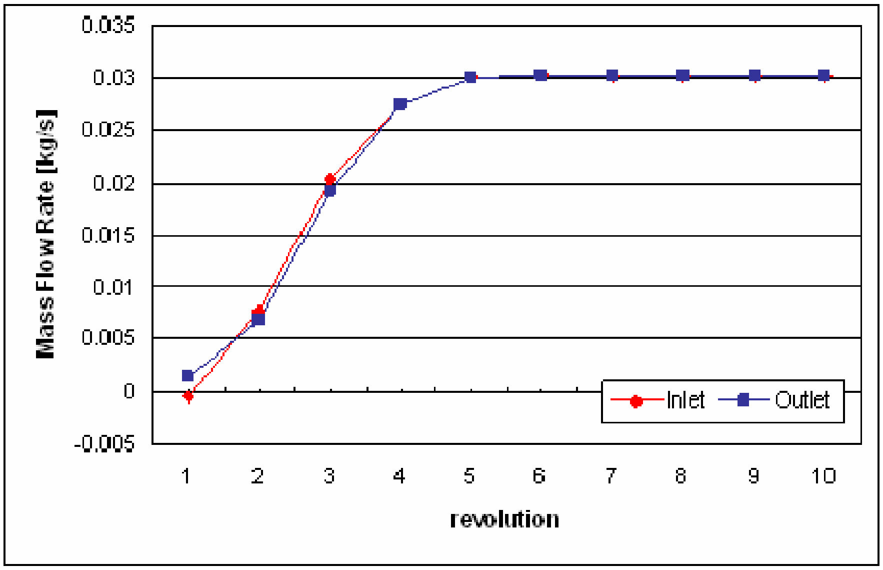

Figure 11. Convergence history of mass flow rate at 3000RPM

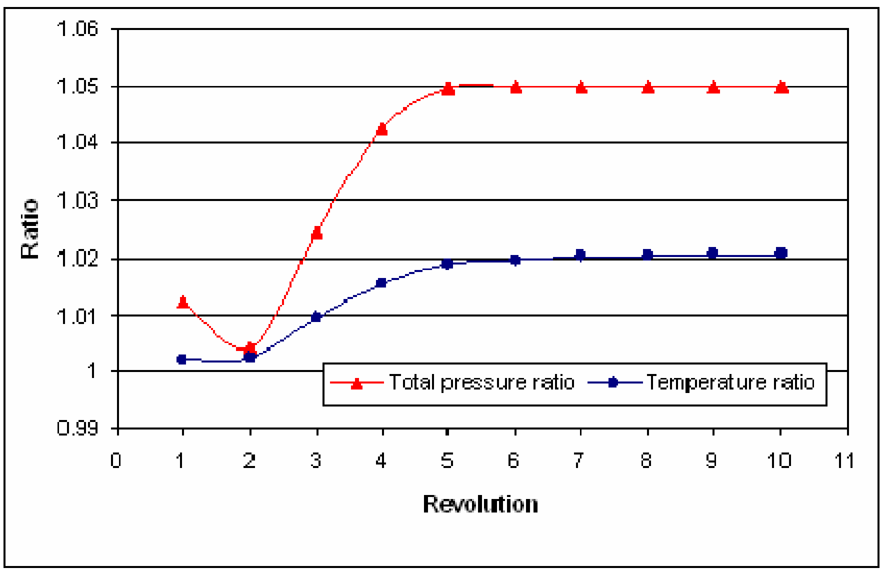

Figure 12. Convergency history of total pressure ratio and total temperature ratio at 3000RPM

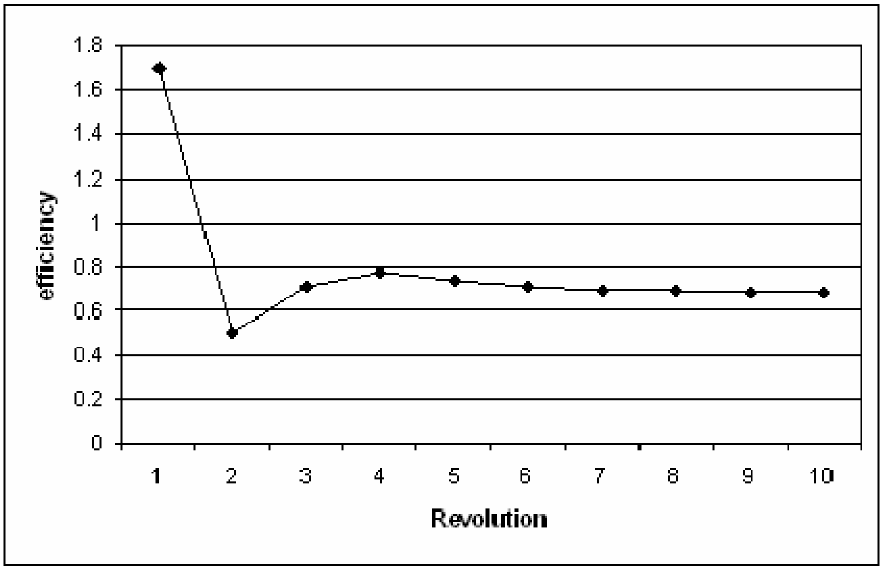

Figure 13. Convergency history of efficiency at 3000RPM

2. Flow Visualization

Figure 14 shows vector distributions of flow velocity for both cavities. In the high pressure cavity (HPC), the direction of flow was clockwise, but counterclockwise in thelow pressure cavity (LPC), which agreed with the observation in [Ref. 4]. Additional vortical flow features occurred between the blades. The highest velocity region was found within the LPC, consistent with the low pressure. Similarly, the lowest velocity region was found within the HPC, consistent with the high pressure, which explained the names of these cavities.

Figure 15 shows that the lowest pressure did not occur within the LPC, but rather within the rotor close to the LPC. The total pressure profile at the outlet boundary suggested more measuring probes should be used to provide more accurate experimental results.

Figure 16 indicates that the most energy lost was due to the vortex that occurred around the LPC. More heat was generated within this region, which caused the temperature at the LPC to be higher than at the HPC. The exit plane total temperature distribution was non-uniform, with the highest temperature close to the top wall; however the variation of temperature was less than 10 degrees.,

Figure 17 shows the distribution of Mach number, which supports the assumption of subsonic flow within the CFF at 3,000 RPM. A large recirculation in the HPC was observed. The highest Mach numbers (~0.39) occurred at three locations, one was within the blades near to the LPC; a second one was in the LPC, and the third one was near to where the flow entered the exhaust duct. The velocity profile at the exhaust duct exit plane is also shown. It was observed that the flow entrainment into the CFF was roughly at the one o'clock position into the rotor..

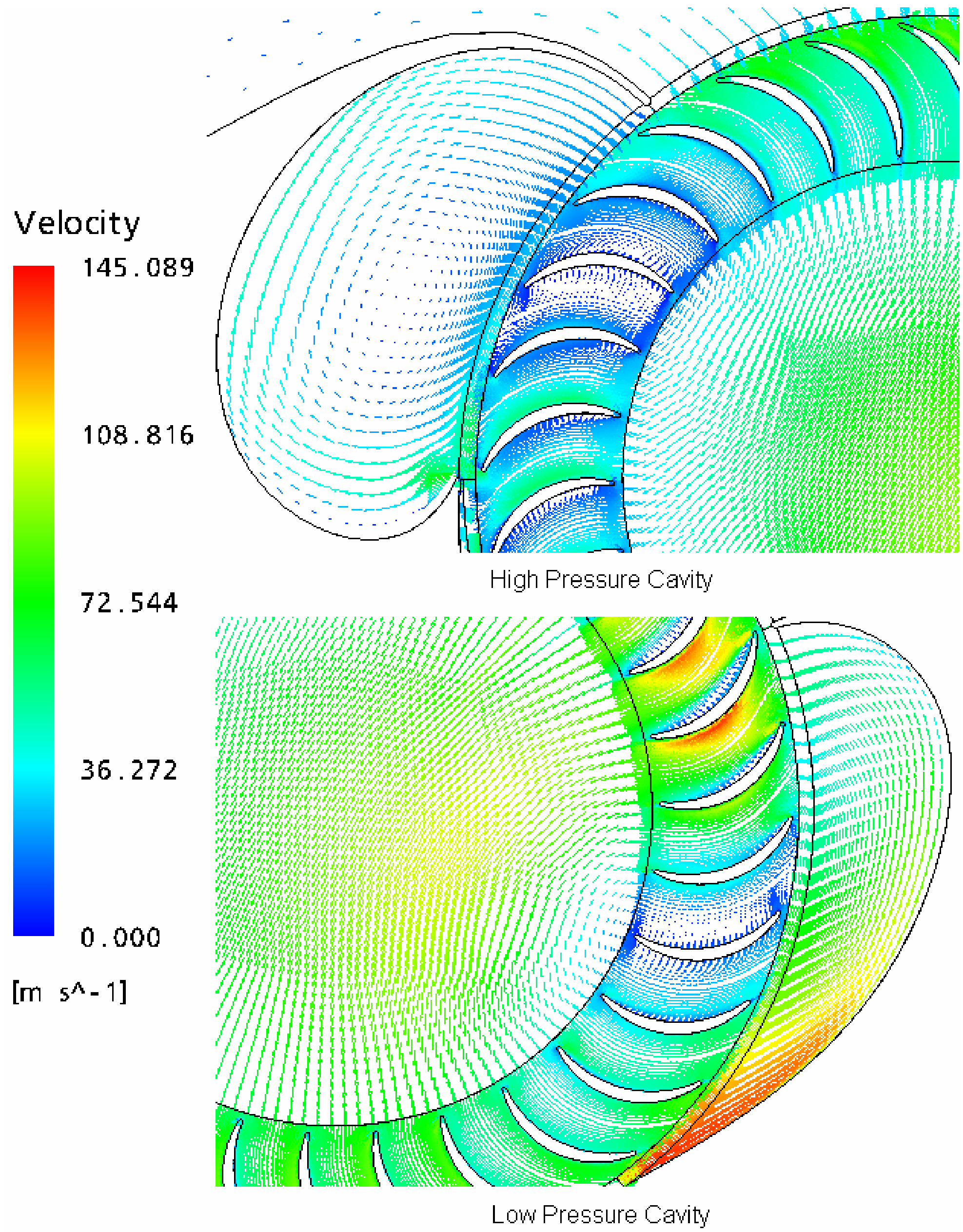

Figure 14. Vector plot of velocity in HPC and LPC at 3000RPM

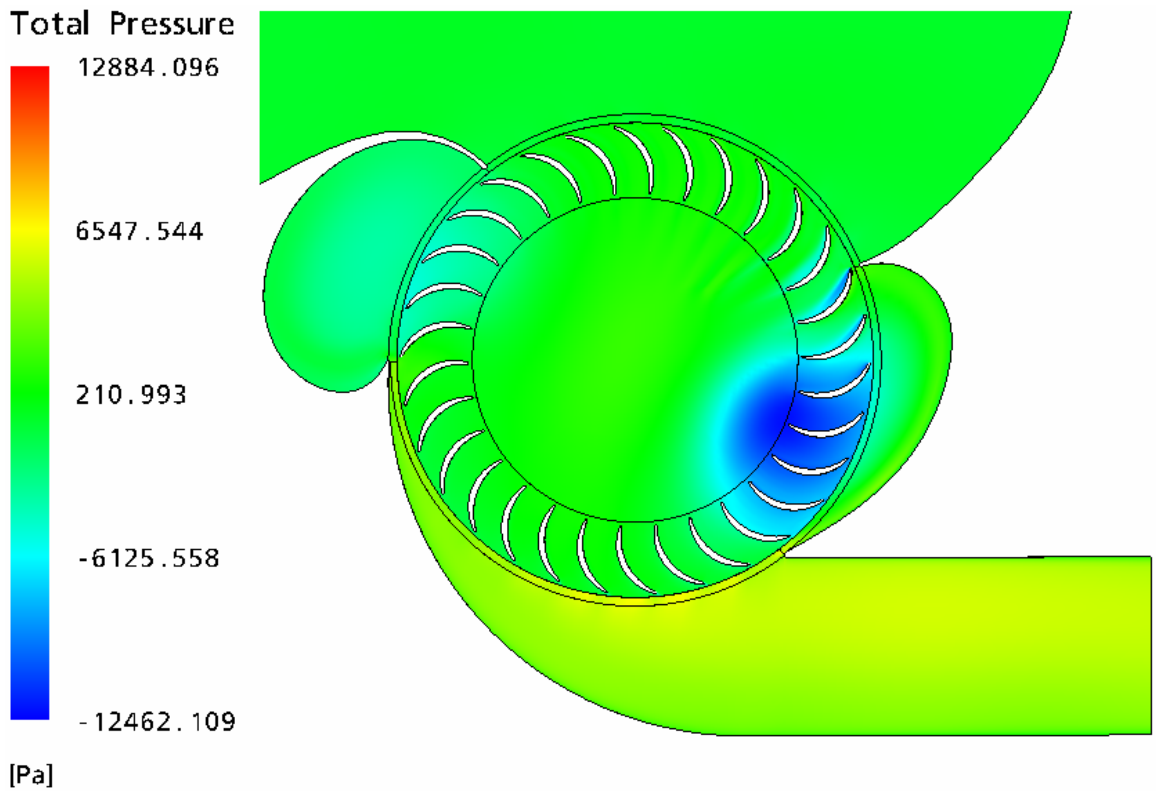

(a) Whole flow field

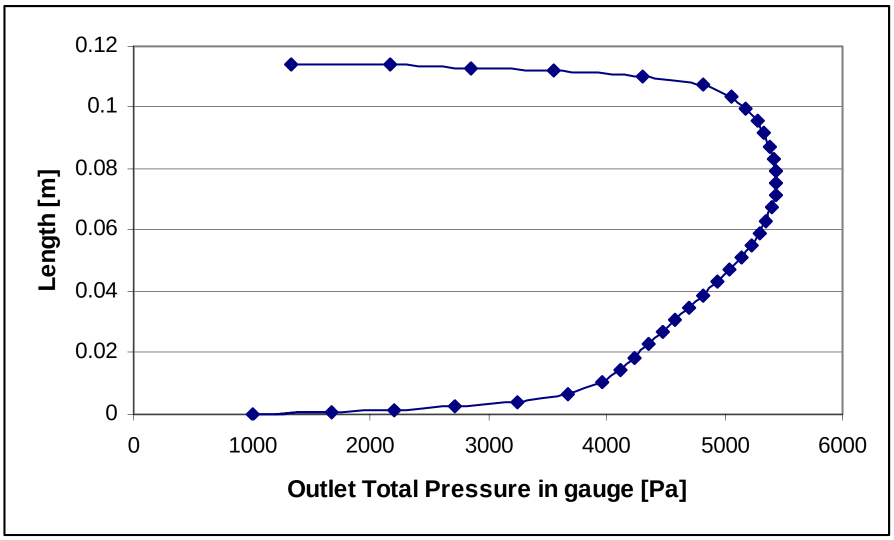

(b) Exit plane

Figure 15. Distribution of total gauge pressure at 3000RPM

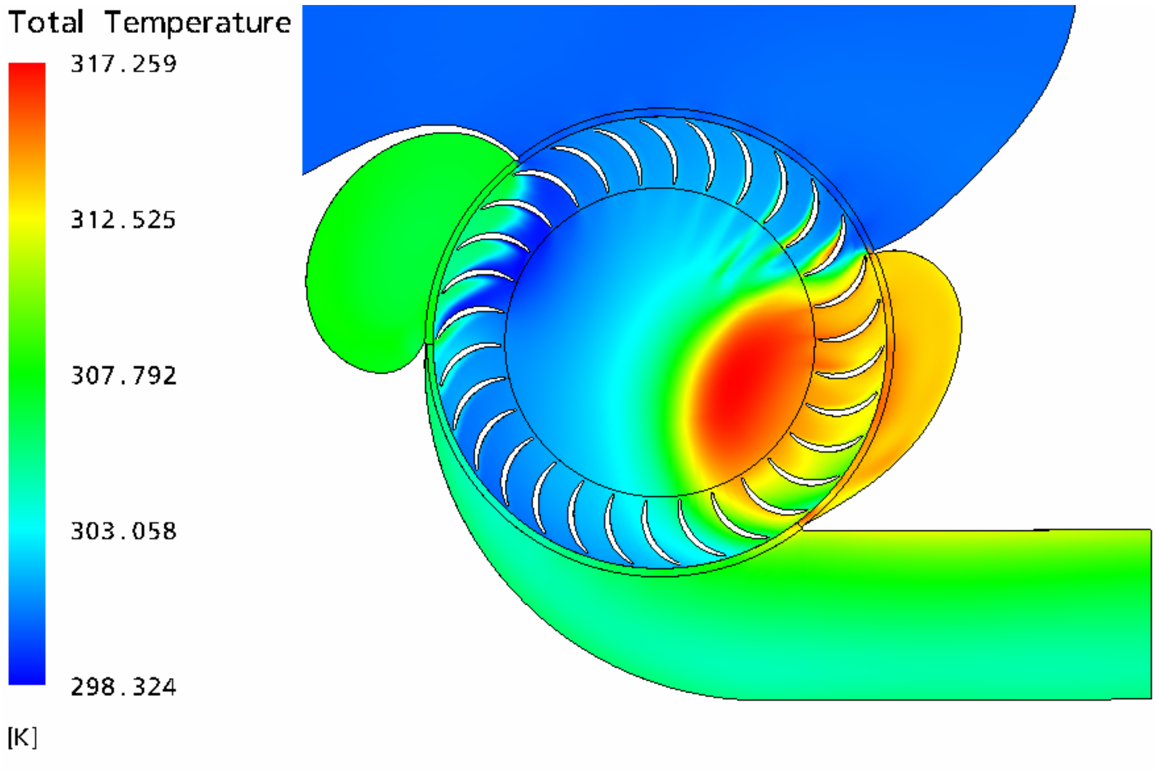

(a) Whole flow field

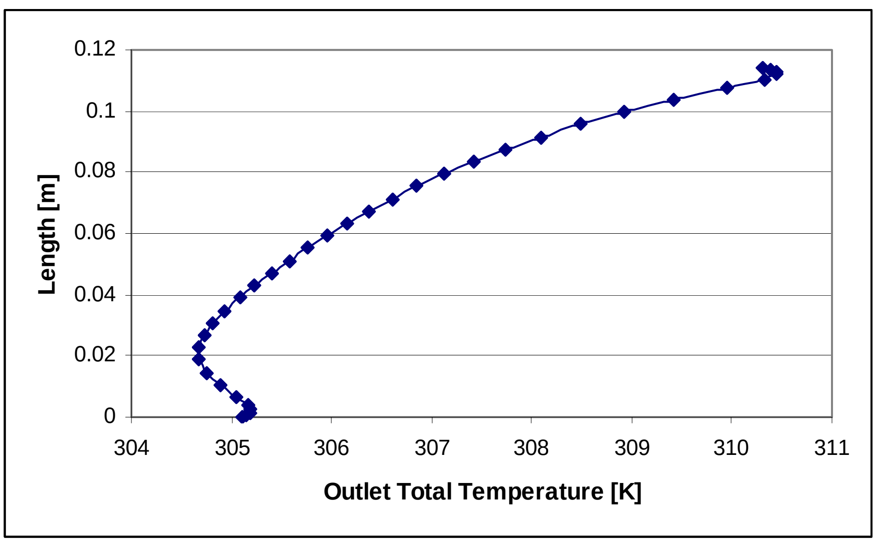

(b) Exit plane

Figure 16. Distribution of total temperature at 3000RPM

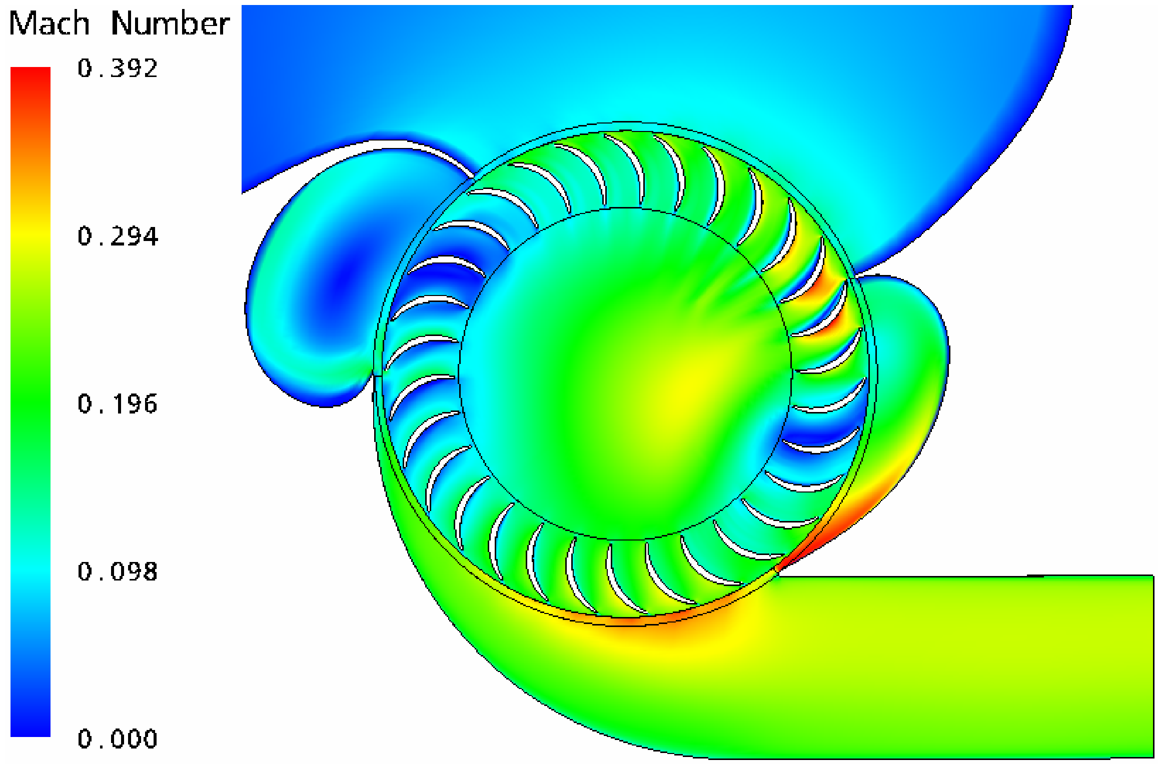

(a) Whole flow field

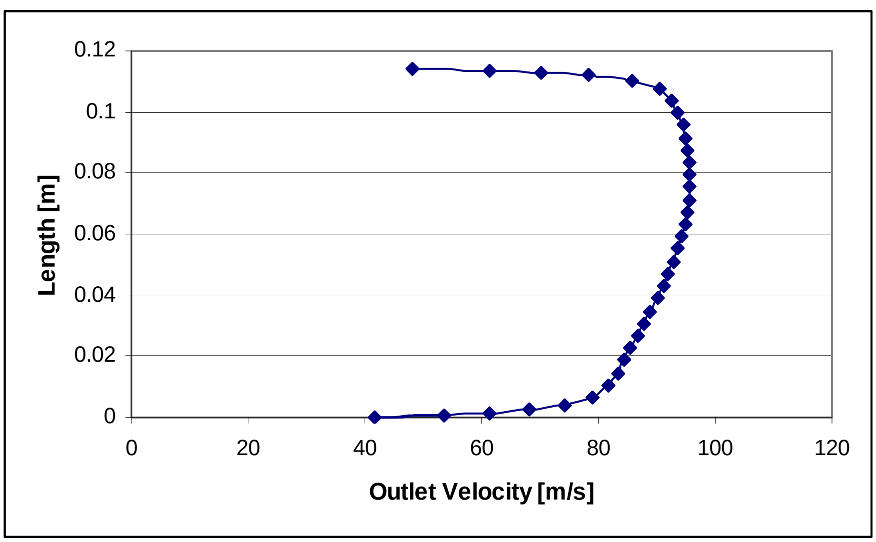

(b) Exit plane

Figure 17. Distribution of Mach number at 3000RPM

D. EXPERIMENTAL DATA CONSISTENCY STUDY

The derived parameters from [Ref. 4] were converted from English Engineering (EE) to SI units, and the raw data sets were re-calculated by the procedure mentioned in

Chapter II, section B. Those two data sets were compared to make sure no inconsistencies occurred during the calculations. Since two test plans, with two cavities opened, were tested in this study, only those cases in [Ref. 4] were considered in the following. The results are shown in Figures 18-25.

1. Test Plan I

It was expected that the curves re-calculated here [shown as Re-cal] would overlap the existing curves [Ref. 4], in Figures 18-21, since the same procedures were applied. However, it was found that at high rotatiional speeds, the differences increased, especially in the mass flow rate. However, the differences in the mass flow rates calculated were small, 1.925% maximum, which was considered to be acceptable.

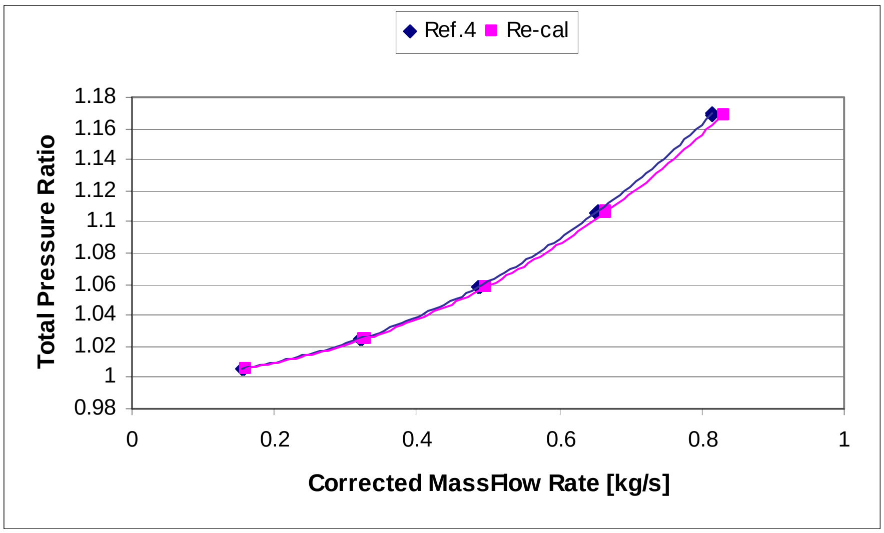

Figure 18. Consistency study of total pressure versus mass flow rate for Test Plan I

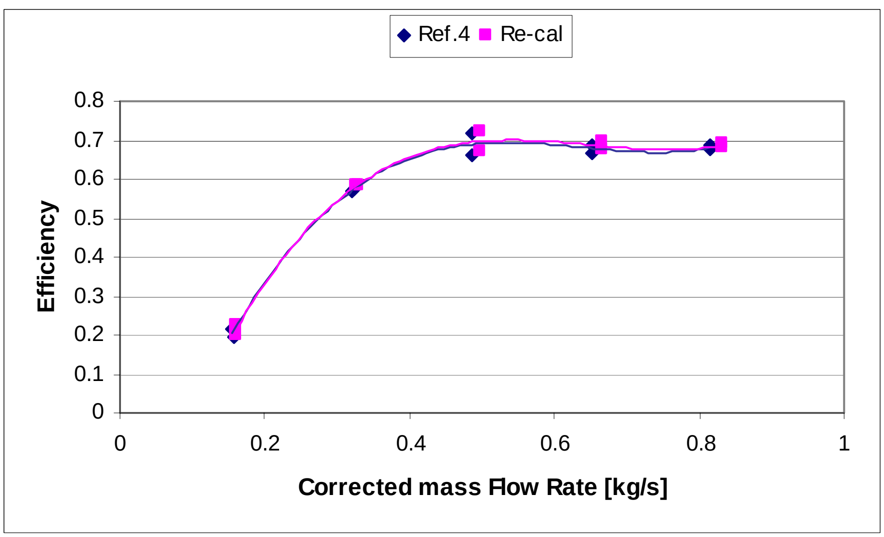

Figure 19. Consistency study of efficiency versus mass flow rate for Test Plan I

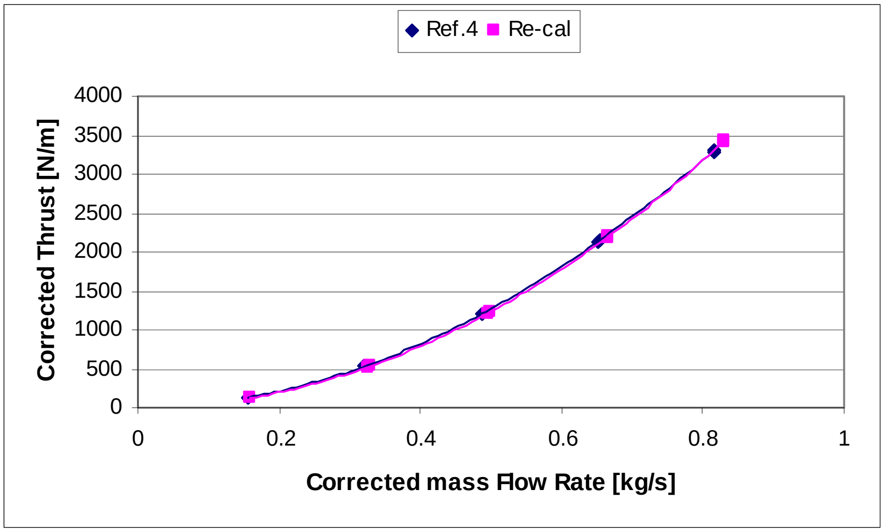

Figure 20. Consistency study of thrust versus mass flow rate for Test Plan I

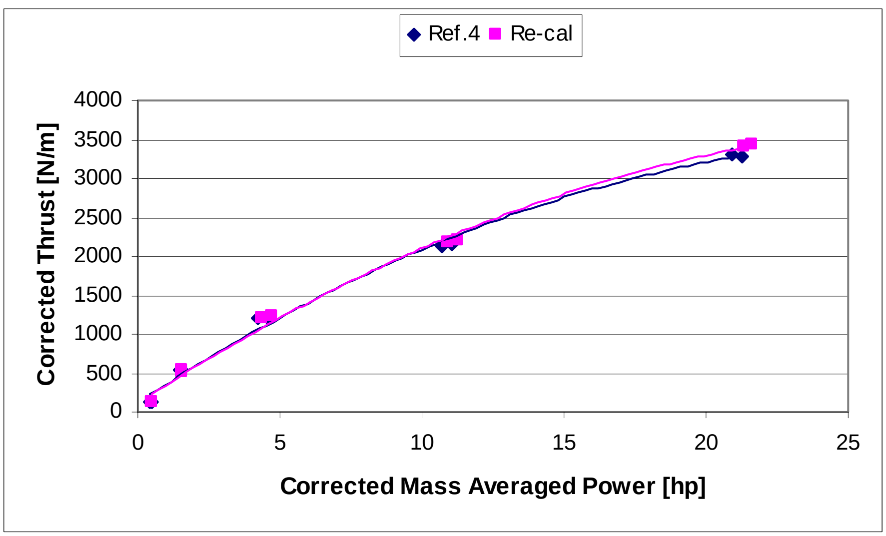

Figure 21. Consistency study of thrust versus power for Test Plan I

2. Test Plan II

As in the comparison for Test Plan I, the characteristic curves, shown in Figures 22-25, were not exactly the same, but the trends of total pressure ratio, total temperature ratio and efficiency versus mass flow rate were acceptable since they were close to the values originally calculated in [Ref. 4]. However, the relationship of thrust versus mass flow rate was linear once it was re-calculated; it was not quadratic as presented in [Ref. 4]. And the curves of the power versus mass flow rate shifted up a lot at higher rotational speeds. Therefore, in order to make the present study consistent, the current calculational procedure was utilized thereafter.

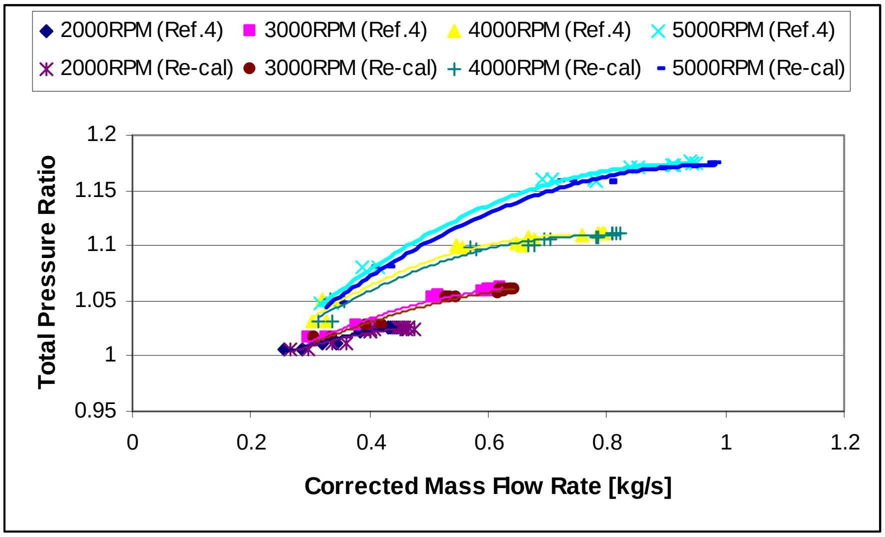

Figure 22. Consistency study of total pressure ratio versus mass flow rate for Test Plan II

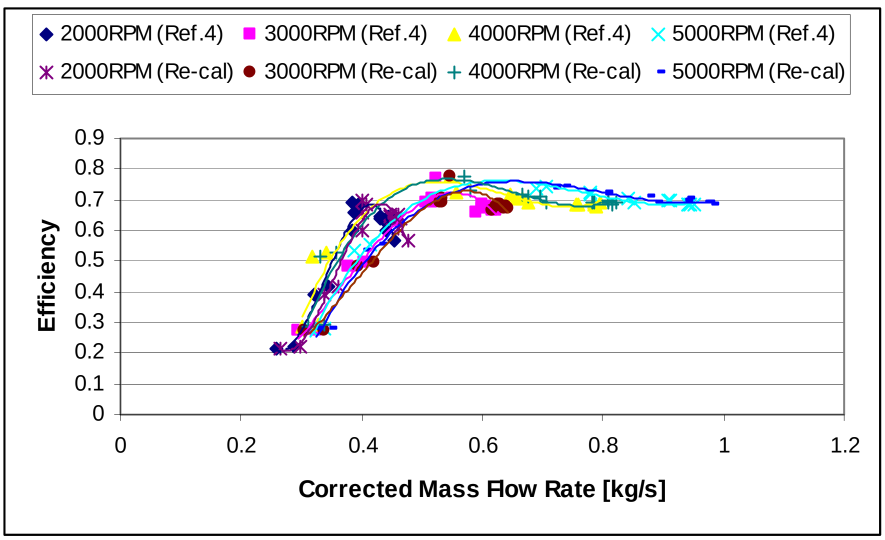

Figure 23. Consistency study of efficiency versus mass flow rate for Test Plan II

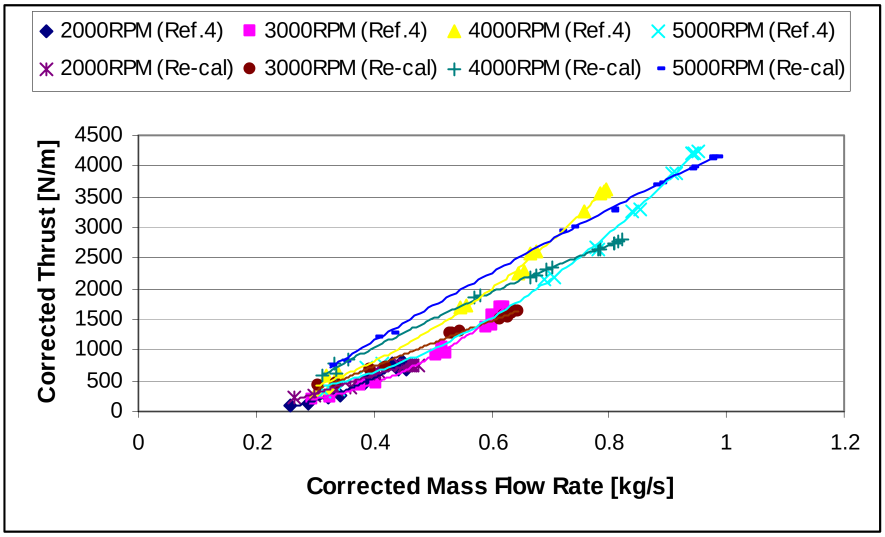

Figure 24. Consistency study of thrust versus mass flow rate for Test Plan II

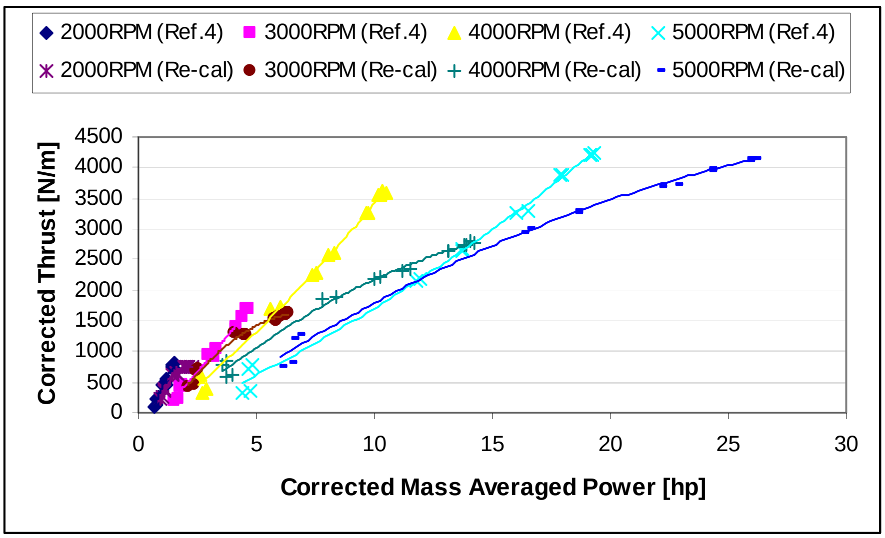

Figure 25. Consistency study of thrust versus power for Test Plan II

E. PERFORMANCE OF THE BASELINE CONFIGURATION AT VARIOUS ROTATIONAL SPEEDS

The results of Test Plan I were compared with the results of Simulation Plan I and the results shown in Figures 26-31. The re-calculated results of Cheng [Ref. 4] are also included. The results show a slight difference in the mass flow rate. There was a slight disagreement of the characteristic curves of total temperature ratio, efficiency and power. When the comparsion was made of the present experimental data but using different calculational procedures, i.e. using 3 exit combination probes vs 5 probes., more measuring probes improved the agreement in the total pressure ratio and efficiency, however total temperature ratio and power deviated slightly. The thrust was similar for all calculational procedures and for both data sets, the present as well as [Ref. 4]. The computed (CFD) results were obtained using the same calculational procedure as in the experiment, i.e. using 3 or 5 exit probes. Over the complete speed range the total pressure ratio comparison was very good. However, the curve of the total temperature ratio (with 5 probes) was higher than the experimental, which resulted in an under prediction of the efficiency. At low speeds the computed efficiency was too high, between 60 and 70%, and the trend was not correct as the drop off of efficiency with decreasing speed was not computed.

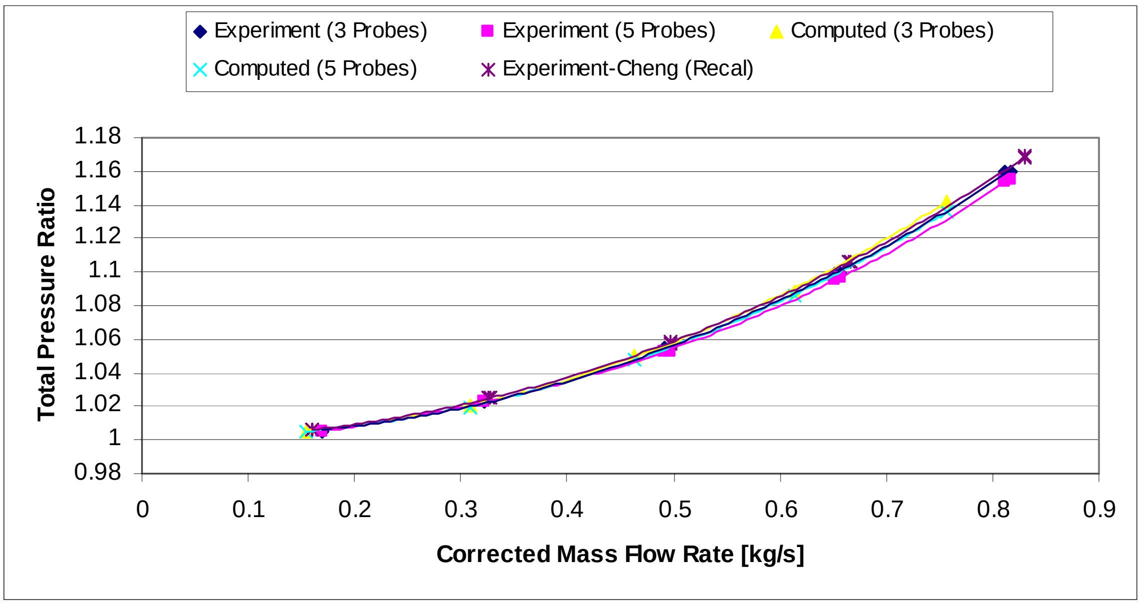

Figure 26. Comparison of total pressure ratio versus mass flow rate for Test Plan I

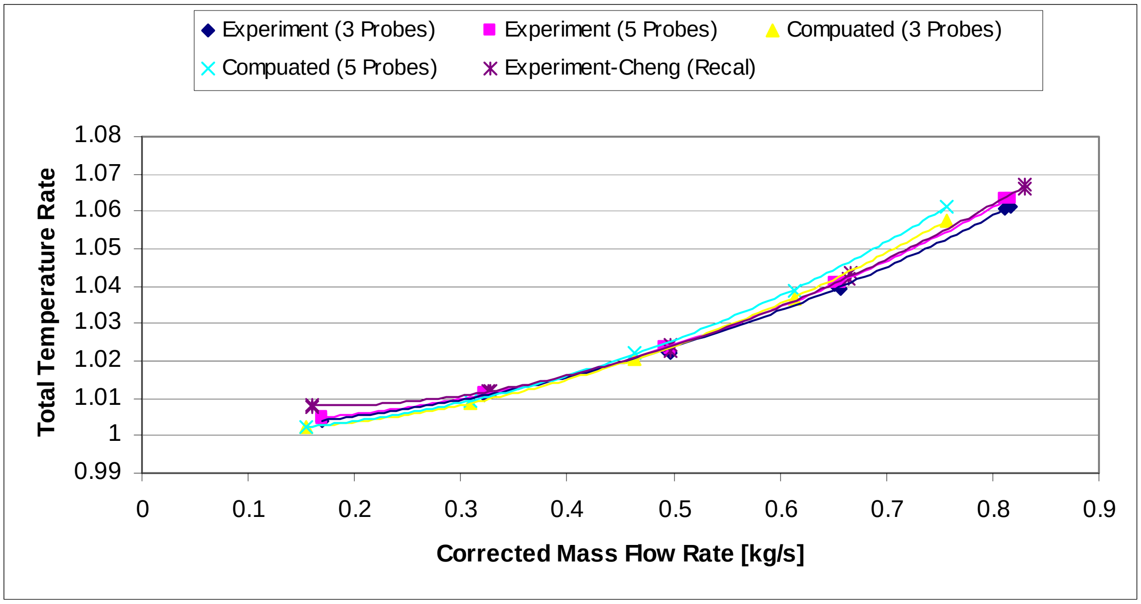

Figure 27. Comparison of total temperature ratio versus mass flow rate for Test Plan I

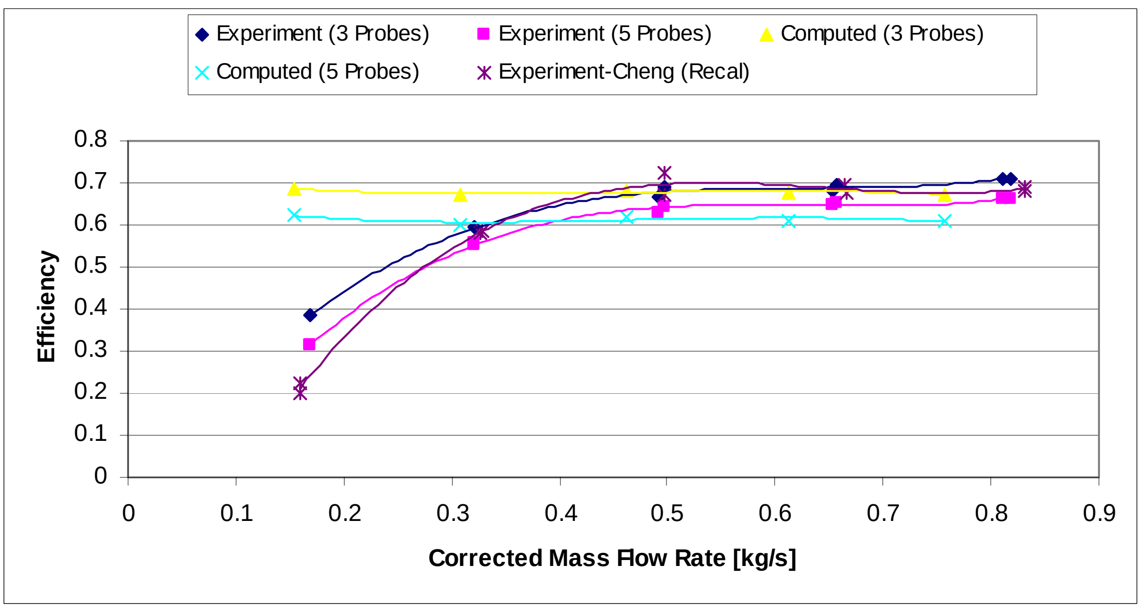

Figure 28. Comparison of efficiency versus mass flow rate for Test Plan I

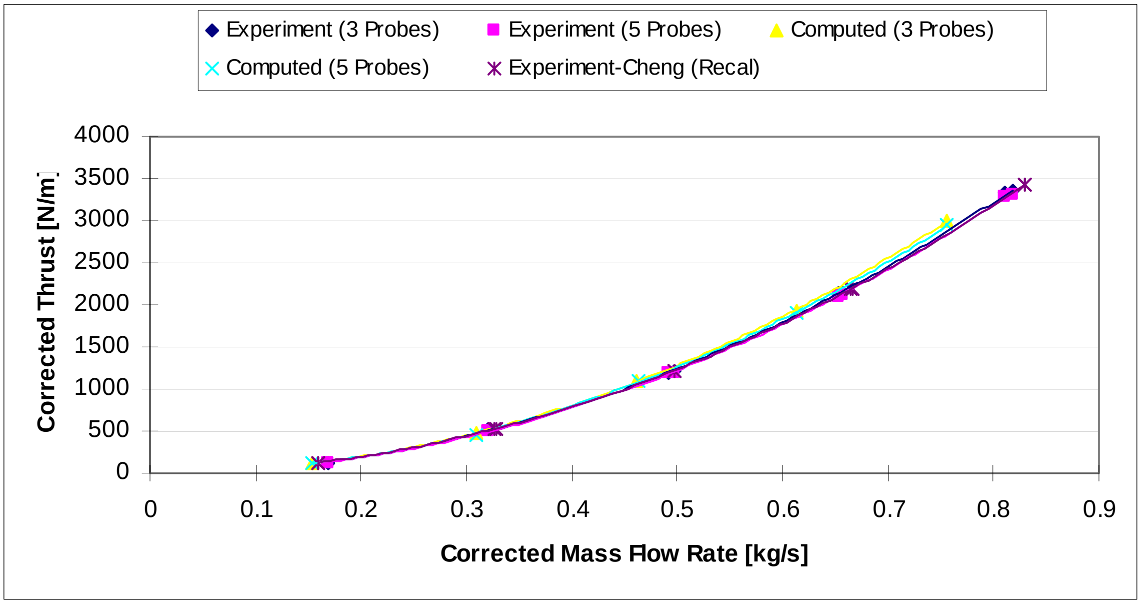

Figure 29. Comparison of thrust versus mass flow rate for Test Plan I

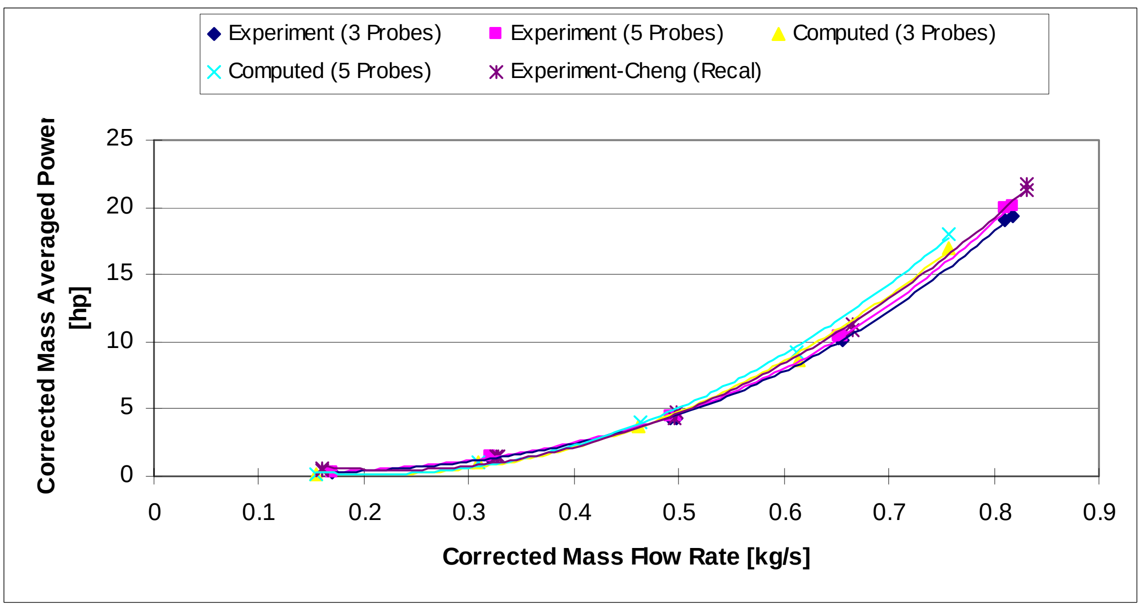

Figure 30. Comparison of power versus mass flow rate for Test Plan I

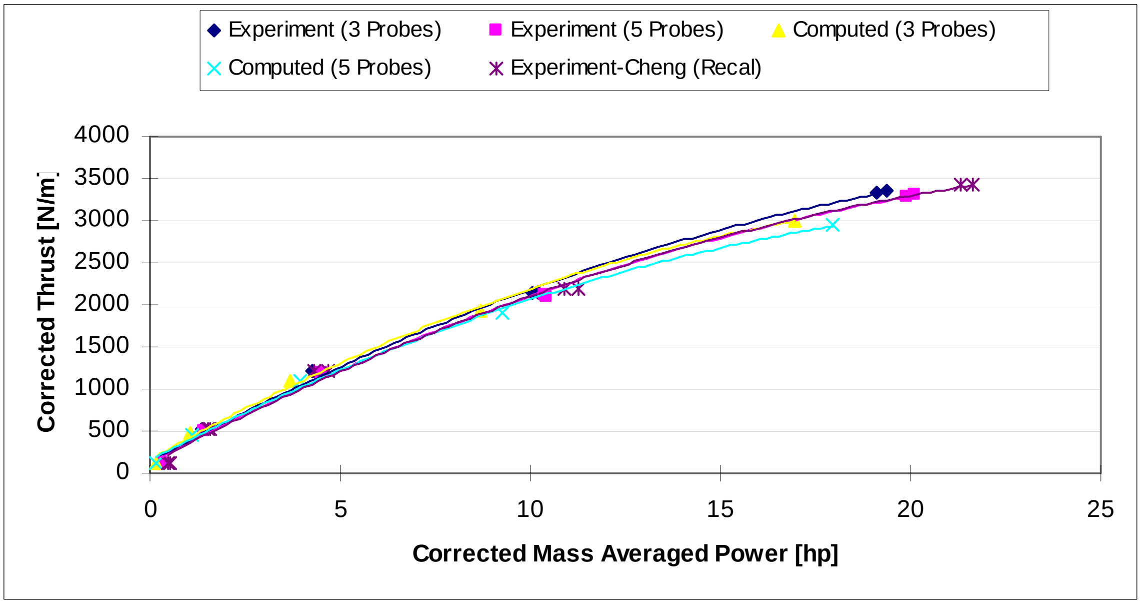

Figure 31. Comparison of thrust versus power for Test Plan I

F. OFF-DESIGN PERFORMANCE AT VARIOUS ROTATIONAL SPEEDS

First, the results of Test Plan II are presented and compared with the recalculated data of Cheng [Ref. 4]. In Figure 32-37, the CFF constant speed characteristics are shown based on the use of 5 probe measurements at the outlet plane. It can be seen that, which the levels of pressure ratio and temperature ratio were fairly similar at the different speeds, the range of mass flow rates from open to closed throttle were quite different, particularly at the lower speeds. At full open and stall throttle setting, the mass flow rate measured at 2000RPM was 15.25% and 77.54% less, respectively. At the higher rotational speed of 5000RPM, the mass flow rate measurements compared more favorably, however, the present measurements were down by 7.69% and 43.93% at open throttle and stall respectively.

A likely explanation for the discrepancy in mass flow rate measurments was that more accurate pressure transducers were used in the present study; i.e. the digital sensor array. To confirm this, an uncertainty analysis was performed. For Test Plan I, the uncertainties at 1000 RPM and 5000RPM were 3.72% and 0.16%, respectively, or averaged uncertainty, 1.94%. For Test Plan II, the uncertainty was 18.62% at the stall throttle position at 2000RPM, and the uncertainty was 0.13% at the full open throttle position at 5000RPM. The overall average uncertainty was 2.39%. Detailed equations for uncertainty are given in APPENDIX C.

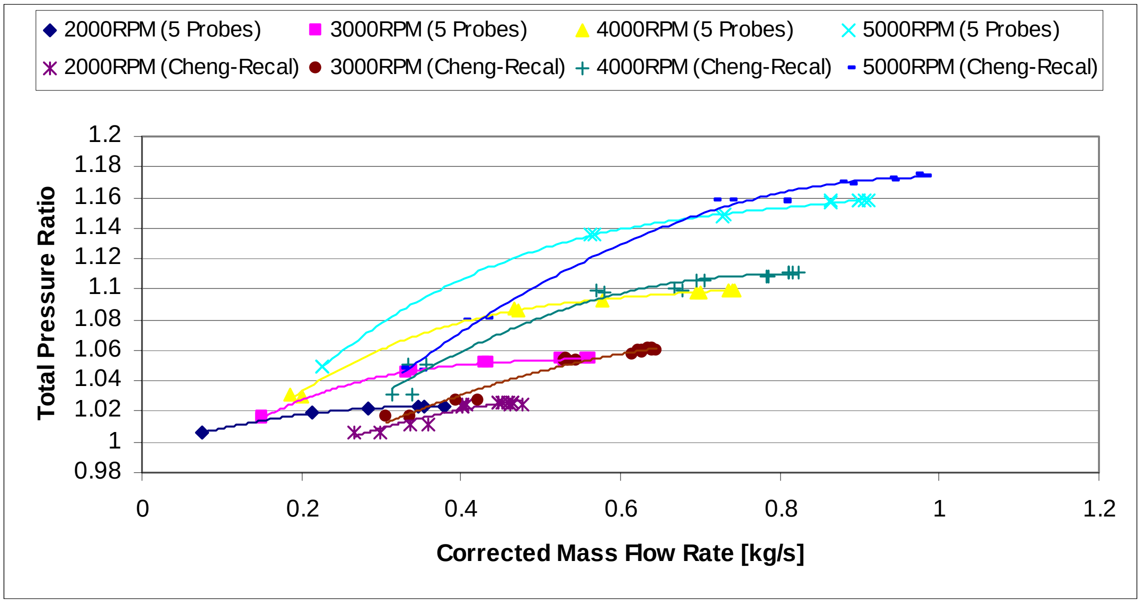

Figure 32. Comparison of total pressure ratio versus mass flow rate for Test Plan II

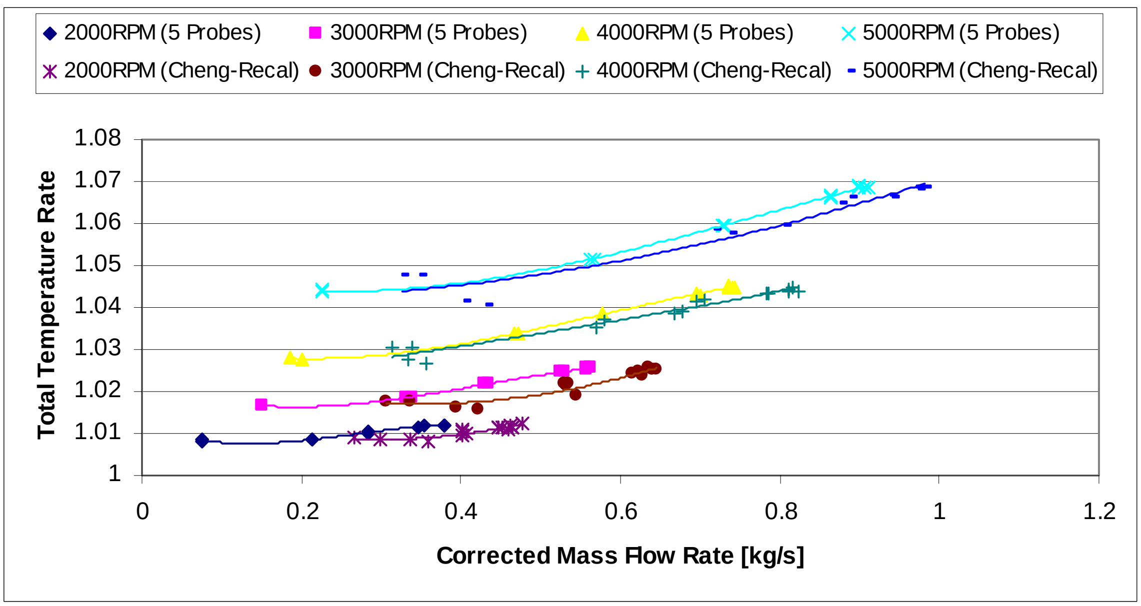

Figure 33. Comparison of total temperature ratio versus mass flow rate for Test Plan II

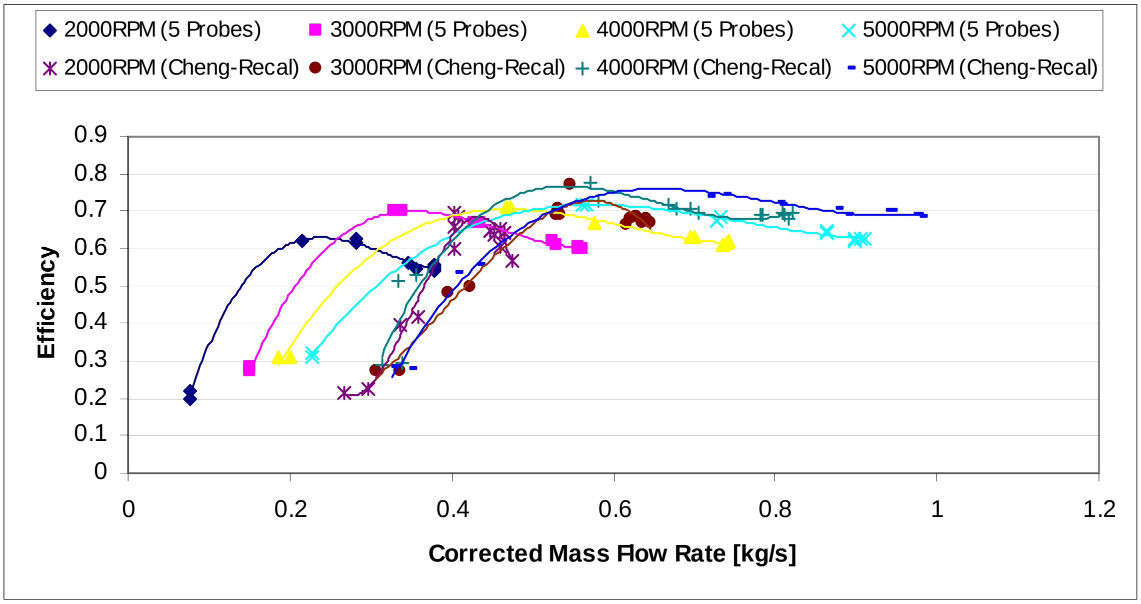

Figure 34. Comparison of efficiency versus mass flow rate for Test Plan II

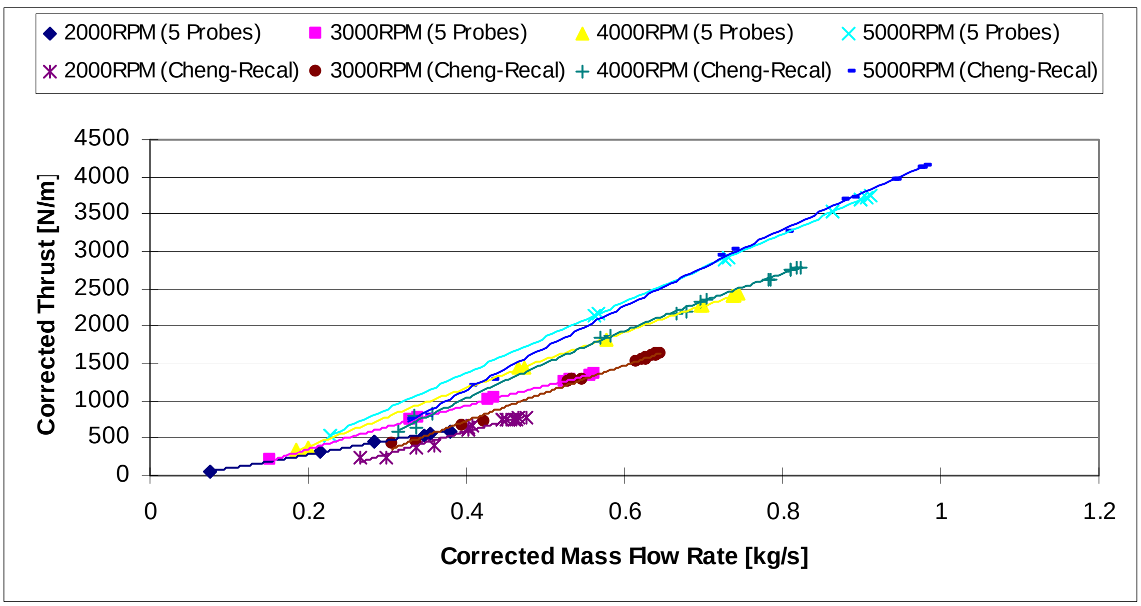

Figure 35. Comparison of thrust versus mass flow rate for Test Plan II

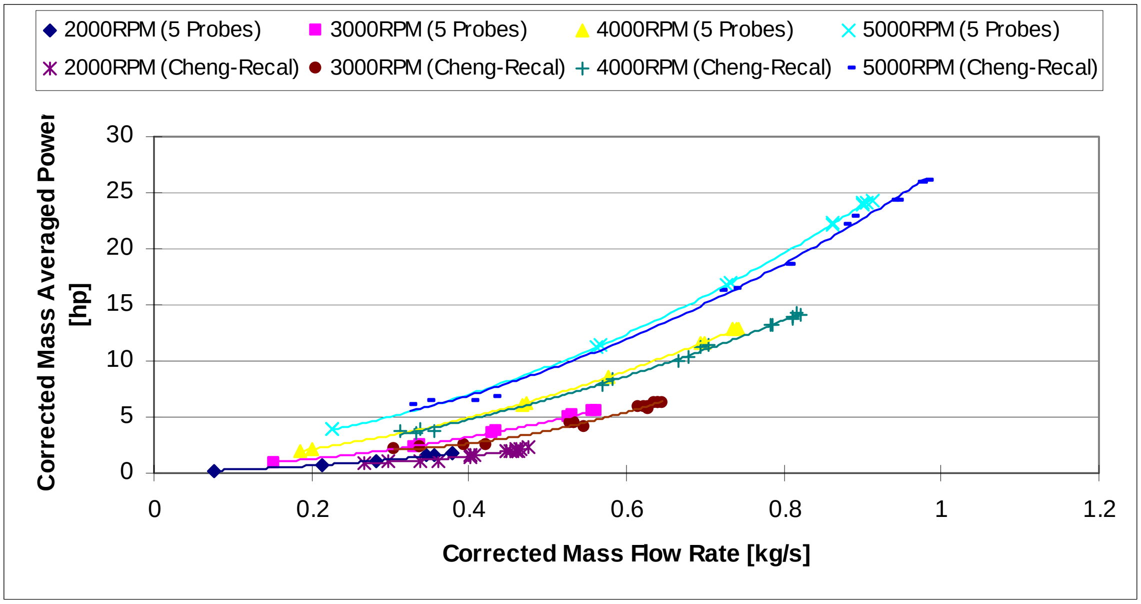

Figure 36. Comparison of power versus mass flow rate for Test Plan II

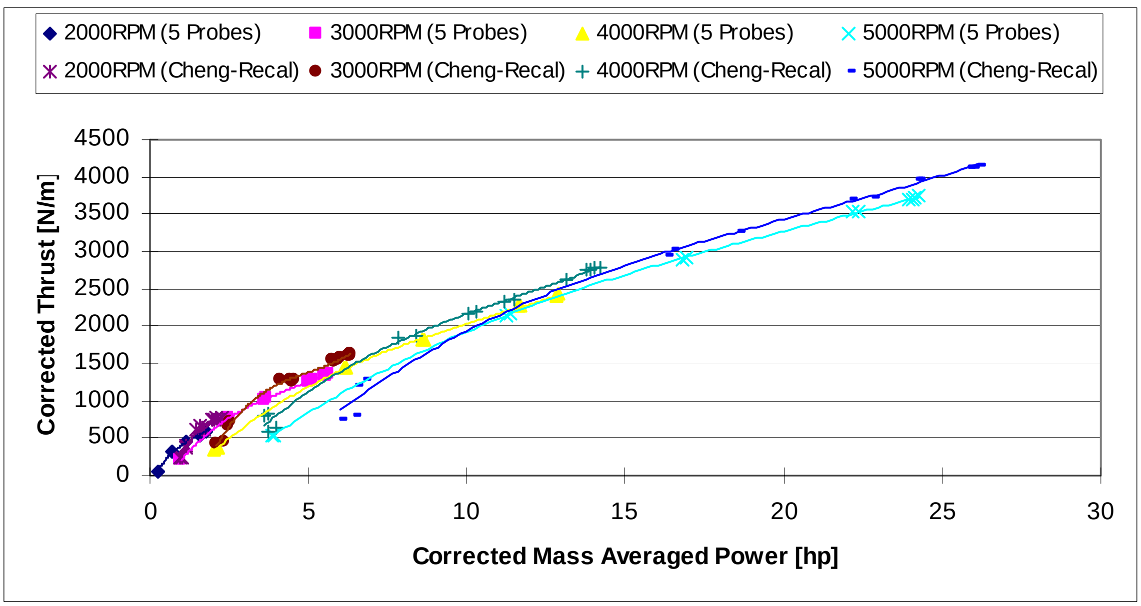

Figure 37. Comparison of thrust versus power for Test Plan II

Next, the combined performance of the baseline configuration (Test Plan I) and throttling test cases (Test Plan II) are shown together in Figures 38–40. As to be expected, the baseline characteristic intersected the constant speed characteristic curves. The exit diffuser extended the performance of the CFF by increasing its open-throttle mass flow rate and the throttle varied the performance up to a stall condition at the low mass flow rates. Peak efficiency occurred after closing the exhaust duct a certain amount at each speed. The peak efficiency was within 62% to 72%, and it increased with increasing speed over the range of speeds tested.

As discussed earlier, the mass flow rate measured in Cheng [Ref. 4] for Test Plan II was higher than that in the present experimental results. If the same combined performance were plotted, there would be no intersection between the two configurations, which supports the questioning of the previous data.

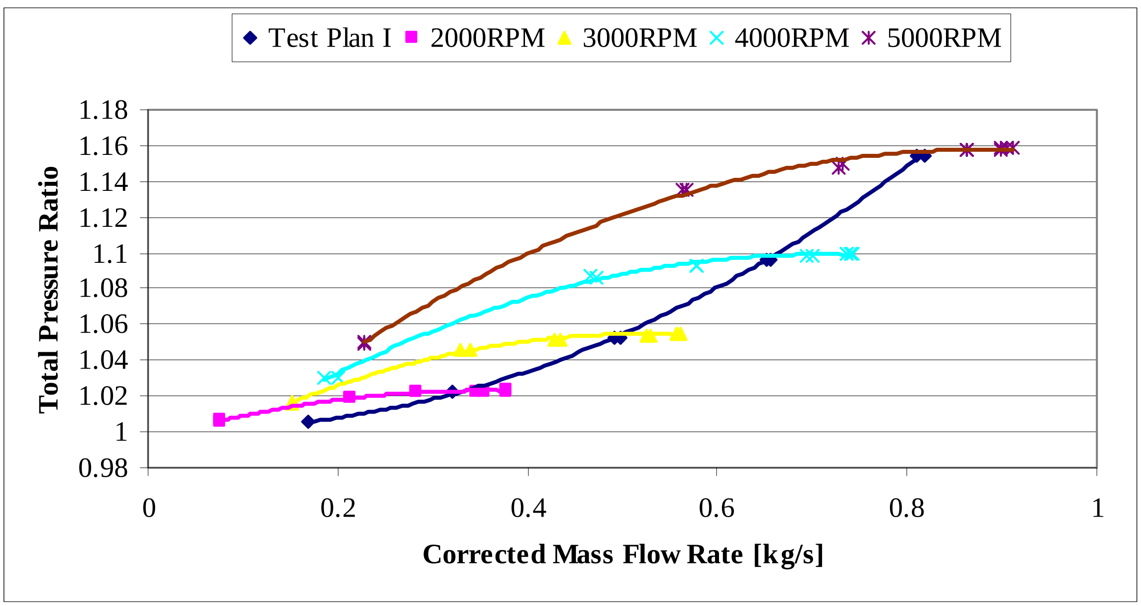

Figure 38. Combination plot of Test Plan I and Test Plan II for total pressure ratio versus mass flow rate

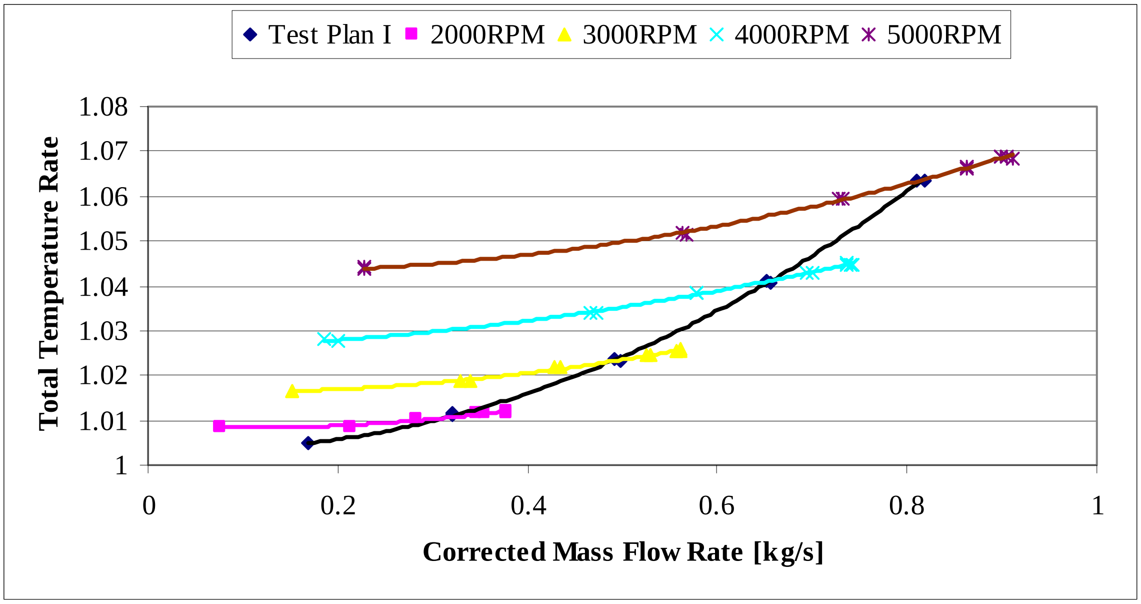

Figure 39. Combination plot of Test Plan I and Test Plan II for total temperature ratio versus mass flow rate

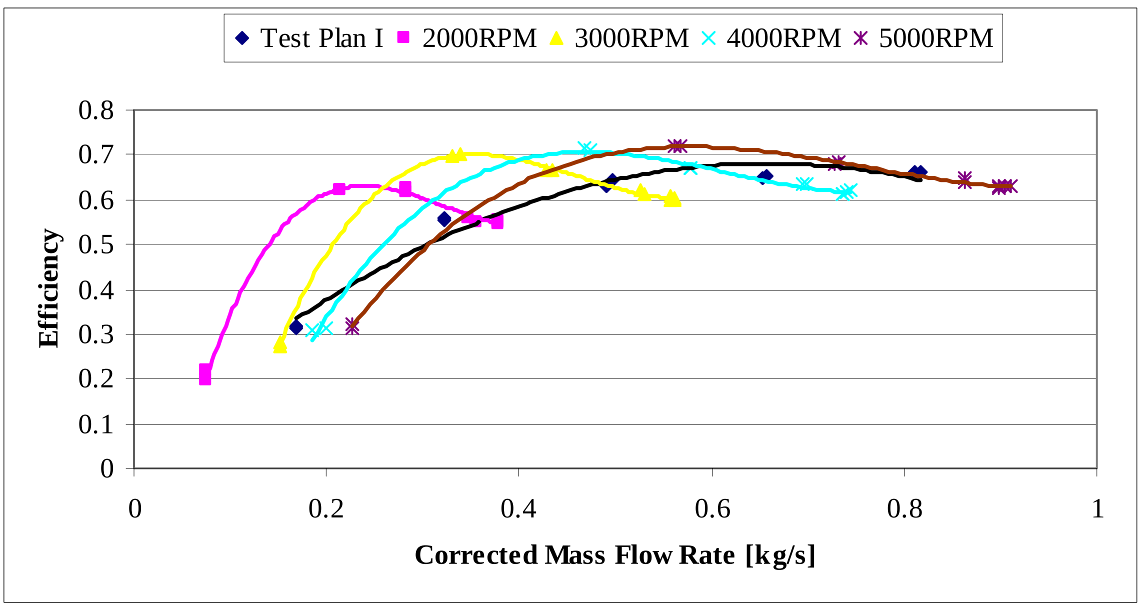

Figure 40. Combination plot of Test Plan I and Test Plan II for efficiency versus mass flow rate

Finally, the present experimental results (Test Plan II) were compared to the computed solutions (Simulation Plan II) as shown in Figures 41-43. The predicted characteristic curves were calculated in the same manner as the experiments except that the mass flow rate in the simulation was obtained directly from the inlet boundary. The numerical solutions for each specific rotational speed followed its corresponding experimental characteristic curve.

Figure 41 shows that the comparison of total pressure ratio versus mass flow rate. For the rotational speed of 2000RPM and 3000RPM, the performance was well predicted. At 5000RPM, it was observed that the difference at the open throttle position was the largest; however, the flow rate prediction was only 2.06% less than the experiment. Near stall the predictions were also very good, particularly since the calculations tended to become unstable. The data presented at the lowest mass flow rates at each speed was the last stable numerical point. Figure 42 shows the comparison of total temperature ratio versus mass flow rate. Although the predicted curves qualitatively followed the experimental curves, the total temperature ratio predicted was lower when stall occurred. The lack of agreement at low flow rates would indicate that the boundary layers within the flow-field were not adequately resolved. Figure 43 shows the efficiency predicted for different rotational speeds. At 5000 RPM the predicted peak efficiency of 72% was very close to that measured and the disagreement in efficiency was largest at open throttle and near stall. The predicted peak efficiency at 2000RPM was off by 15%; however the overall trend was reasonable. At open throttle, the differences between calculation and experiment were 6% and 20% for 2000RPM and 5000RPM respectively. The calculations also showed that the CFF could be run at larger diffuser angles; i.e. higher mass flow rates.

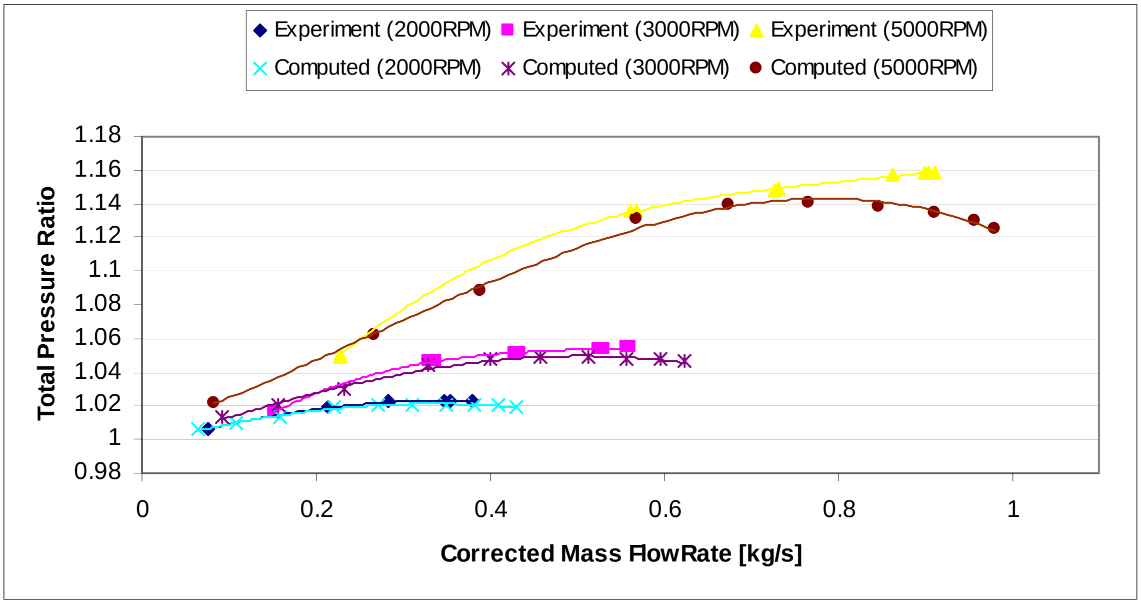

Figure 41. Comparison of experimental and computed results for total pressure ratio versus mass flow rate

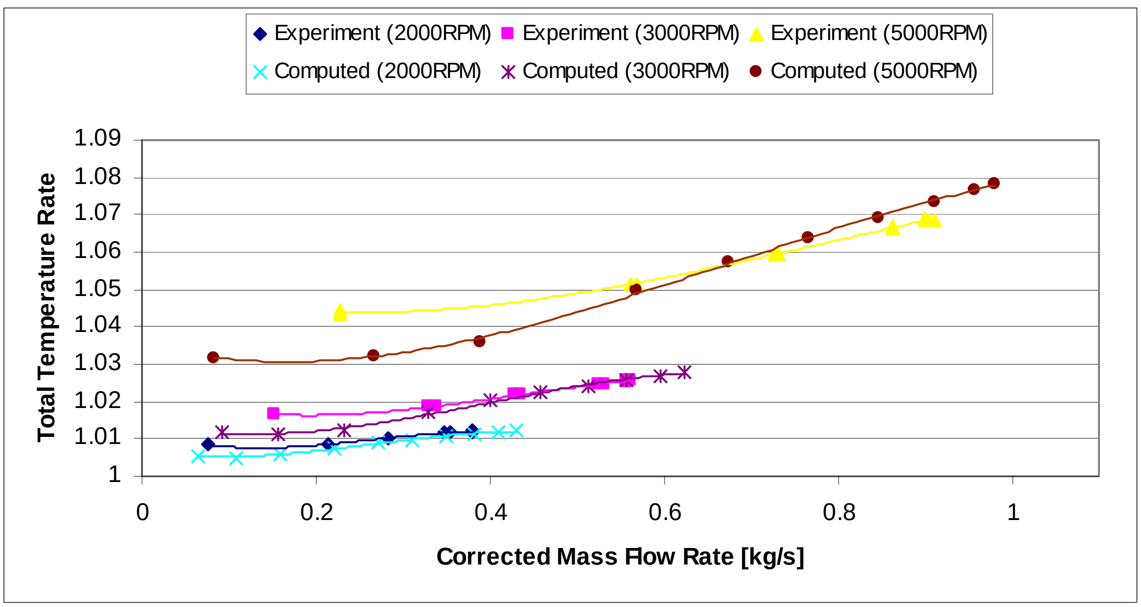

Figure 42. Comparison of experimental and computed results for total temperature ratio versus mass flow rate

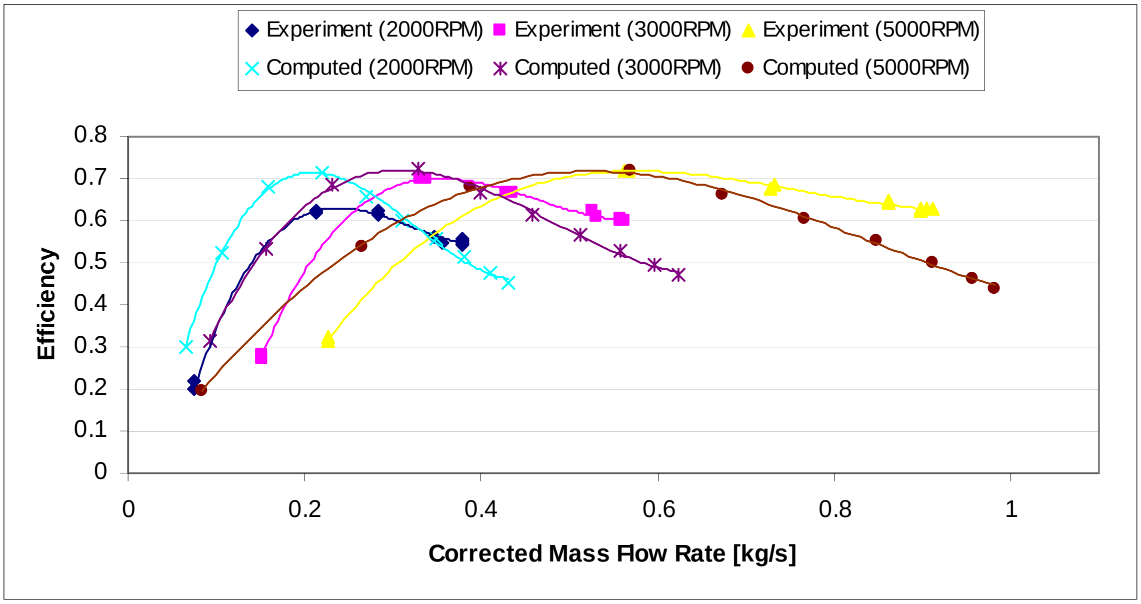

Figure 43. Comparison of experimental and computed results for efficiencies versus mass flow rate

V. SUMMARY AND CONCLUSIONS

The CFD study was initially carried out with the intension of predicting the performance data of Cheng [Ref. 4]. Results of the prediction of the throttling configurations raised the question of the accuracy in the previous experiments. An improved experiment was therefore undertaken as reporeted here. When compared with accurate experimental data, the overall off-design performance of the CFF was numerically well predicted. Specifically, the comparison of computed and experimental results was made by employing the same calculating procedure for both. The study also indicated that the standard day conditions would be a better boundary condition when setting up the model. Moreover, the consistency study supported the contention of some error in the deterimentation of mass flow rate in Cheng [Ref. 4]. The Mach number distribution in the flow field at 3000RPM at stall is shown in Figure 44. The flow entrained into the CFF moved closer to the HPC, while the vortex around the LPC became larger, pushing the flow to the left. The zone of lower velocity increased and the mass flow rate was hence reduced. A dramatic drop-off in efficiency occurred because of the attendant viscous mixing losses.

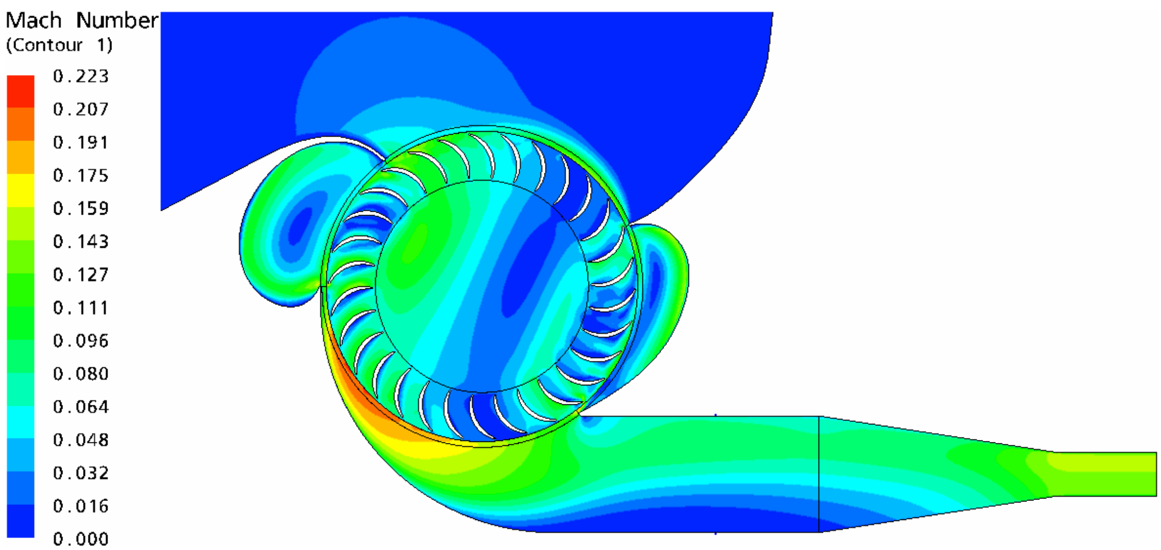

Figure 44. Distribution of Mach at 3000RPM with stall position setting

With the present successful modeling, more configurations of the 12-inch rotor can be computed and compared to the experimental results, particularly at higher rotational speeds and higher exit diffuser angles. Furthermore, a case study of the 6-inch rotor with various spanwise lengths should be computed using the procedures presented.

APPENDIX A. CFF_DAQ STRUCTURAL TREE

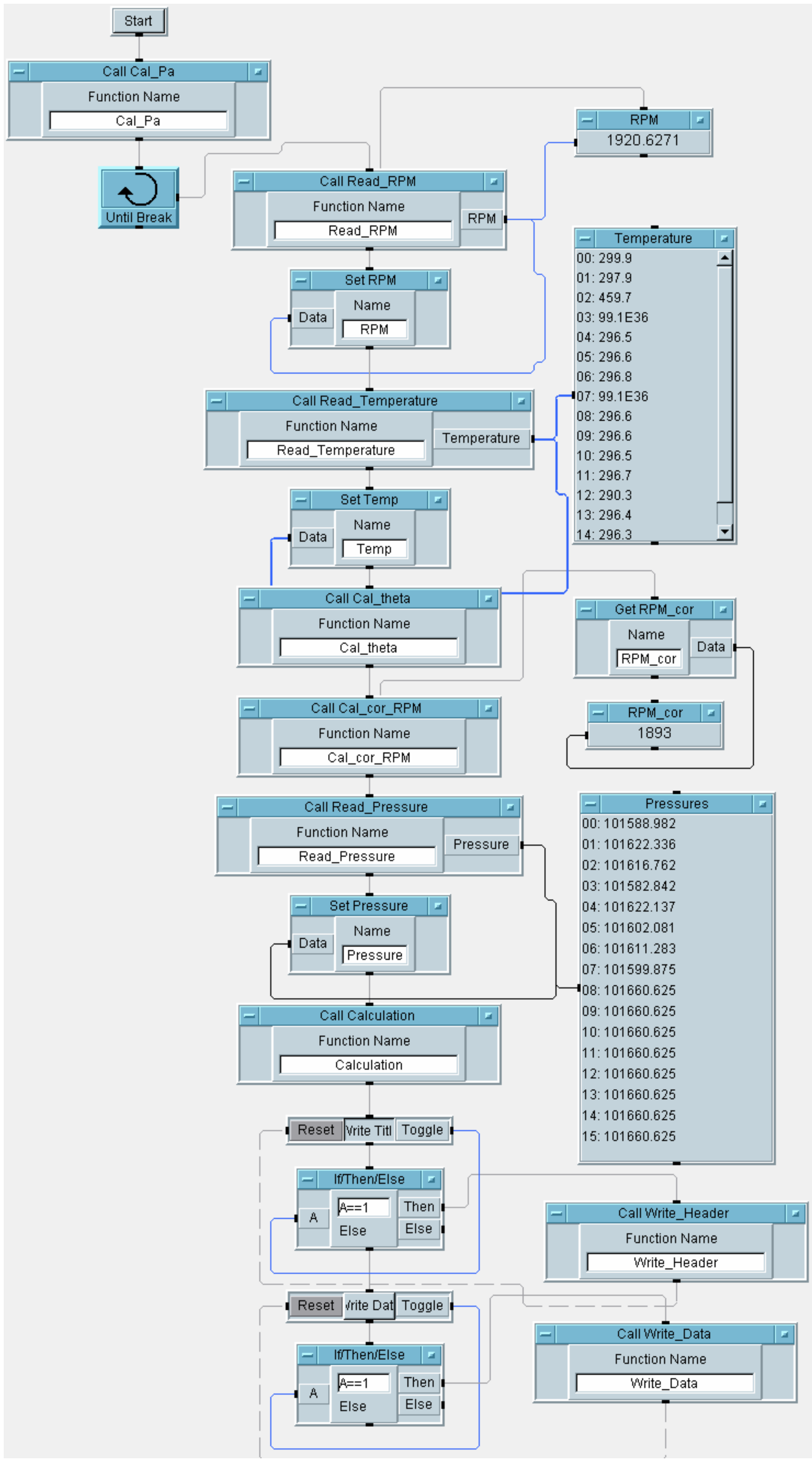

THIS PAGE INTENTIONALLY LEFT BLANK

APPENDIX B. MASS FLOW RATE MEASUREMENT OF THE CFF

Mass flow rate can be obtained using the continuity equation and introducing the equation of state; it is then

$$\dot{m} = \frac{P_1}{RT_1} A V_{in}$$

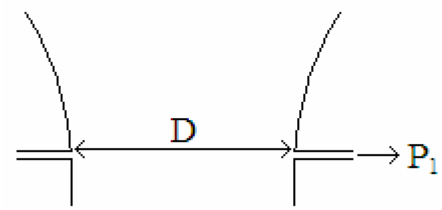

where P_1 is measured directly from static tapes at bell-mouth; A is the cross-sectional area of the bell-mouth, $A = \pi D^2 / 4$, $D = 6.25''$; R is gas constant. However, T_1 and V_{in} are unknown and have to be calculated from parameters which can be measured. The procedure for finding T_1 and V_{in} is as follows:

From steady flow energy equation for a perfect gas;

$$T_{t1} = T_1 + \frac{V_{in}{}^2}{2c_p}, \text{ where } c_p = \frac{\gamma R}{\gamma - 1}$$

then, T_1 is obtained as

$$T_1 = T_{t1} - \frac{(\gamma - 1)}{2\gamma R} V_{in}{}^2$$

From Bernoulli's equation (which assumes small density change), and the equation of state,

$$P_{t1} = P_{atm} = P_1 + \frac{1}{2}\rho V_{in}{}^2$$

$$P_{t1} = P_1 + \frac{1}{2}\frac{P_1}{RT_1}V^2 = P_1\left(1 + \frac{V_{in}{}^2}{2RT_1}\right)$$

By introducing T_1,

$$\frac{P_{t1}}{P_1} = PR = \left\{1 + \frac{V_{in}{}^2}{2R\left[T_{t1} - \left(\frac{\gamma - 1}{2\gamma R}\right)V_{in}{}^2\right]}\right\}$$

Rearrange equation

$$PR = \frac{2R\left[T_{t1} - \left(\frac{\gamma - 1}{2\gamma R}\right)V_{in}{}^{2}\right] + V_{in}{}^{2}}{2R\left[T_{t1} - \left(\frac{\gamma - 1}{2\gamma R}\right)V_{in}{}^{2}\right]}$$

$$PR\left\{2R\left[T_{t1} - \left(\frac{\gamma - 1}{2\gamma R}\right)V_{in}{}^{2}\right]\right\} = 2R\left[T_{t1} - \left(\frac{\gamma - 1}{2\gamma R}\right)V_{in}{}^{2}\right] + V_{in}{}^{2}$$

$$\left[\frac{1}{\gamma} + \left(\frac{\gamma - 1}{2}\right)PR\right]V_{in}{}^{2} = 2RT_{t1}(PR - 1)$$

Therefore, V_{in} is obtained as

$$V_{in} = \sqrt{\frac{2RT_{t1}(PR - 1)}{\frac{1}{\gamma} + \left(\frac{\gamma - 1}{2}\right)PR}}$$

APPENDIX C. UNCERTAINTY STUDY

In APPENDIX B, the description of derivation of mass flow was made, and it can be expressed in the form of

$$\dot{m} = \frac{P_1}{RT_1(T_{t1}, P_{t1}, P_1)} AV_{in}(T_{t1}, P_{t1}, P_1) \quad \text{(C.01)}$$

T_{t1} , P_{t1} , P and A are independent variables and measured from instruments, whose corresponding uncertainties are provided in Table C.01

Variable	Accuracy, w
T_{t1}	$\pm 1°C$ ($w_{T_{t1}}$)
P_{t1}	$\pm 0.001 bar$ ($w_{P_{t1}}$)
P_1	$\pm 0.05\%$ (w_{P_1})
A	$\pm 0.0001\pi\ in^2$ (w_A)

Table C.01 Uncertainty in each measurement

Let w_r be the uncertainty in the mass flow rate, and then it is given as

$$w_r = \left[\left(\frac{\partial \dot{m}}{\partial T_{t1}} w_{T_{t1}} \right)^2 + \left(\frac{\partial \dot{m}}{\partial P_{t1}} w_{P_{t1}} \right)^2 + \left(\frac{\partial \dot{m}}{\partial P_1} w_{P_1} \right)^2 + \left(\frac{\partial \dot{m}}{\partial A} w_A \right)^2 \right]^{1/2} \quad \text{(C.02)}$$

where each w presents the uncertainty in each measurement, and their corresponding derivatives were found as

$$\frac{\partial \dot{m}}{\partial T_{t1}} = \frac{P_1 A}{RT_1} \frac{\partial V_{in}}{\partial T_{t1}} - \frac{P_1 A V_{in}}{R} \frac{1}{T_1^2} \frac{\partial T_1}{\partial T_{t1}} \quad \text{(C.03)}$$

$$\frac{\partial \dot{m}}{\partial P_{t1}} = \frac{P_1 A}{RT_1} \frac{\partial V_{in}}{\partial P_{t1}} - \frac{P_1 A V_{in}}{R} \frac{1}{T_1^2} \frac{\partial T_1}{\partial P_{t1}} \quad \text{(C.04)}$$

$$\frac{\partial \dot{m}}{\partial P_1} = \frac{AV_{in}}{RT_1} + \frac{P_1 A}{RT_1} \frac{\partial V_{in}}{\partial P_1} - \frac{P_1 A V_{in}}{R} \frac{1}{T_1^2} \frac{\partial T_1}{\partial P_1} \quad \text{(C.05)}$$

$$\frac{\partial \dot{m}}{\partial A} = \frac{P_1 V_{in}}{RT_1} \quad \text{(C.06)}$$

Now, there are six more derivatives to be determined,

$$\frac{\partial V_{in}}{\partial T_{t1}},\ \frac{\partial V_{in}}{\partial P_{t1}},\ \frac{\partial V_{in}}{\partial P_{1}},\ \frac{\partial T_{1}}{\partial T_{t1}},\ \frac{\partial T_{1}}{\partial P_{t1}},\ \frac{\partial T_{1}}{\partial P_{1}}$$

These six derivatives were derived as follows:

$$\frac{\partial V_{in}}{\partial T_{t1}}=\frac{\partial}{\partial T_{t1}}\left[\frac{2RT_{t1}\left(\frac{P_{t1}}{P_1}-1\right)}{\frac{1}{\gamma}+\left(\frac{\gamma-1}{2}\right)\frac{P_{t1}}{P_1}}\right]^{1/2}=\frac{1}{2}\left[\frac{2RT_{t1}\left(\frac{P_{t1}}{P_1}-1\right)}{\frac{1}{\gamma}+\left(\frac{\gamma-1}{2}\right)\frac{P_{t1}}{P_1}}\right]^{-1/2}\left[\frac{2R\left(\frac{P_{t1}}{P_1}-1\right)}{\frac{1}{\gamma}+\left(\frac{\gamma-1}{2}\right)\frac{P_{t1}}{P_1}}\right]\quad \text{(C.07)}$$

$$\begin{aligned}\frac{\partial V_{in}}{\partial P_{t1}}&=\frac{\partial}{\partial P_{t1}}\left[\frac{2RT_{t1}\left(\frac{P_{t1}}{P_1}-1\right)}{\frac{1}{\gamma}+\left(\frac{\gamma-1}{2}\right)\frac{P_{t1}}{P_1}}\right]^{1/2}\\&=\frac{1}{2}\left[\frac{2RT_{t1}\left(\frac{P_{t1}}{P_1}-1\right)}{\frac{1}{\gamma}+\left(\frac{\gamma-1}{2}\right)\frac{P_{t1}}{P_1}}\right]^{-1/2}\left\{\frac{2RT_{t1}\frac{1}{P_1}}{\frac{1}{\gamma}+\left(\frac{\gamma-1}{2}\right)\frac{P_{t1}}{P_1}}-\frac{2RT_{t1}\left(\frac{P_{t1}}{P_1}-1\right)\left(\frac{\gamma-1}{2}\right)\frac{1}{P_1}}{\left[\frac{1}{\gamma}+\left(\frac{\gamma-1}{2}\right)\frac{P_{t1}}{P_1}\right]^2}\right\}\end{aligned}\quad \text{(C.08)}$$

$$\begin{aligned}\frac{\partial V_{in}}{\partial P_{1}}&=\frac{\partial}{\partial P_{1}}\left[\frac{2RT_{t1}\left(\frac{P_{t1}}{P_1}-1\right)}{\frac{1}{\gamma}+\left(\frac{\gamma-1}{2}\right)\frac{P_{t1}}{P_1}}\right]^{1/2}\\&=\frac{1}{2}\left[\frac{2RT_{t1}\left(\frac{P_{t1}}{P_1}-1\right)}{\frac{1}{\gamma}+\left(\frac{\gamma-1}{2}\right)\frac{P_{t1}}{P_1}}\right]^{-1/2}\left\{\frac{2RT_{t1}\left(\frac{P_{t1}}{P_1}-1\right)\left(\frac{\gamma-1}{2}\right)\frac{P_{t1}}{P_1^2}}{\left[\frac{1}{\gamma}+\left(\frac{\gamma-1}{2}\right)\frac{P_{t1}}{P_1}\right]^2}-\frac{2RT_{t1}\frac{P_{t1}}{P_1^2}}{\frac{1}{\gamma}+\left(\frac{\gamma-1}{2}\right)\frac{P_{t1}}{P_1}}\right\}\end{aligned}\quad \text{(C.09)}$$

$$\frac{\partial T_1}{\partial T_{t1}}=\frac{\partial}{\partial T_{t1}}\left(T_{t1}-\frac{\gamma-1}{2\gamma R}V_{in}{}^2\right)=1-\left(\frac{\gamma-1}{2\gamma R}\right)(2V_{in})\left(\frac{\partial V_{in}}{\partial T_{t1}}\right)\quad \text{(C.10)}$$

$$\frac{\partial T_1}{\partial P_{t1}}=\frac{\partial}{\partial P_{t1}}\left(T_{t1}-\frac{\gamma-1}{2\gamma R}V_{in}{}^2\right)=-\left(\frac{\gamma-1}{2\gamma R}\right)(2V_{in})\left(\frac{\partial V_{in}}{\partial P_{t1}}\right)\quad \text{(C.11)}$$

$$\frac{\partial T_1}{\partial P_{1}}=\frac{\partial}{\partial P_{1}}\left(T_{t1}-\frac{\gamma-1}{2\gamma R}V_{in}{}^2\right)=-\left(\frac{\gamma-1}{2\gamma R}\right)(2V_{in})\left(\frac{\partial V_{in}}{\partial P_{1}}\right)\quad \text{(C.12)}$$

Substituting Eq. (C.07), (C.08) and (C.09) into Eq. (C.10), (C.11) and (C.12), respectively, then all derivatives were expressed in terms of independent variables.

Once all derivatives required were found, substitute them back to Eq. (C.02), then the uncertainty in the mass flow rate was determined.

THIS PAGE INTENTIONALLY LEFT BLANK

APPENDIX D. GEOMETRY GENERATION IN ICEM-CFD

1. Starting a New Project

a) Launch ANSYS ICEMCFD-CFX

Select **File > New Project** from the Main menu and click on  (Create New Directory) and enter Directory name as in Figure D01.

Figure D01: New Project Window

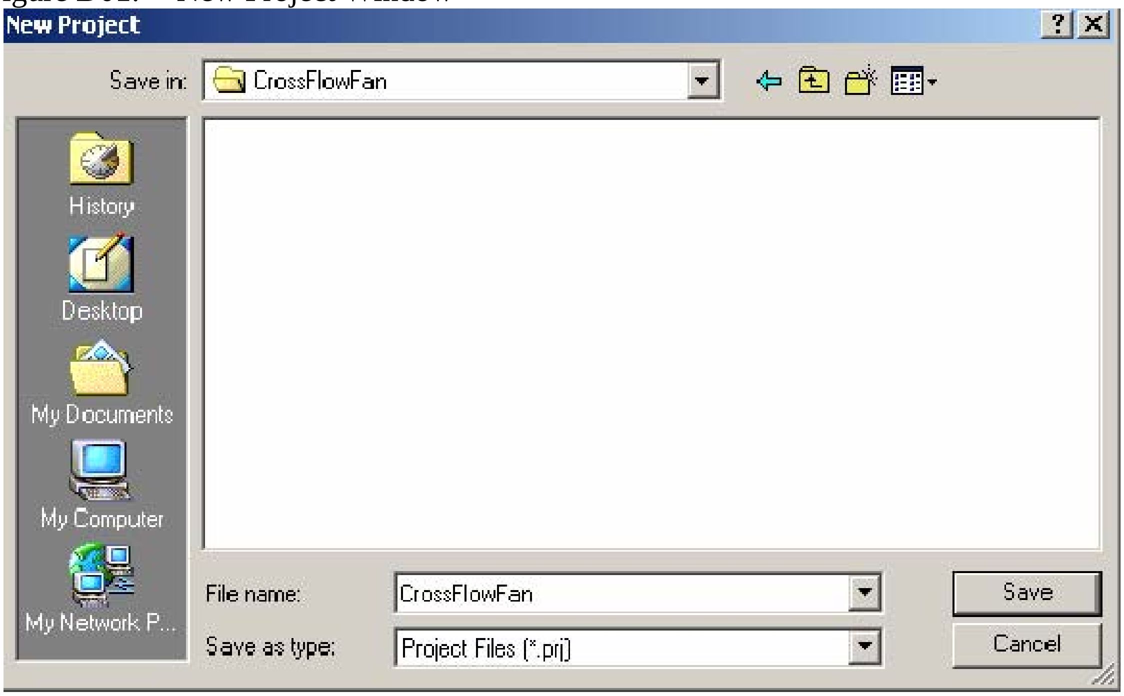

2. 2-D Model Generation

2.1. Blade generation

a) Point Creation

Geometry > Create Point > Explicit Coordinates: Select the  (Explicit coordinate) to open the *Explicit Location* window as shown in Figure D02.

As shown in Figure D02, Select **Create 1 point**, and assign coordinates (0 0 0). Input the **Part** name POINTS, and the **Name** as POINTS.00 and press **Apply** to create a point. This is a reference point *when* **Import Geometry** is required.

Figure D02: Point creation window

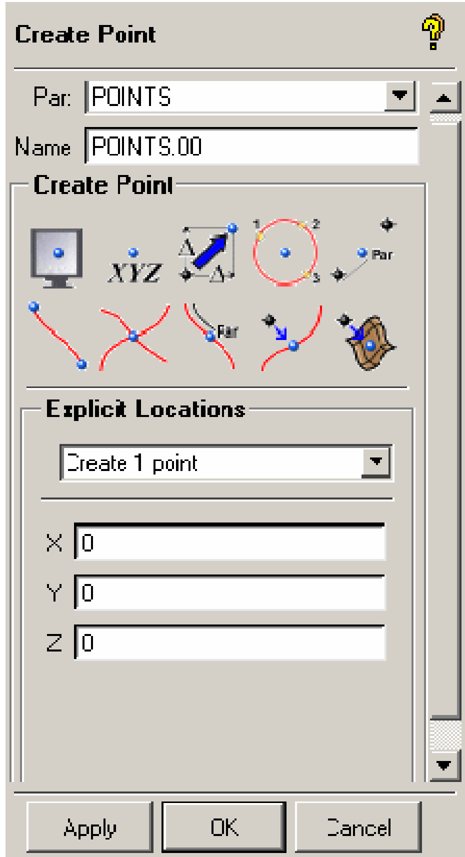

Figure D03: Select point-data window

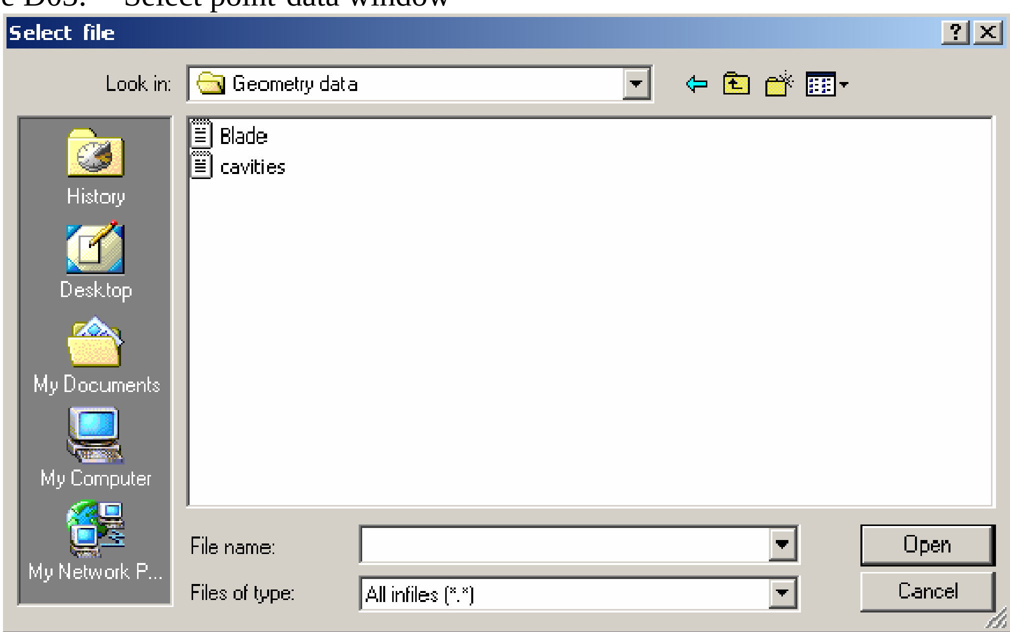

Select **File** > **Import Geometry** > **Formatted point data** from the Main menu and choose **Blade.txt** as shown in Figure D03. Press **Open**, the window shown as Figure D04 appears. Uncheck **Import Curves**, **Import Surfaces** and **Plot3D Format,** Then Set **Approximation Tolerance** to **0**. Keep the name of **Point Part** as default. To accept the points by click **Apply**, then it is read and shown in Figure D05.

Figure D04: Import formatted point data window

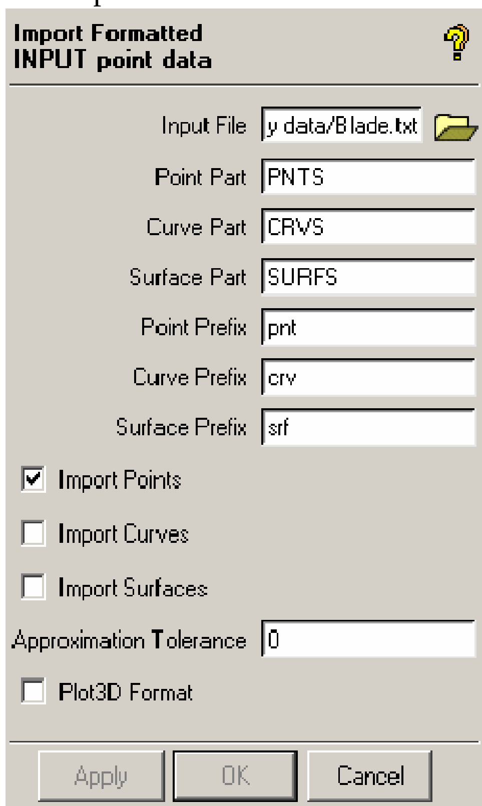

Figure D05: Points after importing

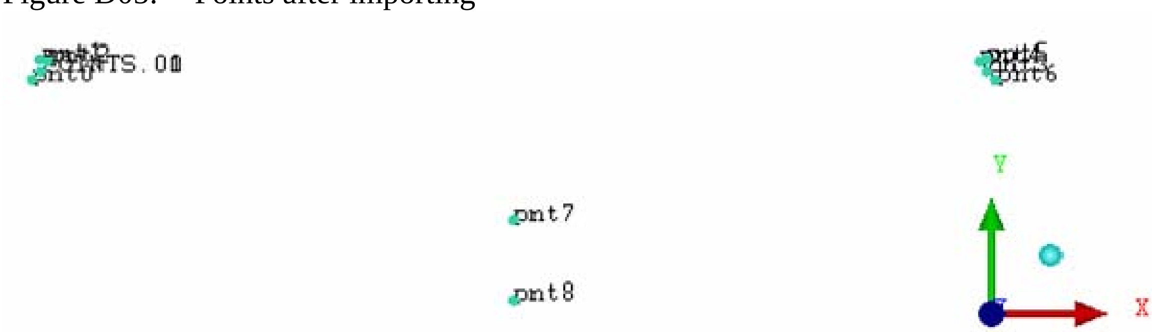

TIP1: Switch ON the **Points** in the left side *model Tree window*. To see the names of the points, use the **right mouse** and select **button Points > show Points Names** in the *model Tree window*. To turn Off Points **Names**, click button **Points > show Points Names** in the *model Tree window* again.

b) Line Creation

Geometry > Create/Modify Curve > Arc from 3 Points: Select the 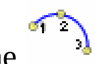 (Are from 3 Points) to open the *From Points* window as shown in Figure D06.

Figure D06: Are from 3 points window

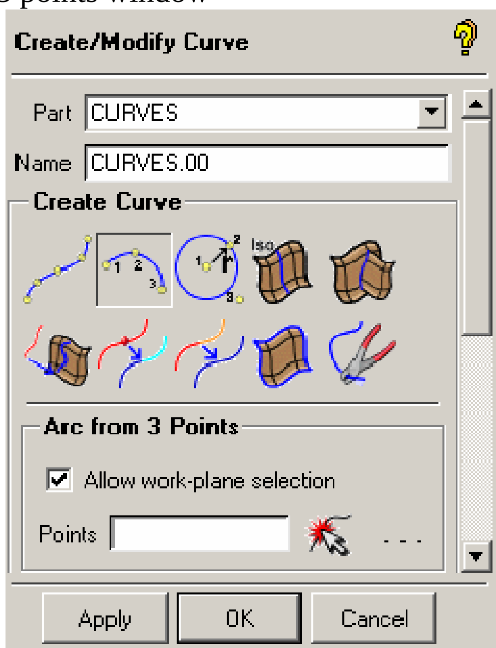

Unclick on **Allow work-plane selection**. To select Points, click on  (Entity chooser icon) and then select **pnt0**, **pnt1** and **pnt2** with the left-mouse button. Press the middle mouse button to accept the points. The points name will appear in the select window. Enter the **Part** to **BLADES**, and **Name** to **BLADES.00**. Press **Apply** to create a curve.

Similarly make other lines by just selecting the points below, the curves name will then change by default.

BLADES.01: pnt4, pnt5 and pnt6

BLADES.02: pnt0, pnt8 and pnt6

BLADES.03: pnt2, pnt7 and pnt4

TIP2: At any time during the selection process, pressing F9 will allow the user to zoom, rotate or pan to get a better view. Toggle F9 again will return the user to selection mode.

TIP3: To see the names of curves, use the right mouse and select **button Curves > show Curves Names** in the *model Tree window*. It is shown in Figure A07.

Figure D07: Geometry after blade curves generated

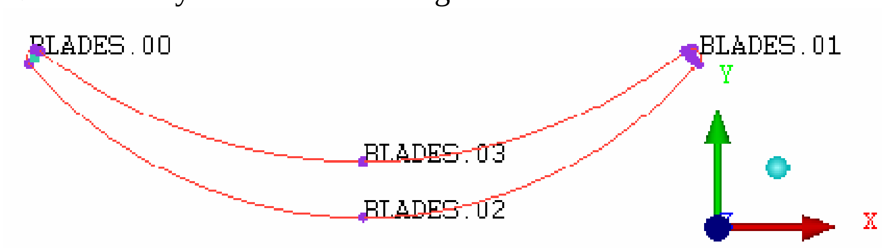

Geometry > Transform Geometry > Translate Geometry: Select the 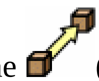 (Translate Geometry) to open the *Select* window as shown in Figure D08.

Figure D08: Translation method window

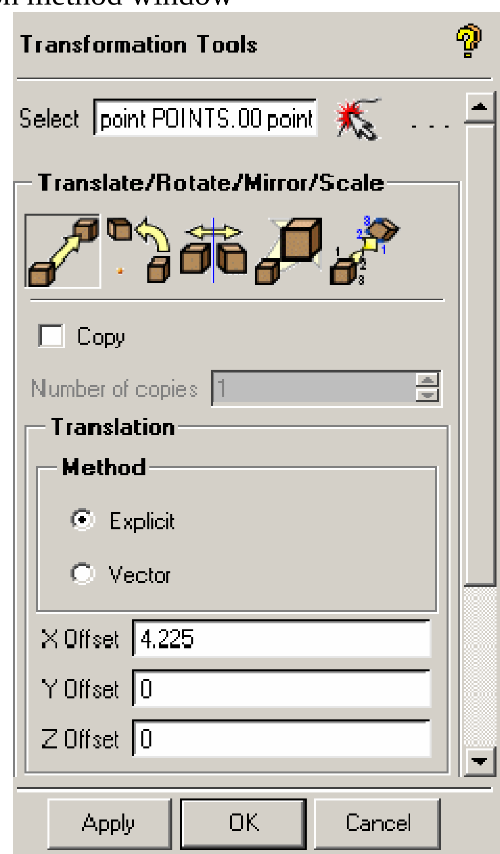

Switch ON **Points** and **Curves** in the left side *model Tree window*.

To select **Translating objects**, click on  (Entity chooser icon) and there is a **Select Geometry** bar popping up. Switch off  (Toggle selection of surfaces or shells) and  (Toggle selection of bodies or volume element) at the right side of this bar as shown in Figure D09. Then select  (all appropriate visible objects). Click off **Copy** and set **X Offset** to **4.225**, **Y and Z Offset** to **0**. Press **Apply** to translate points and curves.

Figure D09: Selection geometry tool bar window

Geometry > **Transform Geometry** > **Rotate Geometry**: Select the  (Rotate Geometry) to open the *Select* window as shown in Figure D10.

Figure D10: Rotation select window

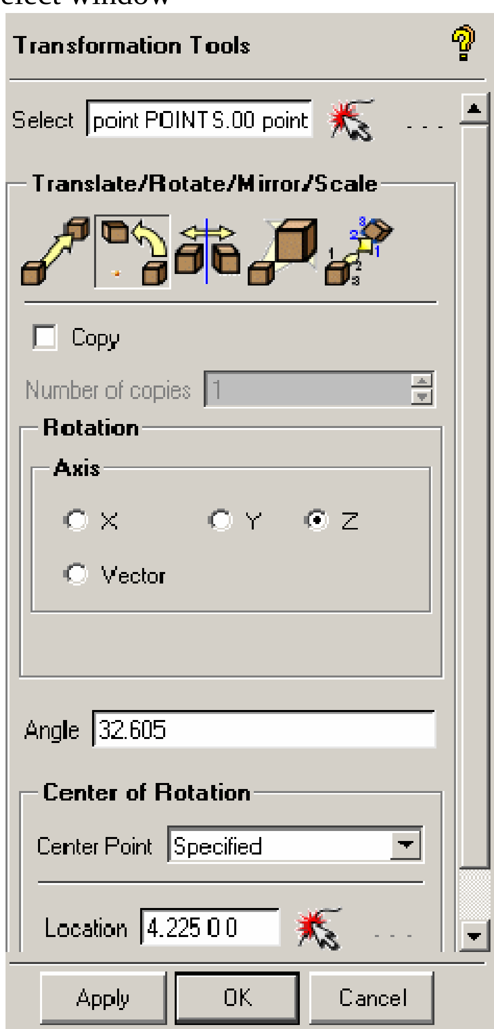

To select **Rotating objects**, click on and Click on from **Select Geometry** after switching off and . Under **Rotation**, set on **Axis** to **Z**, and set **Angle** to **32.605**. Under **Center of Rotation**, set **Center** Point to **Specified** and **Location** to (4.225 0 0). Press **Apply** to rotate points and curves.

c) Blade Surface Creation

Geometry > Create/Modify Surface > From Curves: Select the (From Curves) to open the *Select Curves* window as shown in Figure D11.

Figure D11: Select curves window

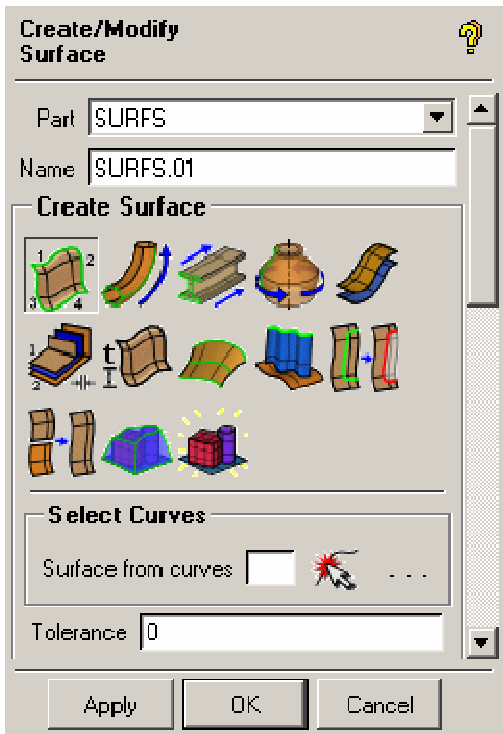

To select Curves, click on and select BLADES.00, BLADES.01, BLADES.02 and BLADES.03 with the left mouse button. Press the middle mouse button to accept the curves. The curves name will appear in the select window. Set **Tolerance** to 0, and enter the **Part** as **BLADES**, and **Name** as **BLADES.00**. Press **Apply** to create the surface.

TIP4: To regroup **Parts**, double-click **Parts** in the left side *model Tree window* with the left-mouse button, the **Create Part** window appear as shown in Figure A12. Switch OFF **Curves** and **Surfaces** in the left side *model Tree window*. Set **Parts** to **POINTS** and click on from **Select Geometry**. The imported points are joining into **POINTS** by pressing **Apply**.

TIP5: To delete **empty Parts**, click **Parts > Delete Empty Parts** in the *model Tree window*.

Geometry > Transform Geometry > Rotate Geometry: Switch ON **Curves** and **Surfaces** in the left side model Tree window. Switch OFF **Points**. To select rotating objects, click on and select from **Select Geometry** after switching , and on, then Check **Copy** and Set **Number of copies** to **29**. Under **Rotation**, set **Axis** to **Z**. Set **Angle** to **12** and **Center of Point** to **Origin**. Press **Apply** to copy curves and surfaces. The result is shown in Figure D13.

Figure D12: Create part window

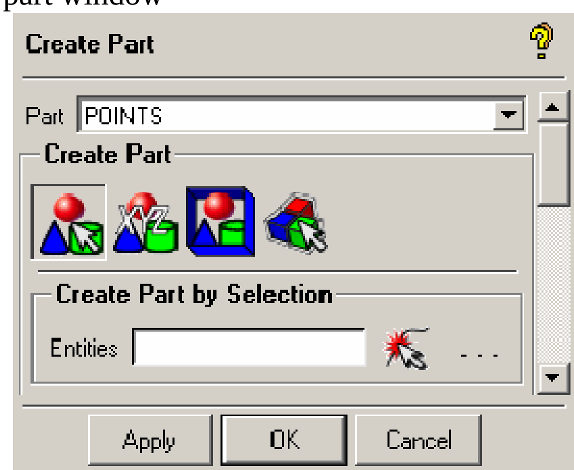

Figure D13: Geometry after blade surface generated

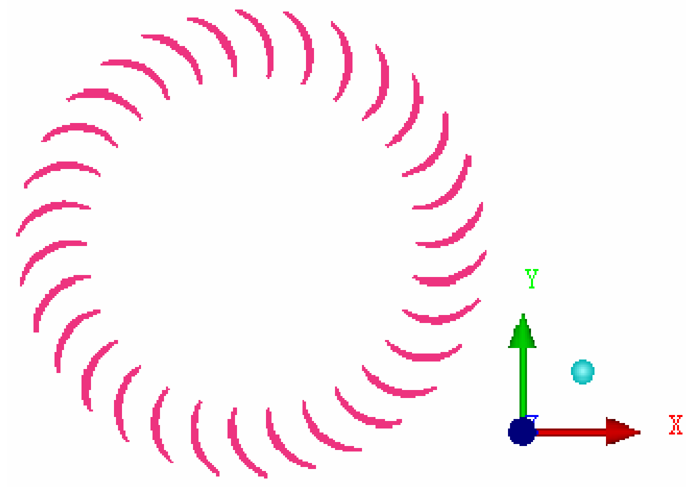

Figure D14: Center and 2 points window

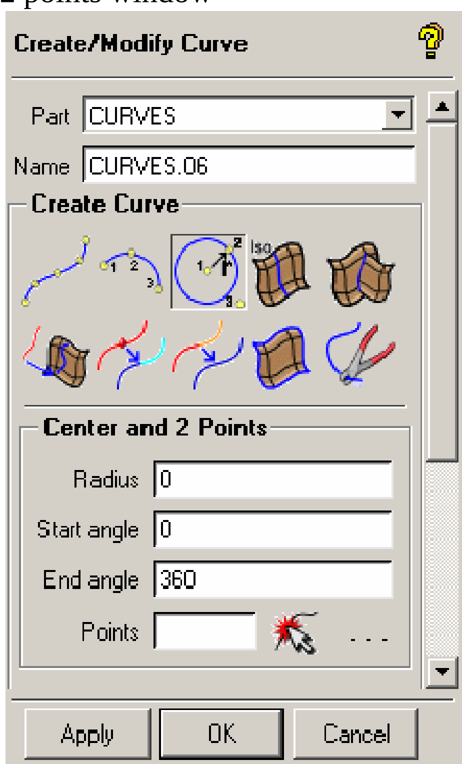

d) Surface around blade Creation

Geometry > Create/Modify Curves > Circle or arc from Center point and 2 points on plane: Select the 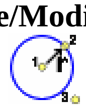 (Circle or arc from Center point and 2 points on plane) to open *Center and 2 points* window as shown in Figure D14.

To select Center Point, click on  and select point with coordinate **(0 0 0)** with the left mouse button. Press the middle mouse button to accept the point. If there is no such point, then create one. The point name will appear in the select window. Enter the **Part** to **INNERCIRCLE**, and set **Name** to **INNERCIRCLE.00**. Set **Radius** to **4.1**, and Press **Apply** to create the circle. Similarly make other circle with **Radius equal to 6**. Enter the **Part** to **OUTERCIRCLE**, and set **Name** to **OUTERCIRCLE.00**.The result is shown in Figure D15.

Figure D15: Geometry after two circles created

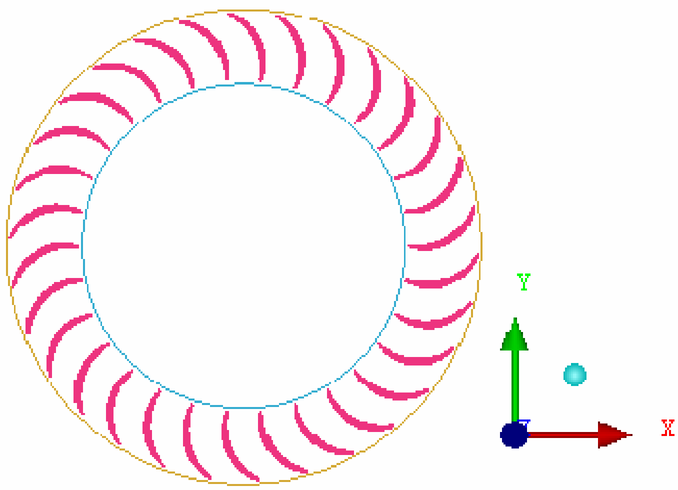

Geometry > **Create Points** > **Parameter along a curve**: Select the 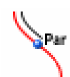 (Parameter along a Curve) to open *Parameter along a Curve* window as shown in Figure D16.

To select Curve, click on  and select BLADES.00 with the left mouse button. Press the middle mouse button to accept the curve. Enter the **Part** as **POINTS**, and set **Name** by default. Set **Curve parameters** to **0.5**. Press **Apply** to create the point. Similarly make center points for other three edges of a blade.

Repeat the same steps to create center points for other blades. The final result is shown in Figure D17.

Figure D16: Parameter along a curve window

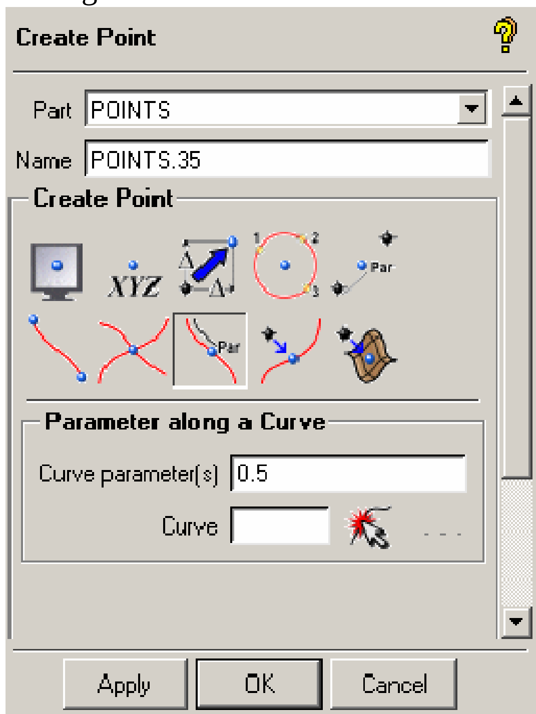

Figure D17: Geometry after center point at each edge of blades created

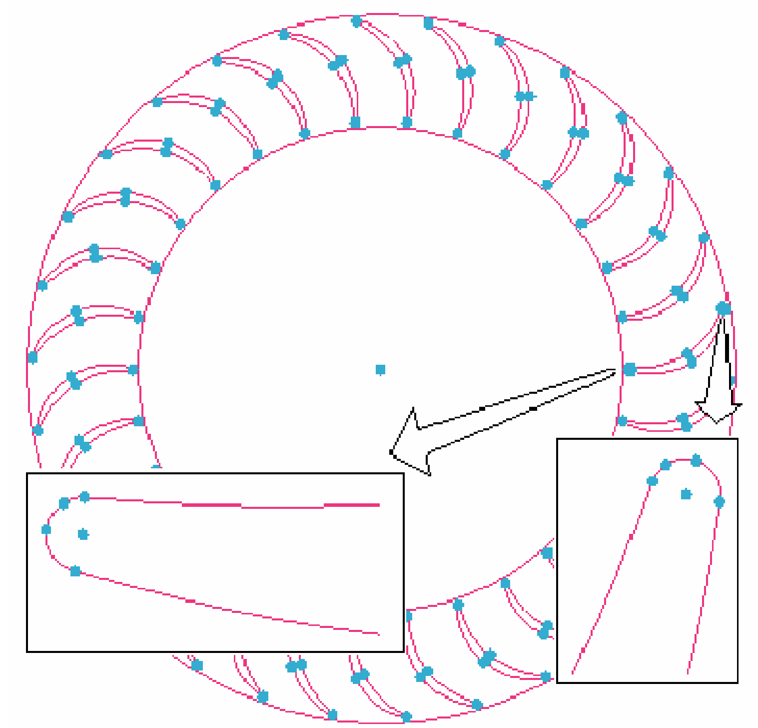

Geometry > Create Points > Project point to curve: Select the (Project point to Curve) to open *Project Point to Curve* window as shown in Figure D18.

Figure D18: Project point to curve

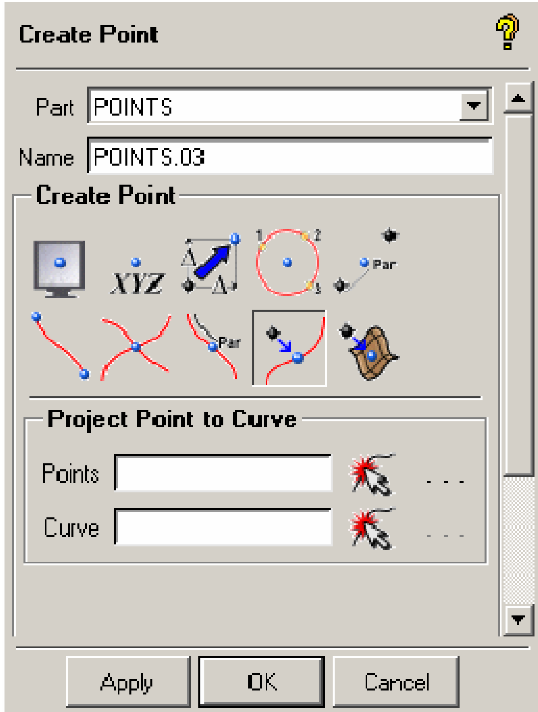

Project points created at leading edge and trailing edge previously to INNERCIRCLE and OUTERCIRCLE respectively. Enter the **Part** to **POINTS**, and set **Name** by default.

Geometry > **Create/Modify Curve** > **Segment curve**: Select the 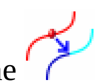 (Segment Curve) to open *Segment Curve* window as shown in Figure D19.

To Segment INNERCIRCLE by selecting four points with almost even distance. Enter the **Part** as **INNERCIRCLE**, and set **Name** by default.

Geometry > **Create/Modify Surface** > **From Curves**: To make inner circle surface by selecting four segmented curves with **tolerance** equal to **0.000001**. Enter the **Part** as **SYM1**, and set **Name** by default.

Geometry > **Create/Modify Curve** > **Segment curve**: Continue to split INNERCIRCLE and OUTERCIRCLE by other points on them respectively. Enter the **Part** to **INNERCIRCLE** for INNERCIRCLE and **OUTERCIRCLE** for OUTERCIRCLE. Set **Name** by default for both cases.

In the same manner, split curves BLADES.00 and BLADES.01 with the points at the center respectively. Repeat the same steps for other blades. Enter the **Part** as **BLADES**, and set **Name** by default.

Geometry > Create/Modify Curve > From Points: Select the 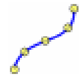 (From Points) to open *From Points* window as shown in Figure D20.

To create curves between blades and circles by joining two points and set **Tolerance** to **0**, enter the **Part** to **CURVES**, and set **Name** by default. The result is shown in Figure D21.

Geometry > Create Points > Parameter along a curve: Select each segment curve on INNERCIRCLE and OUTERCIRCLE. Enter the **Part** as **POINTS**, and set **Name** by default. Set **Curve parameters** to **0.5**. Press **Apply** to create the points.

Geometry > Create/Modify Curve > Segment curve: Segment circles again by the points just created.

Geometry > Create Point > Parameter Along a Vector: Select the  (Parameter along a Vector) to open *Parameter along a Vector* window as shown in Figure D22.

To select 2 points, click on  and select points at the center of the pressure edge and suction edge with the left mouse button. Press the middle mouse button to accept the point. Set **Parameter(s)** to **0.5**, Enter the **Part** as **POINTS**, and set **Name** by default. Press **Apply** to create points.

Geometry > Create/Modify Curve > Arc from 3 Points: Create Curves between blades as shown in Figure D23, Enter the **Part** as **CURVES**, and **Name** by default.

Geometry > Create/Modify Surface > From Curves: To select Curves, click on  and select curves shown in Figure D24 with the left mouse button. Press the middle mouse button to accept the curves. Enter the **Part** as **SYM1**, and **Name** by default, Set **Tolerance** to **0.001**. Press **Apply** to create the surface.

Follow the same steps and Repeat **59** times to create other surfaces around blades, be sure that curves can enclose an area.

Figure D19: Segment curve windowmove this to the next page – check all the way through

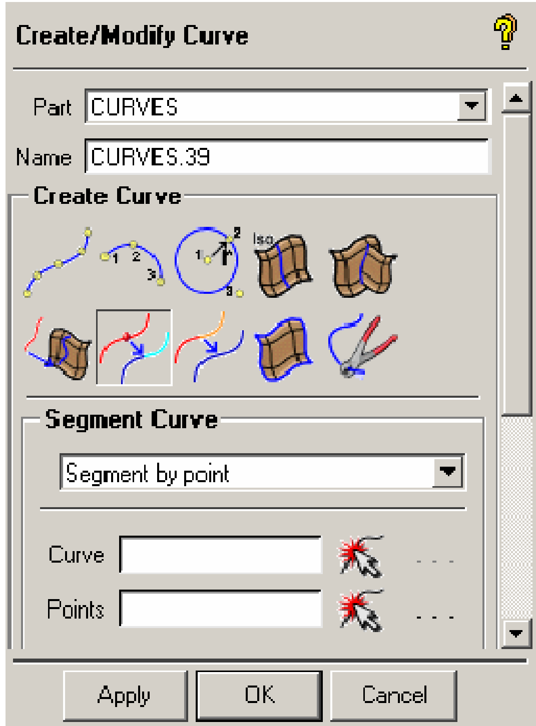

Figure D20: Form points window

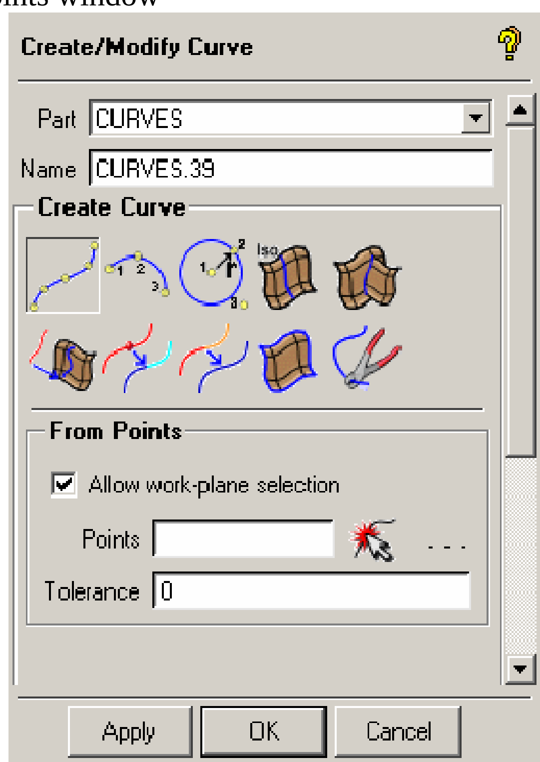

Figure D21: Geometry after assistant curves created

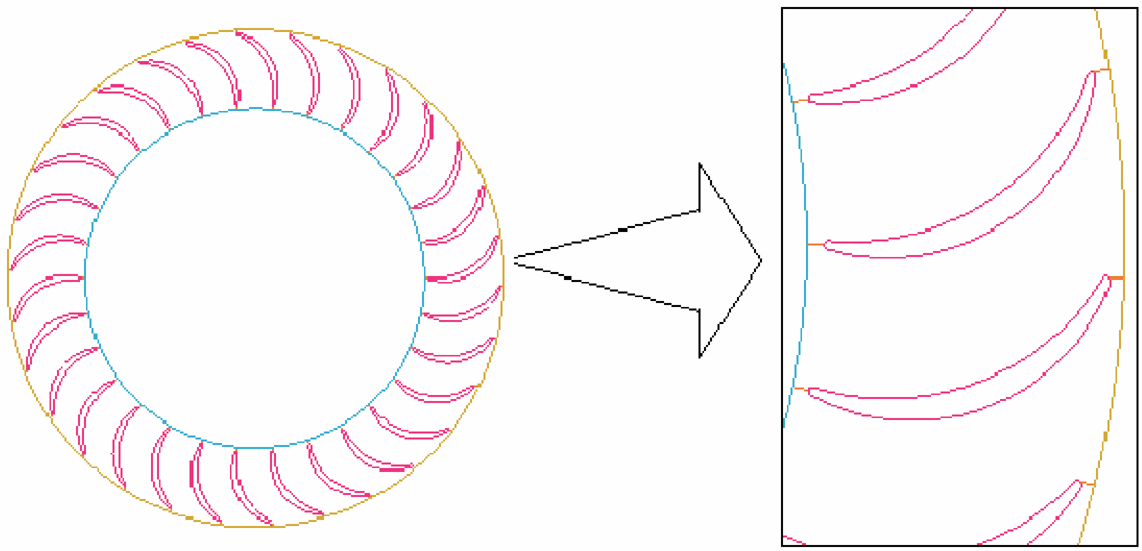

Figure D22: Parameter along a vector window

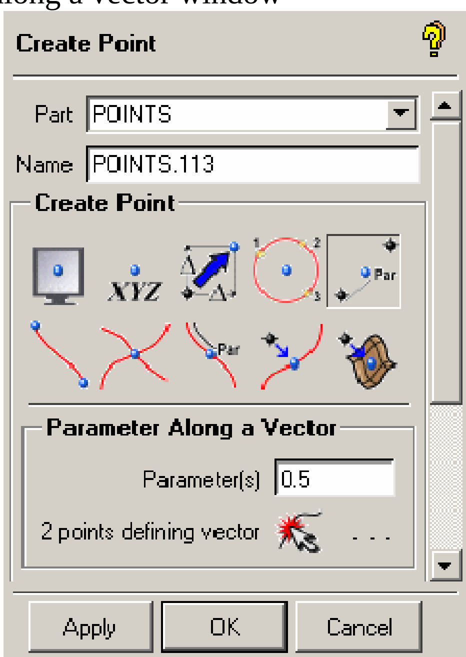

Figure D23: Geometry after assistant curves created

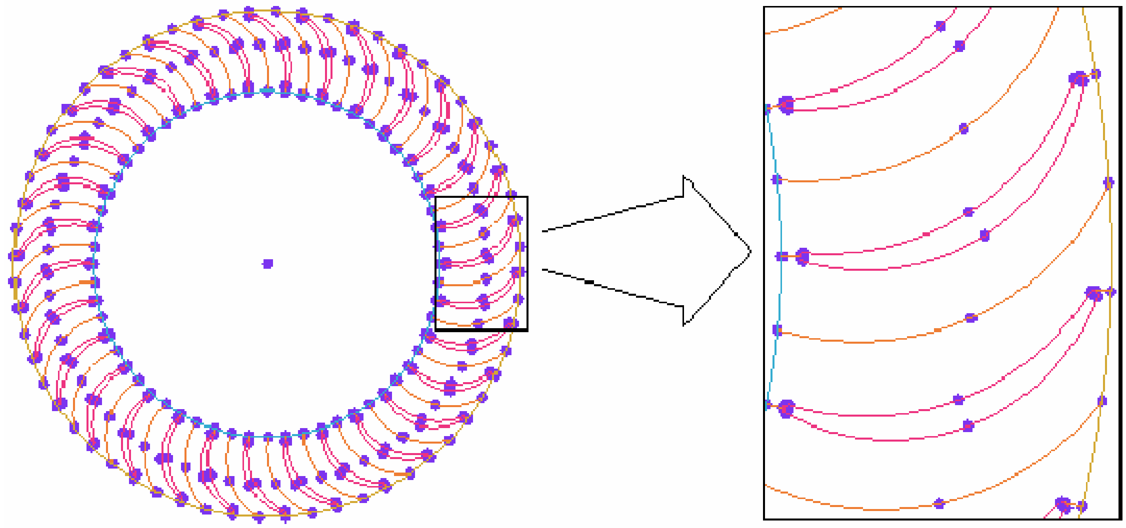

Figure D24: The selection of surface creation around the blade

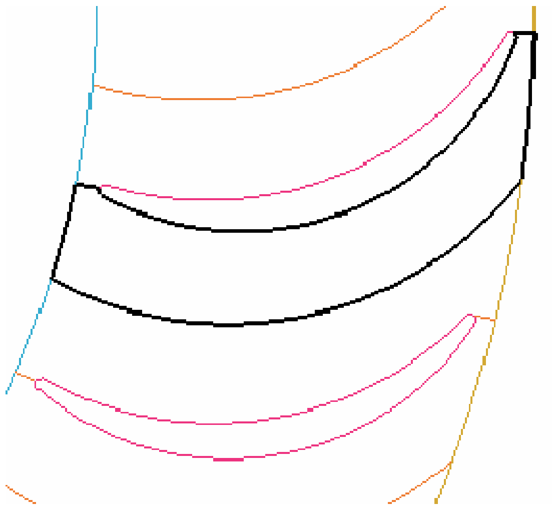

2.2. Cavities, Inlet, Outlet Section Generation

a) Points Creation

Select **File > Import Geometry > Formatted point data** from the Main menu and choose **Cavities.txt** as shown in Figure D03. Uncheck **Import Curves**, **Import Surfaces** and **Plot3D Format**, then Set **Approximation Tolerance** to **0**. To accept the points by click **Apply**, then it is read and shown in Figure D25.

Figure D25: Geometry after cavities points imported

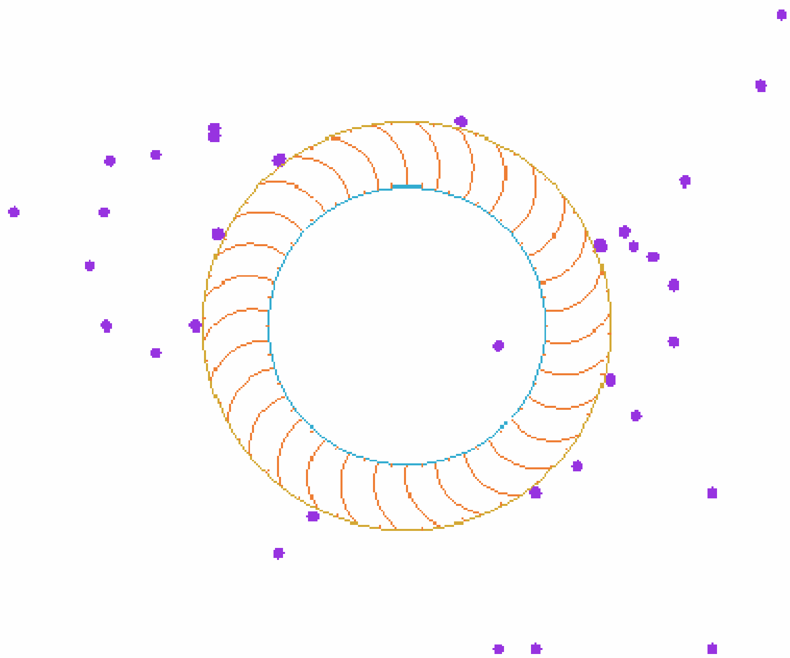

b) Line Creation

Geometry > Create/Modify Curve > From Points: To select Points, click on  and then select **pnt9, pnt10, pnt11, pnt12, pnt13, pnt14, pnt15 and pnt16** with the left mouse button. Press the middle mouse button to accept the points. The points name will appear in the select window. Set **Tolerance** to **0**, Enter the **Part** to **WALL**, and **Name** to **WALL.00**. Press **Apply** to create the curve for high pressure cavity.

Similarly make other curves by selecting the following points, Leave the **Part** as **WALL** and **Name** by default.

WALL.01: pnt28, pnt29, pnt30, pnt31, pnt32, pnt33, pnt34 and pnt35 (Low Pressure Cavity)

WALL.02: pnt18, pnt19, pnt20 and pnt21 (Inlet Section)

WALL.03: pnt37, pnt38, pnt39, pnt40 and pnt41 (Inlet Section)

WALL.04: pnt25, pnt26 and pnt.27 (Set **Tolerance** to **0.00001**, others are 0) (Outlet Section)

WALL.05: pnt43 and pnt44 (Outlet Section)

OUTLET.00: pnt27 and pnt44 (Set **Part** as **OUTLET** and **Name** as **OUTLET.00**) (Outlet Section)

Geometry > Create/Modify Curve > Arc from 3 Points: Click on  and then select **pnt16**, **pnt17** and **pnt18** with the left mouse button. Press the middle mouse button to accept the points. The points name will appear in the select window. Enter the **Part** as WALL and **Name** as WALL.06. Press **Apply** to create the curve.

Similarly make other lines by selecting the group of points shown below separately:

WALL.07:	pnt9, pnt22 and pnt23
WALL.08:	pnt23, pnt24 and pnt25
WALL.09:	pnt28, pnt42 and pnt43
WALL.10:	pnt35, pnt36 and pnt37
INT0.00:	pnt23, pnt49 and pnt43 (Set **Part** as **INT0** and **Name** as **INT0.00**)
INT1.00:	pnt28, pnt47 and pnt35 (Set **Part** as **INT1** and **Name** as **INT1.00**)
INT2.00:	pnt37, pnt48 and pnt18 (Set **Part** as **INT2** and **Name** as **INT2.00**)
INT3.00:	pnt22, pnt46 and pnt16 (Set **Part** as **INT3** and **Name** as **INT3.00**)

Figure D26: Geometry after wall, outlet and interface created

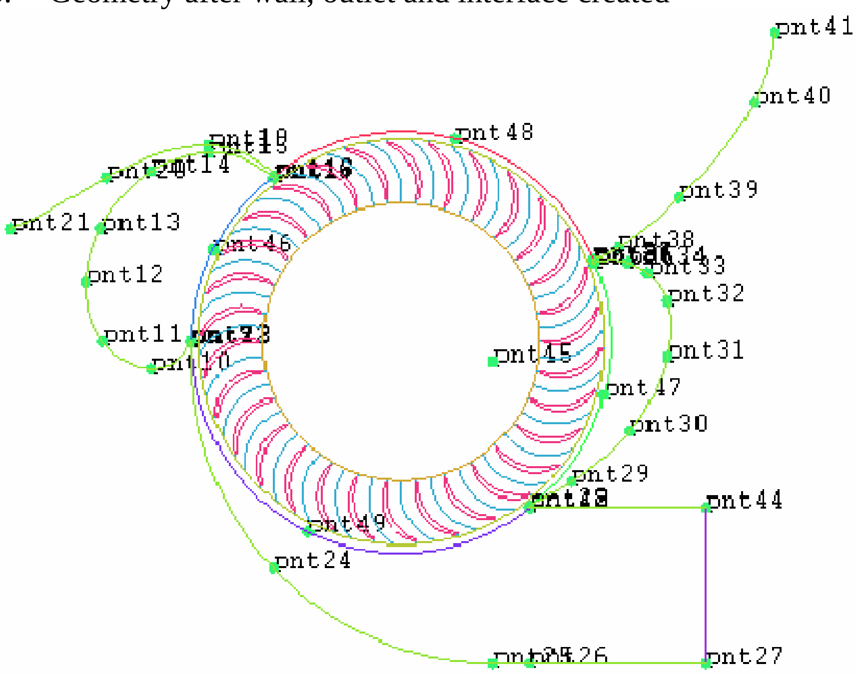

Since Inlet section is not complete, it is needed to continue the curve generation:

Geometry > Create/Modify Curve > Segment curve: Split curve WALL.02 by point pnt20.

Geometry > **Delete Any Entity**: Select the  (Delete Any Entity) from the main toolbar. Delete the curve between points: pnt20 and pnt21.

Geometry > **Create/Modify Curve** > **Modify Curves**: Select the  (Modify Curves) to open *Modify Curves* window as shown in Figure D27.

To select Curve, click on  and then select previous segment curve with the left mouse button. Press the middle mouse button to accept the curve. In the same manner, set **Location** to pnt21. Enter the **Part** as **WALL**, and **Name** by default. Press **Apply** to create the curve.

Continue to extend the curve, under **End point selection,** click Length and the window is shown in Figure D28, Set **Length** to **25**. Under **Extend as**, Click on **Line**. Enter the **Part** as **WALL**, and **Name** by default. Press **Apply** to extend the curve.

Similarly extend a curve WALL.03 by setting **Length** to **25**, and extend as a **Line**. The final curves are shown is Figure D29.

Figure D27: Modify curves by selecting end point window

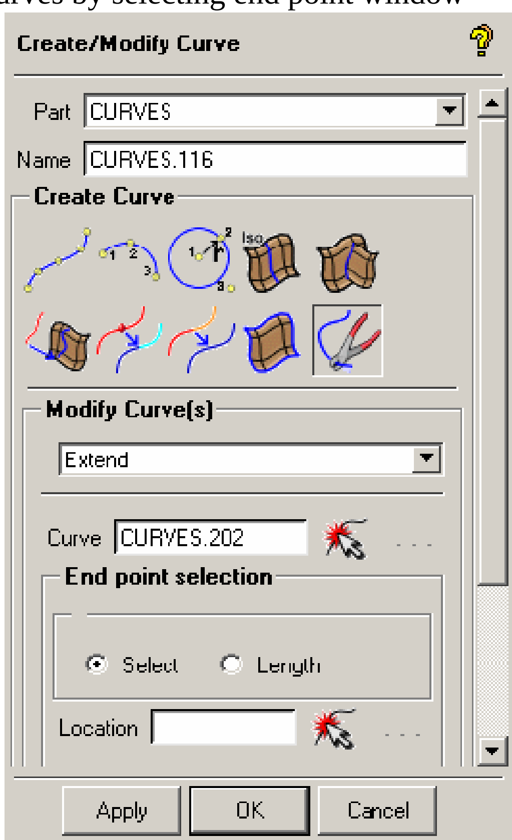

Figure D28: Modify curves by extending length window

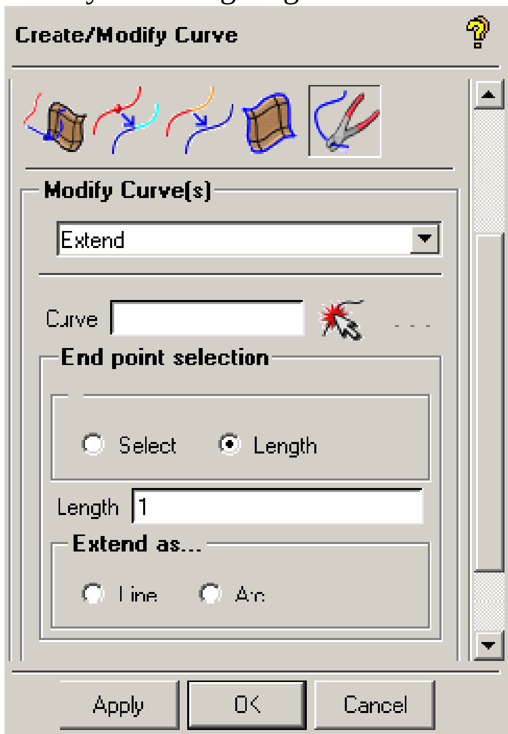

Figure D29: Geometry after curves extended at inlet section

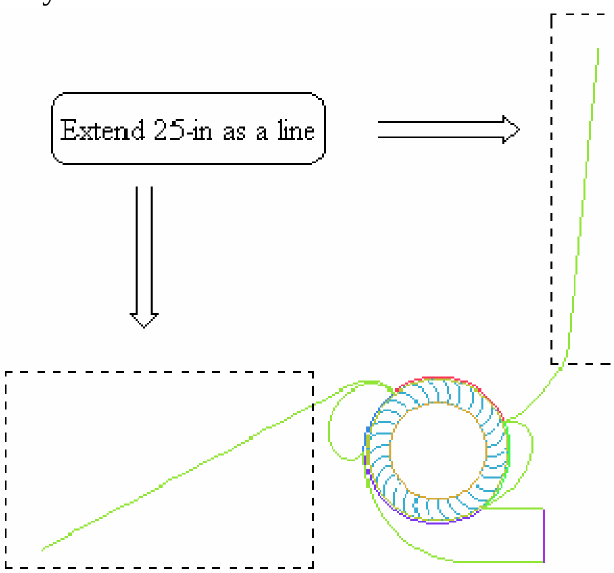

Geometry > Create/Modify Curves > Circle or arc from Center point and 2 points on plane: To create a circle with radius **25** along center point (0 0 0). Enter the **Part** as **INLET**, and set **Name** to **INLET.00**. Press **Apply** to create a circle.

Geometry > Create Point > Curve-Curve Intersection: Select the 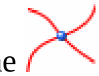 (Curve- Curve Intersection) to open the *Curve-Curve Intersection* window as shown in Figure D30.

Figure D30: Curve-Curve intersection window

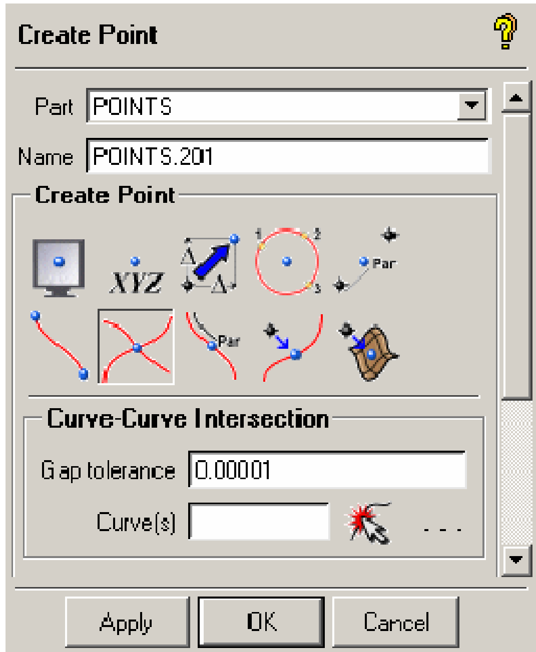

To select Curve, click on  and then select **INLET.00** and **extended Curves** with the left mouse button. Press the middle mouse button to accept the curve. Set **Gap tolerance** to 0.000001, Enter the **Part** as **POINTS**, and **Name** by default. Press **Apply** to create point as shown in Figure D31.

Figure D31: Geometry after circle with radius 25 inch and intersection points created

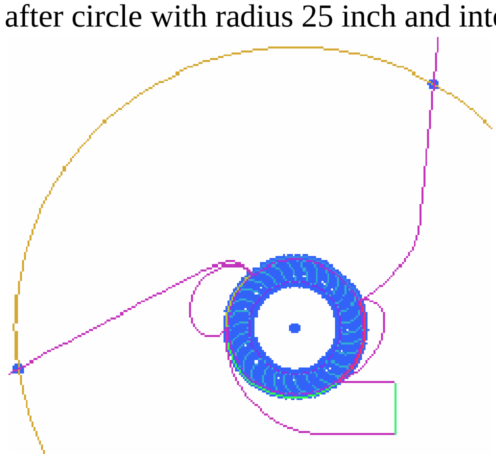

Geometry > Create/Modify Curve > Segment curve: Spilt Curve INLET.00 and extended curves WALL.03 and WALL.04 with two intersection points.

Geometry > Delete Any Entity: Select the  from the main toolbar. Delete the curves and the final geometry is shown in Figure D32.

Figure D32: Geometry after inlet section created

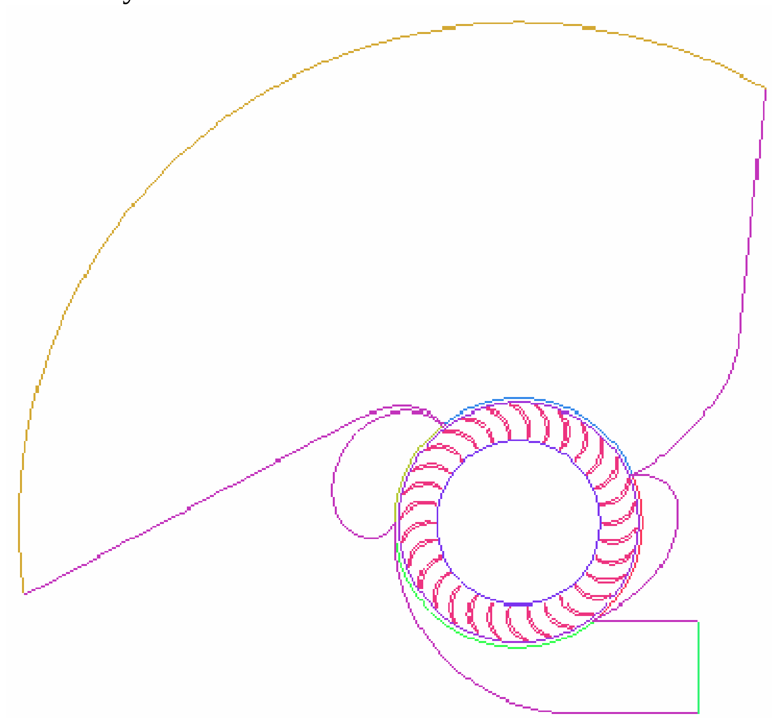

> **TIP6**: To see the better color distribution, use the **right mouse** and select **button Part > Good Colors** in the *model Tree window*.

c) Surface for Inlet Section, Outlet Section, High Pressure Cavity and Low Pressure Cavity generation

Geometry > Create/Modify Surface > From Curves: Select curves around with the left mouse button. Press the middle mouse button to accept the curves. No matter there is four curves or not, as long as the area is closed, the surface will be generated. For Inlet Section, High Pressure and Low Pressure Cavity, set **Tolerance** to 0. For Outlet Section, set **Tolerance** to 0.00001. And it is shown in Figure D33.

Figure D33: Geometry after surface at inlet section, outlet section, high pressure cavity and low pressure cavity created

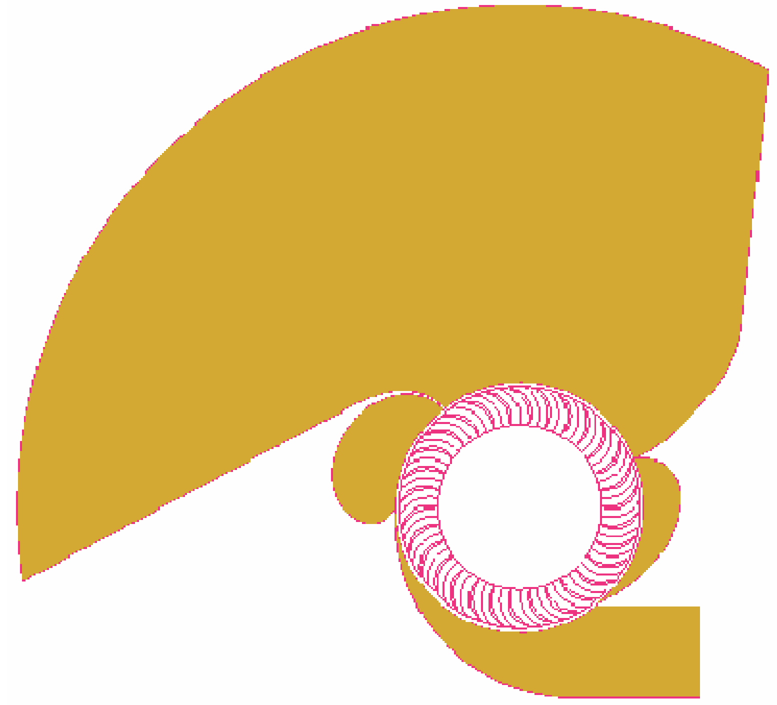

In order to generate the surface between OUTERCIRCLE.00 (A circle with radius 6-in) and 4 sections (inlet section, outlet section, high pressure cavity and low pressure cavity), there are more assistant points and curves required.

Geometry > **Create Points** > **Project point to curve**: Project points on OUTERCIRCLE to its outer curves corresponding to inlet section, outlet section, high pressure cavity and low pressure cavity. Enter the **Part** as **POINTS**, and leave **Name** by default. Similarly create four points on curve OUTERCIRCLE by project points: pnt17, pnt23, pnt42, and pnt36.

Geometry > **Create/Modify Curve** > **Segment curve**: Split the curves by the points projected previously.

Geometry > **Create/Modify Curve** > **From Points**: Create curve between the gaps by two corresponding points created previously. Set **Tolerance** to **0**, enter the **Part** as **CURVES** and set **Name** by default. However, there are four curves excluded and shown in Figure D34.

INT5.00 pnt17 and its projected point on OUTERCIRCLE (Set **Part** as **INT5** and **Name** as **INT5.00**)

INT6.00 pnt23 and its projected point on OUTERCIRCLE (Set **Part** as **INT6** and **Name** as **INT6.00**)

INT7.00 pnt42 and its projected point on OUTERCIRCLE (Set **Part** as **INT7** and **Name** as **INT7.00**)

INT8.00 pnt36 and its projected point on OUTERCIRCLE (Set **Part** as **INT8** and **Name** as **INT8.00**)

PS: The part INT4 is kept for an assistant curve for future mesh generation and it will be created at next section.

Geometry > Create/Modify Surface > From Curves: Select curves, basically four curves create a surface, but even there are no four curves, a surface will be created due to enclosed area. Follow the steps indicated and Set **Tolerance** to **0.001**. Enter the **Part** as **SYM1**, and leave **Name** by default.

If there are more points or curves needed, follow the steps above to create them. The result is shown in Figure D34 and four particular areas are indicated.

d) Assistant Curves for Future Mesh Generation

There is a curve which will be used for future Mesh Generation, and it is created by following steps:

Geometry > Create Points > Parameter along a curve: Set **Curve Parameter(s)** to 0.8 and select curve shown at the right of Figure D35. Similarly make a point as shown in a middle of Figure D35. Enter the **Part** as **POINTS**, and set **Name** by default.

Geometry > Create/Modify Curve > Segment curve: Split the curve by point created previously.

Geometry > Create/Modify Curve > Arc from 3 Points: Click on three points (2 points are created previously, other one is pnt42) and make an arc shown in Figure D35. Enter the **Part** as **INT4**, and set **Name** to **INT4.00**.

Figure D34: Geometry after surface between outer circles generated

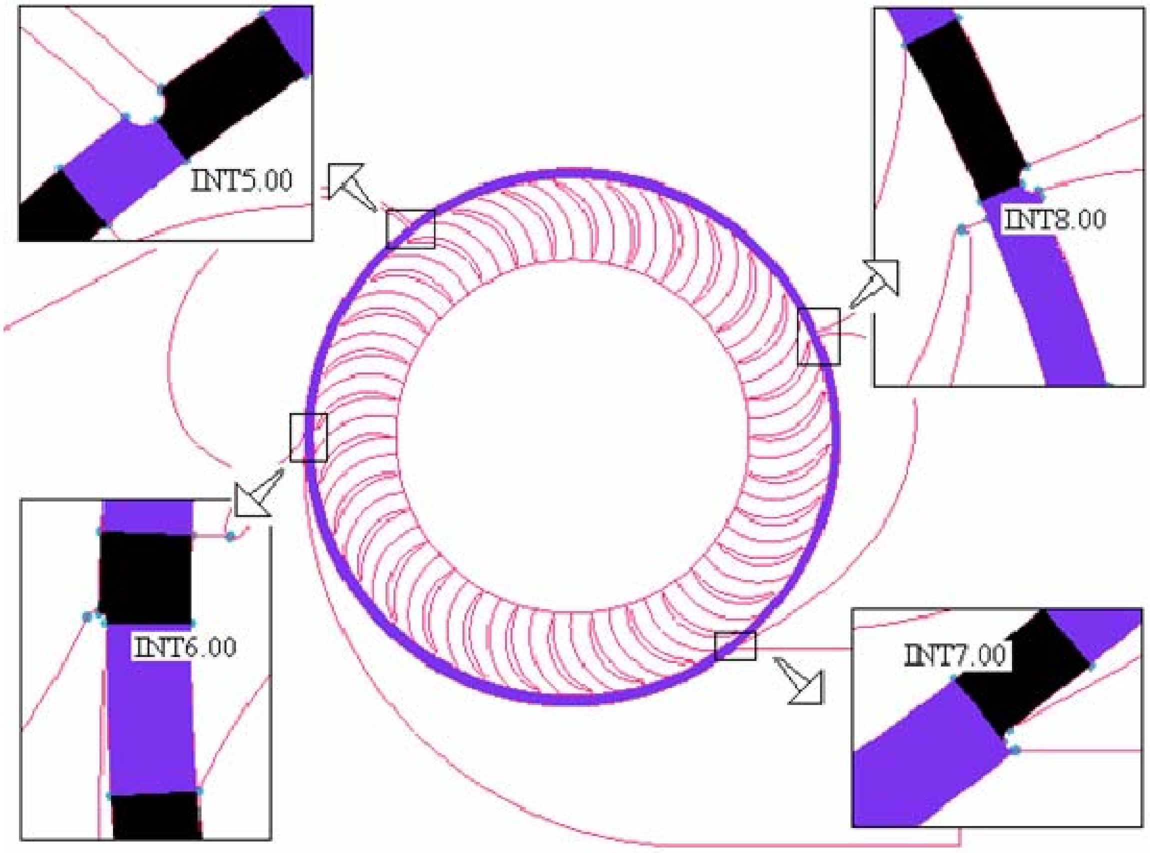

Figure D35: Geometry after assistant curve for future mesh generation

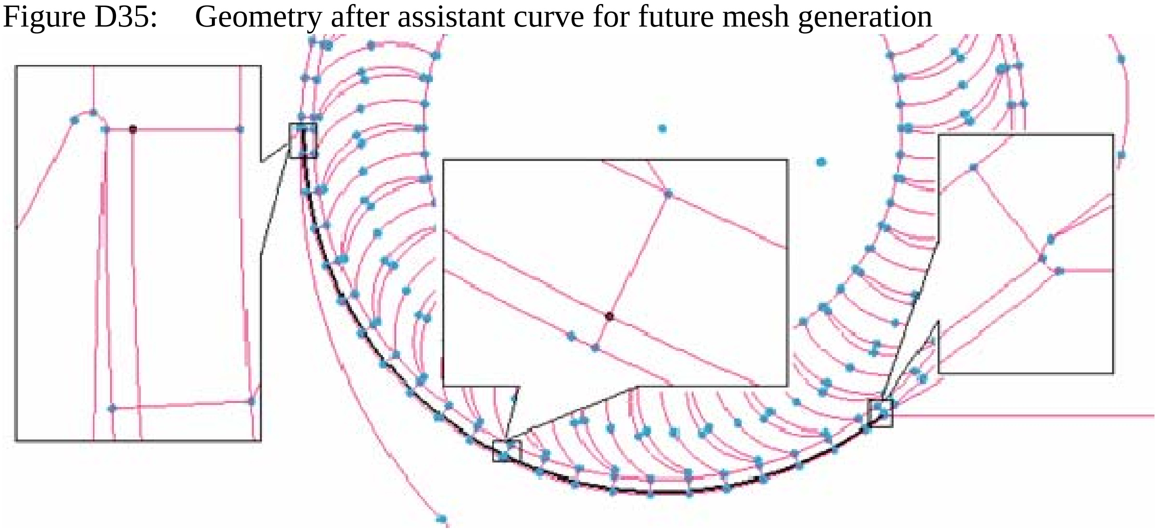

3. 3-D Model Generation

a) Extrude 0.1 inch along Z-axis

Geometry > **Create Point** > **Explicit Coordinates**: Create a point (0 0 0.1). Enter the **Part** as **POINTS**, and leave **Name** by default.

Geometry > **Create/Modify Surface** > **Sweep Surface**: Select the 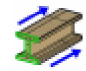 (Sweep Surface) to open the *Select* window as shown in Figure D36.

Figure D36: Sweep surface window

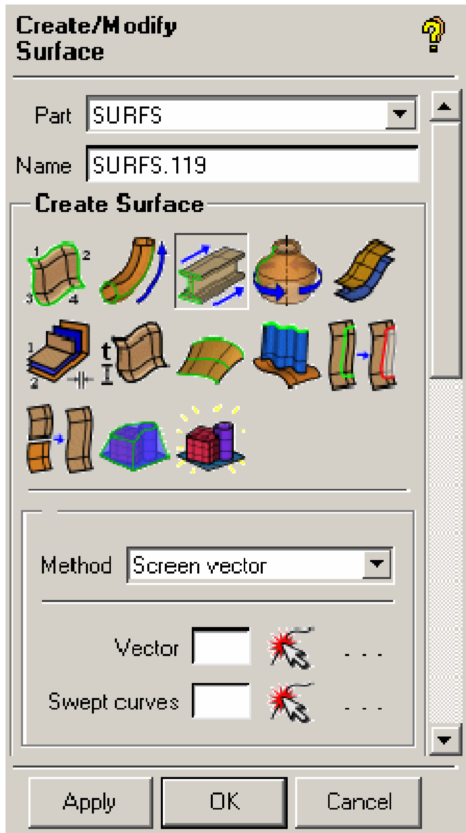

Set **Method** to **Screen Vector**, and set **Vector** to two points **(0 0 0) and (0 0 0.1)**. Switch ON **Curves** in the left side model Tree window. Switch OFF the **Part** of **CURVES** and **INT0** in the left side model Tree window. Enter **Part** as **SURFS** and **Name** as **SURFS.00**. After clicking on **Entity chooser icon**, select  from **Select Geometry**. Then press **Apply**, geometry is created.

Regroup each Part by following the TIP4 mentioned previously, and let all curves to the **Part** of **CURVES**, all points to the **Part** of **POINTS**. Others are indicated and shown in Figure D37.

Figure D37: Geometry after extruded

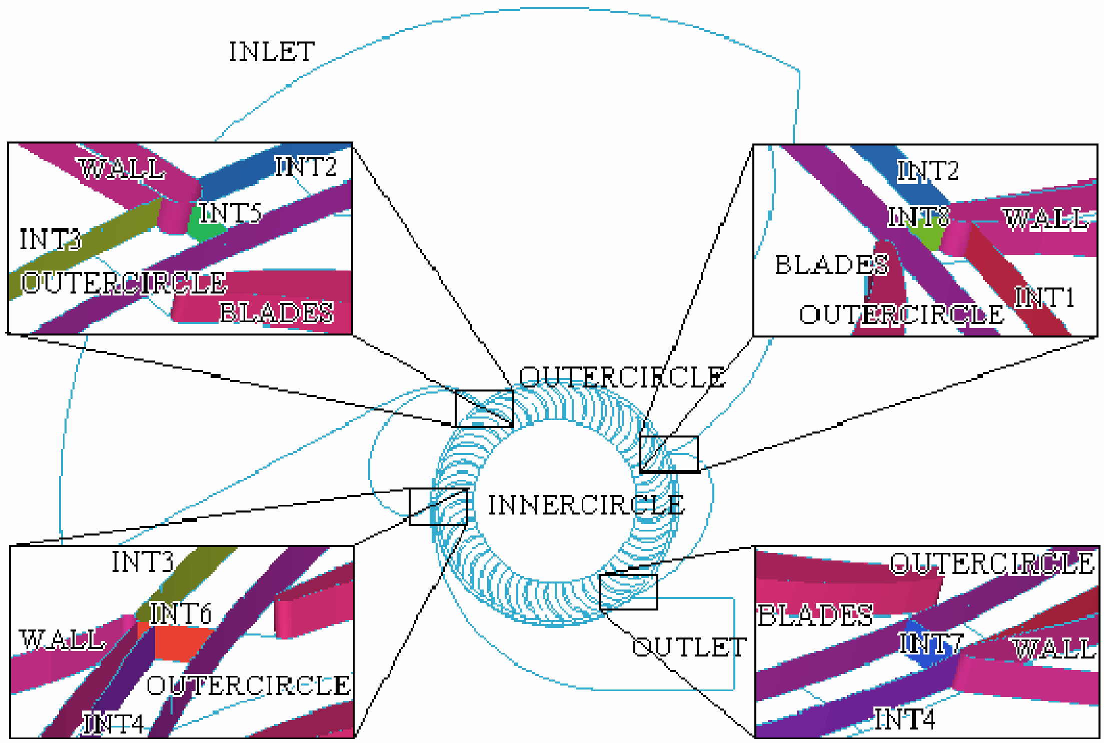

Geometry > Transform Geometry > Translate Geometry: Translate **SYM1,** including curves and surfaces, and copy along Z-axis about 0.1-inch by selecting **Explicit Method**.

Regroup the translated surface by following the TIP4 mentioned previously, and Let its **Part** as **SYM2**.

Similarly translate blade surfaces about 0.1-inch along Z-axis to enclose the blades.

b) Body Creation

Geometry > Create Body > Material Point > Centroid of 2 points: Select the  (Create Body) to open create body window as shown in Figure D38. Enter **Part** name **FLUID** and select two point (0 0 0) and (0 0 0.1) with the left mouse button. Press the middle to accept the selection. Press **Apply** to create the material point.

Figure D38: Create body window

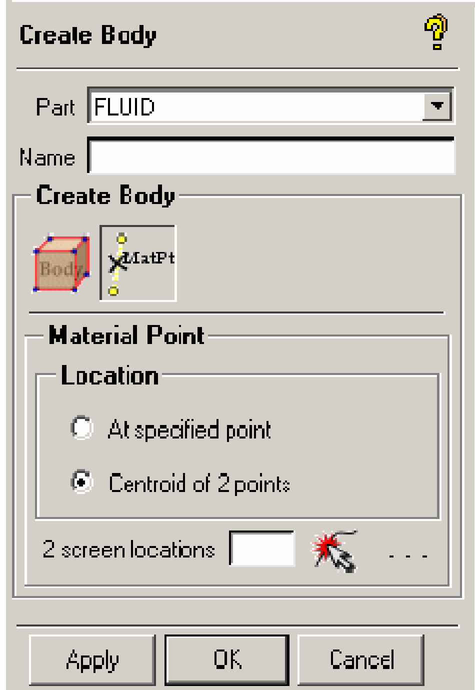

4. Mesh Generation

4.1. Inner Circle Mesh

a) Starting Blacking

Blocking > **Create Block** > **Initialize block**: It will open the C*reate Block* window as shown in Figure D39.

Under **Initialize Block**, set **Type** to **3D**. And select two inner-circle surfaces on planes **SYM1** and **SYM2**. Name **Part** as **FLUID** and press **Apply** to create block.

Blocking > **Associate** > **Associate Vertex**: It will open the window as shown in Figure D40. Toggle **ON** Geometry > Points and Blocking > vertices > Numbers from tree widget. Under **Entity**, select **Point** and associate vertex to point as shown in Figure D41.

Figure D39: Create block window

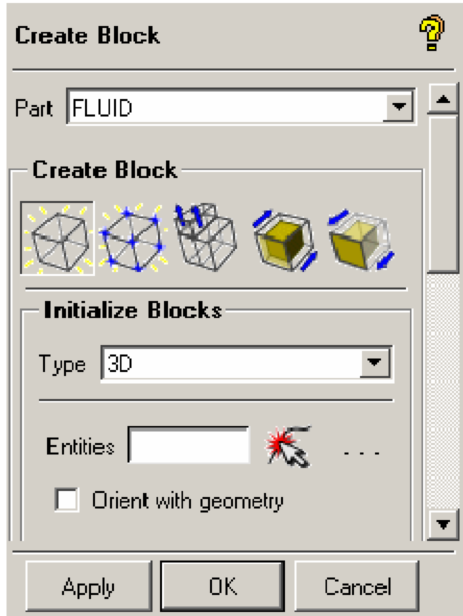

Figure D40: Associate vertex window

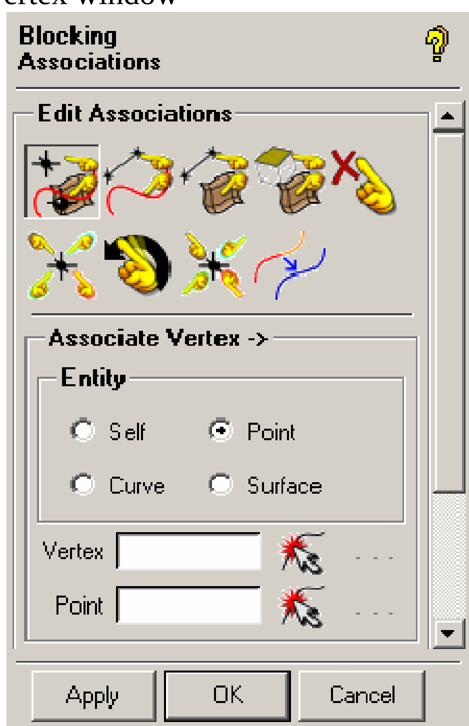

Figure D41:   Moving vertices

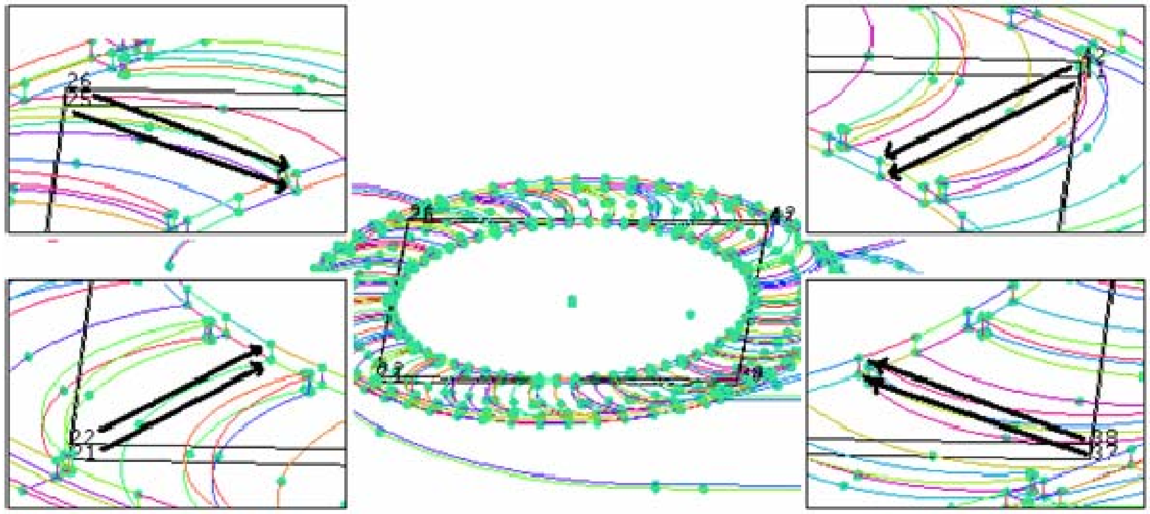

Blocking > **Associate**  > **Associate Edge to Curve**  : It will open the window as shown in Figure D42 and Associate edges to curves as shown in Figure D43.

Figure D42:   Associate edge to curve window

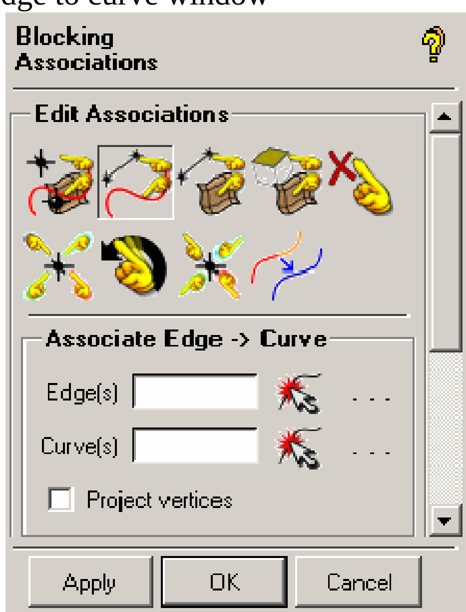

TIP: To make sure the association is correct by selecting **Edges** > **Show Association** from the *Tree Widget* and switch on Curve

Figure D43:   Associating edges to curves

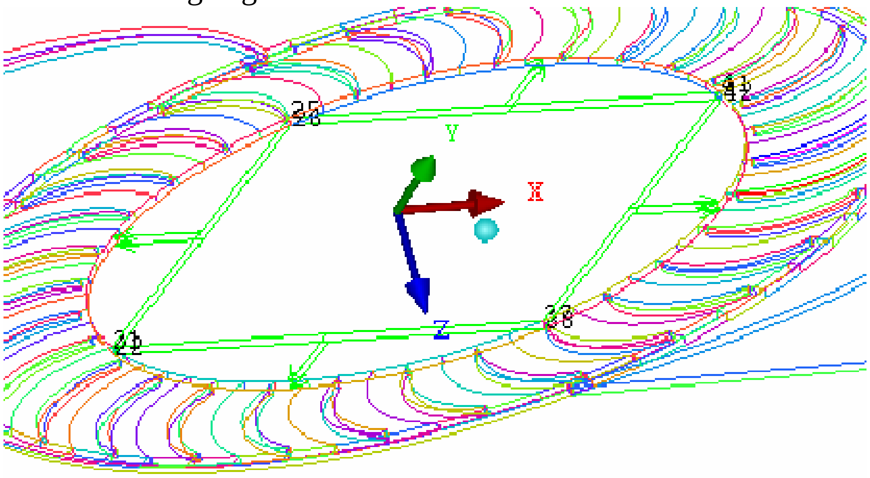

Blocking > **Split Block**  > **Ogrid Block**  : It will open the *Ogrid block* window as shown in Figure D44. Select **Face(s)** as shown in Figure D45, Set **Offset** to 1. Press **Apply** to create O-grid block.

Figure D44:   O-grid block window

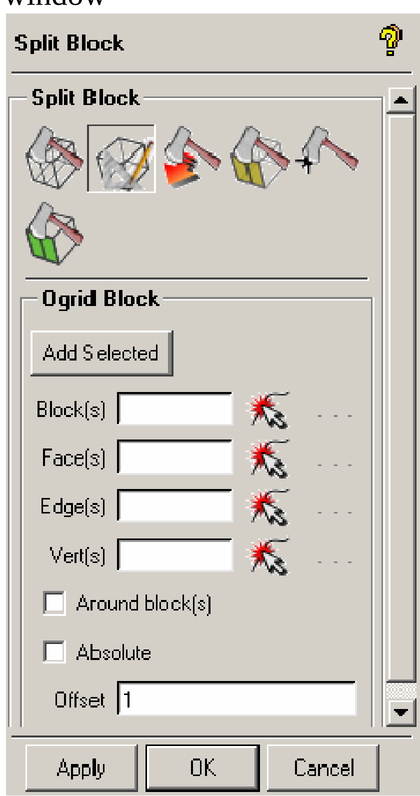

Figure D45:

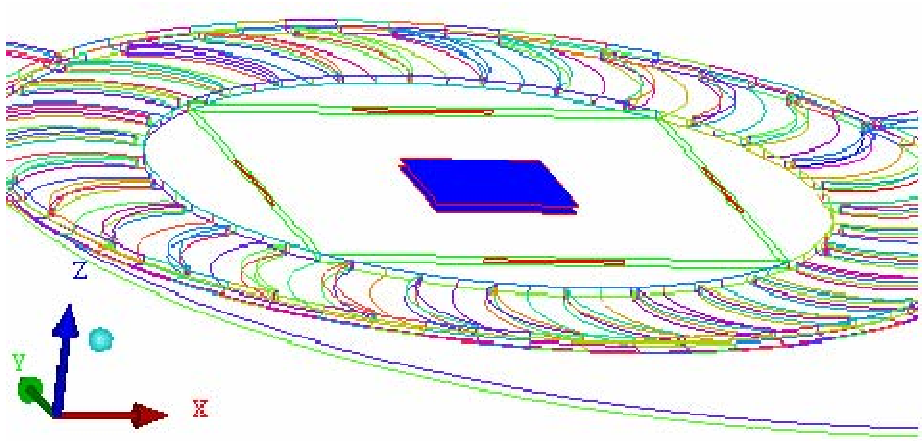

Blocking > **Pre-Mesh Params** >**Edge Param(s)**: It will open the *Meshing Parameters* window as shown in Figure D46. To create the mesh as shown in Figure D47, Select edges and enter their nodes as 36 or 18. Let **Mesh law** as BiGeometric and Check **Copy to parallel edges**.

After setting up the parameters on each edge, toggle **Pre-Mesh** from *tree widget*, then the mesh is created. Convert it to Unstruct Mesh before saving the file by following steps:

Use the **right mouse** and select **Pre-Mesh > Convert to Unstruct Mesh** in the model *Tree window*.

Figure D46: Meshing parameters window

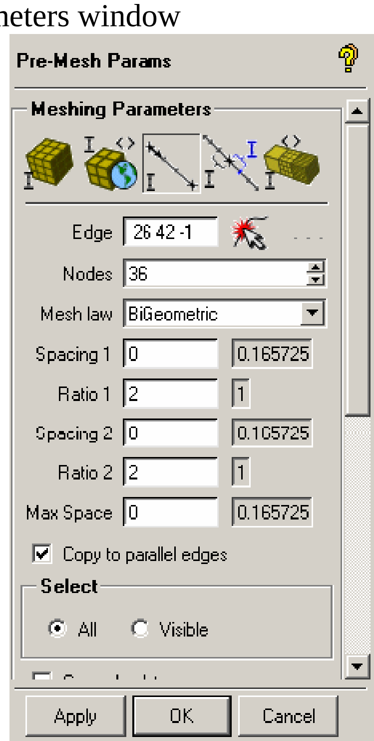

Figure D47: Completed center-circle mesh

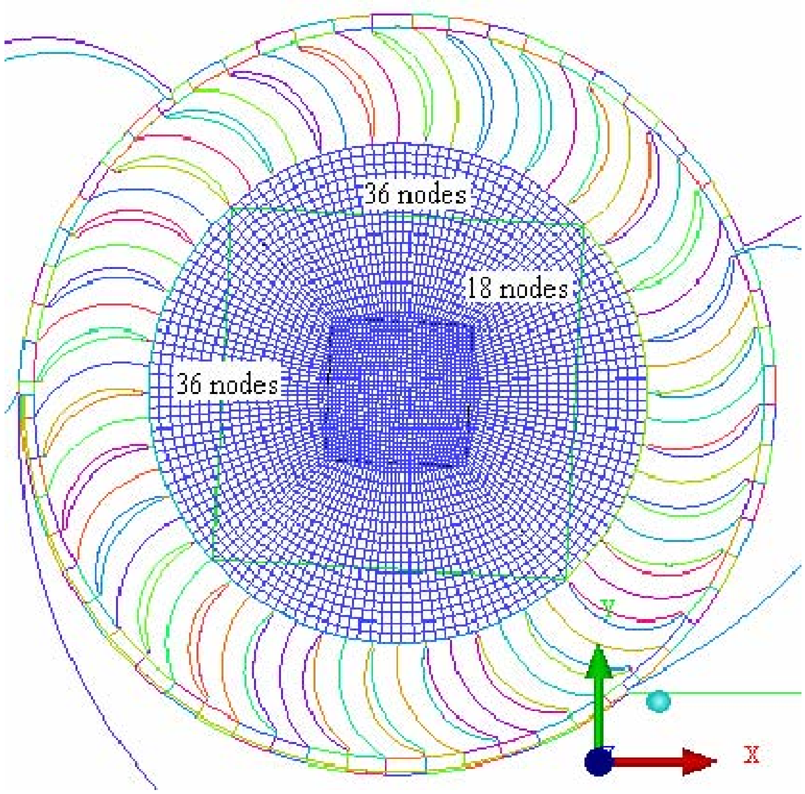

4.2. Blades Mesh

Blocking > Create Block > **Initialize block**: Under **Initialize Block**, set **Type** to **2D Planer.** Name **Part** as **FLUID** and press **Apply** to create a single block.

Blocking > Associate > **Associate Vertex**: Toggle **ON Geometry > Points** and **Blocking > vertices > Numbers** from *tree widget*. Under **Entity**, select **Point**. And associate vertex to appropriate point as shown in Figure D48.

Figure D48: Moving vertices to points

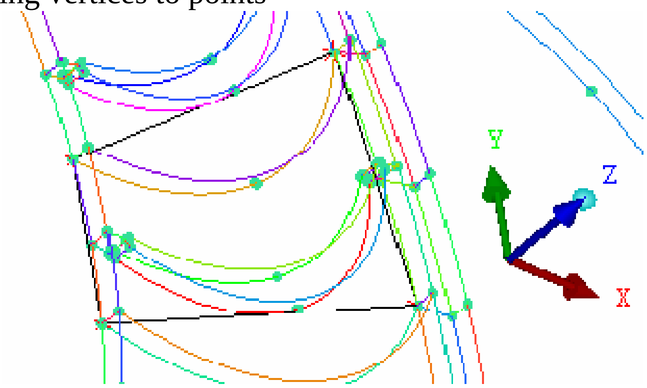

Blocking > **Associate** > **Associate Edge to Curve** : To associate block edges to appropriate curves as shown in Figure D49.

Figure D49: Associating edges to blade-curves

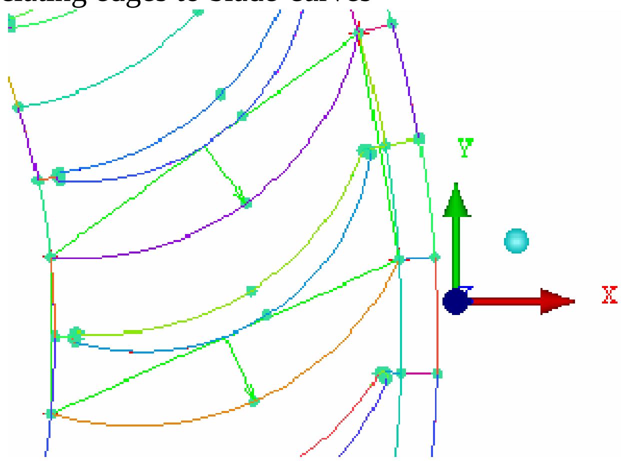

Blocking > **Split Block** > **Split Block** : Select the Top edge with the left mouse button, try to position the edge at the required position as shown in Figure D50, then press the middle mouse button to accept the selection. Create other split also.

Figure D50:

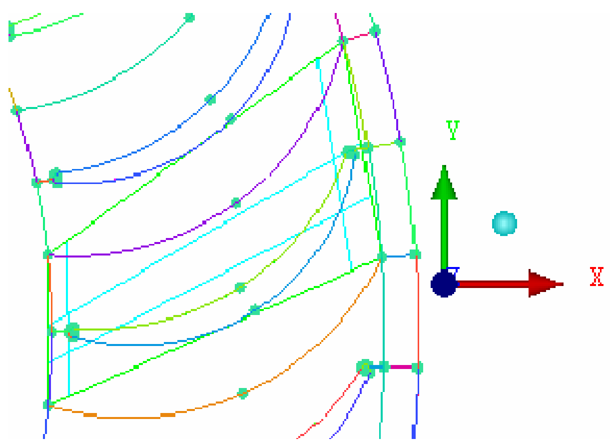

Blocking > **Associate** > **Associate Edge to Curve** : Associate inner block edges to appropriate blade-curves.

Blocking > **Associate** > **Associate Vertex** : Associate vertices at inner block to appropriate points at the blade.

Blocking > **Move Vertex** > **Move Vertex** : Directly click on edges and move them to appropriate location as shown in Figure D51.

Figure D51: After moving vertices to appropriate location

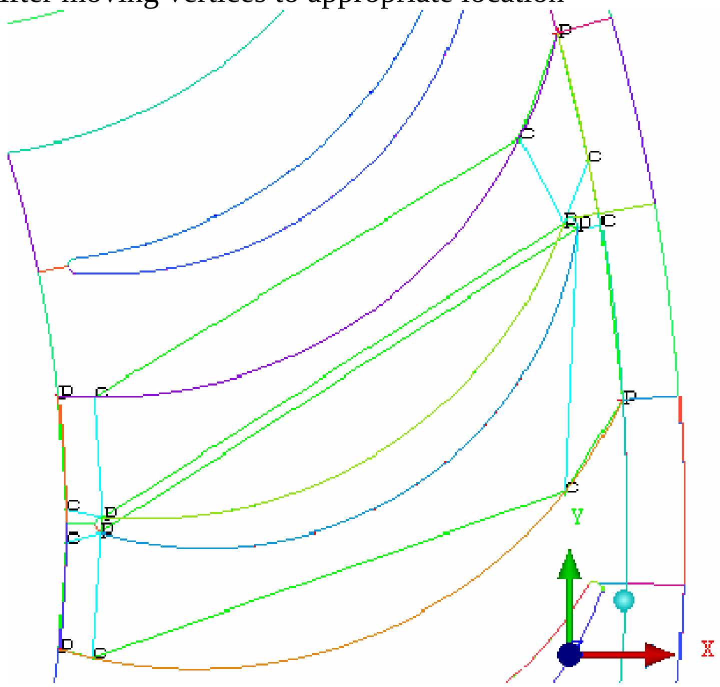

Blocking > **Split Block** > **Ogrid Block** : Set **Offset** to 0.3 and Check **Around Block(s)**. Select the block at center one as shown in Figure D52, and **Apply** to create O-grid block.

Figure D52: Select the block for the O-grid

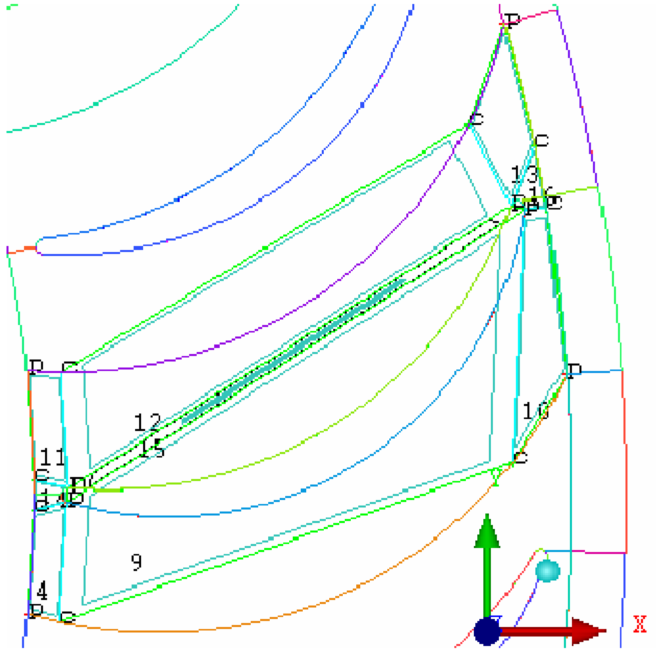

Blocking > **Edit Edge** > **Split Edge** : To open *Edit Edge(s)* window as shown in Figure D53. Set **Split type** to Linear, then to split appropriate edges. Also use **Blocking** > **Move Vertex** > **Move Vertex** to move and arrange the edge as shown in Figure D54.

Figure D53: Edit edge window

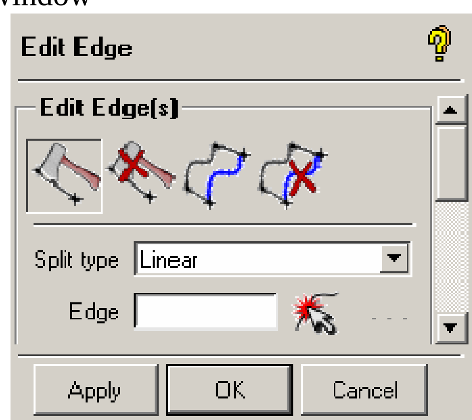

Figure D54: After arranging the shape of the block

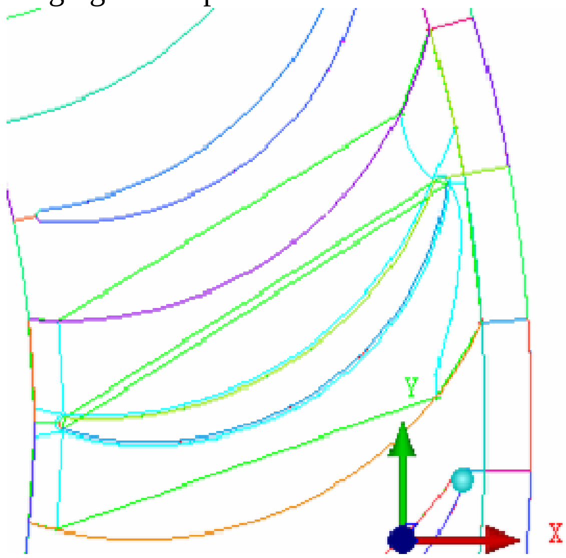

Blocking > Pre-Mesh Params **>Edge Param(s)** : Set the number of nodes on each edge as shown in Figure D55. Check **Copy to parallel edges** and **Copy absolute**. Then press **Apply** to accept.

Figure D55: Nodes at each edge

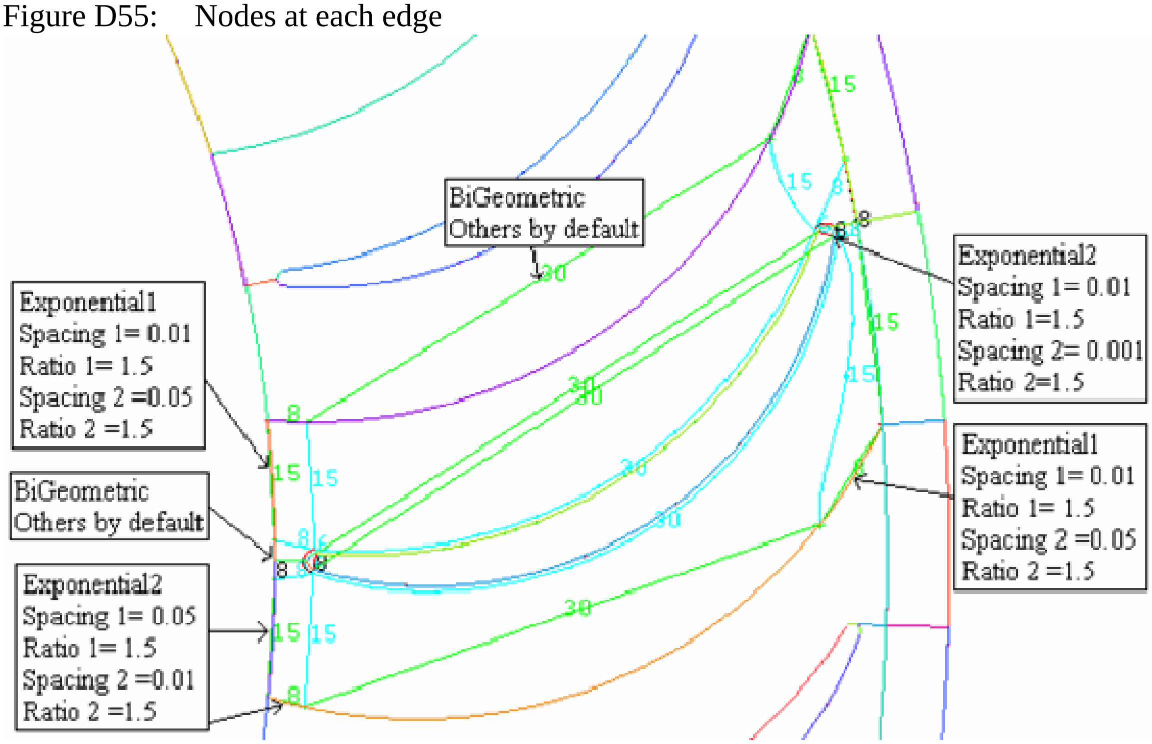

After setting up the parameters on each edge, toggle **Pre-Mesh** from *tree widget*, then the mesh is created as shown in Figure D56.

Figure D56: Mesh created around single blade

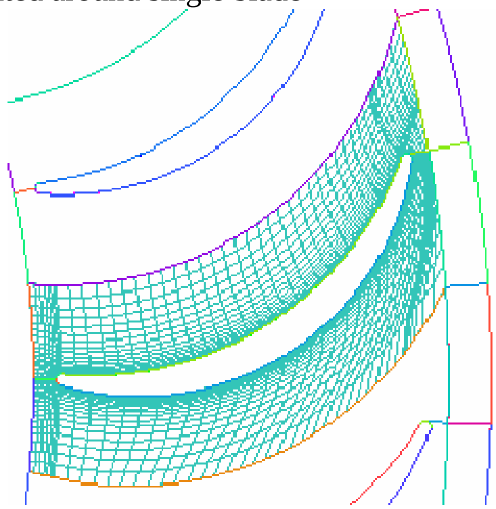

Since this mesh is good enough, there are 29 blades remaining, it is suggested to rotate and copy this Block to other corresponding blades. Before the action, disassociate Edges and Vertices first.

Toggle **Pre-Mesh** from *tree widget* again to close the mesh

Blocking > **Associate** > **Disassociate form Geometry** : To open *Disassociate* window as shown in Figure D57.

To select Edges, click on and then select from **Select Blocks** bar window. Press **Apply** to disassociate the edges.

Blocking > **Transform Blocks** > **Rotate Blocks** : To open *selection* window.

To select **Rotating objects**, click on and Click on from **Select Blocks**. Check **Copy** and set **Number of copies** to **29**. Under **Rotation**, set on **Axis** to **Z**, and set **Angle** to **12**. Under **Center of Rotation**, set **Center Point** to **Origin**. Press **Apply** to rotate blocks.

Blocking > **Associate** > **Associate Edge to Curve** : Re-associate edges to appropriate curves. And check if the nodes on edge are changed or not. If there are extra vertices, delete them by **Blocking** > **Edit Edge** > **Unsplit Edge**, under **Remove splits,** set **Single**.

After complete the previous step, to see how the meshes look like, toggle **Pre-Mesh** from *tree widget*, then the mesh is created as shown in Figure D59

Figure D57: Disassociate window

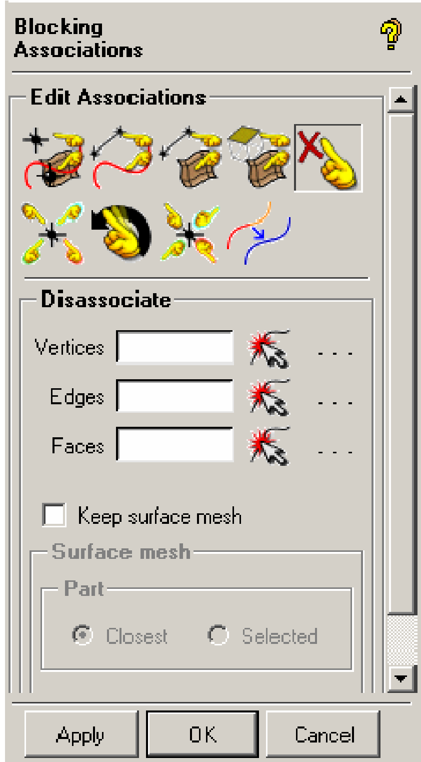

Figure D58: Rotation block selection window

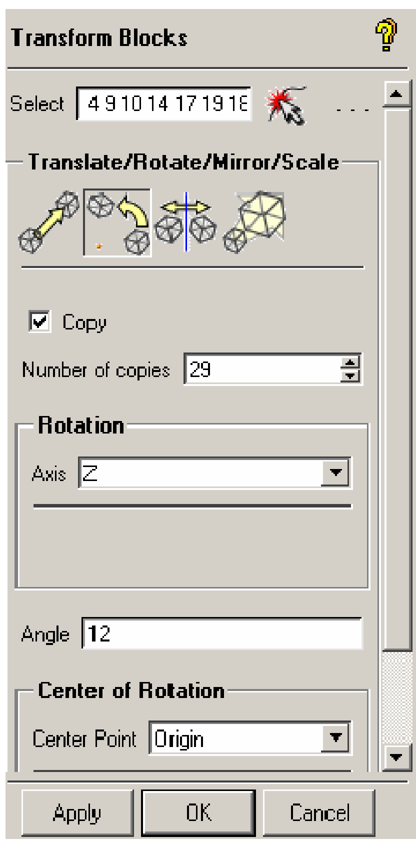

Figure D59: After 2D blade mesh creation

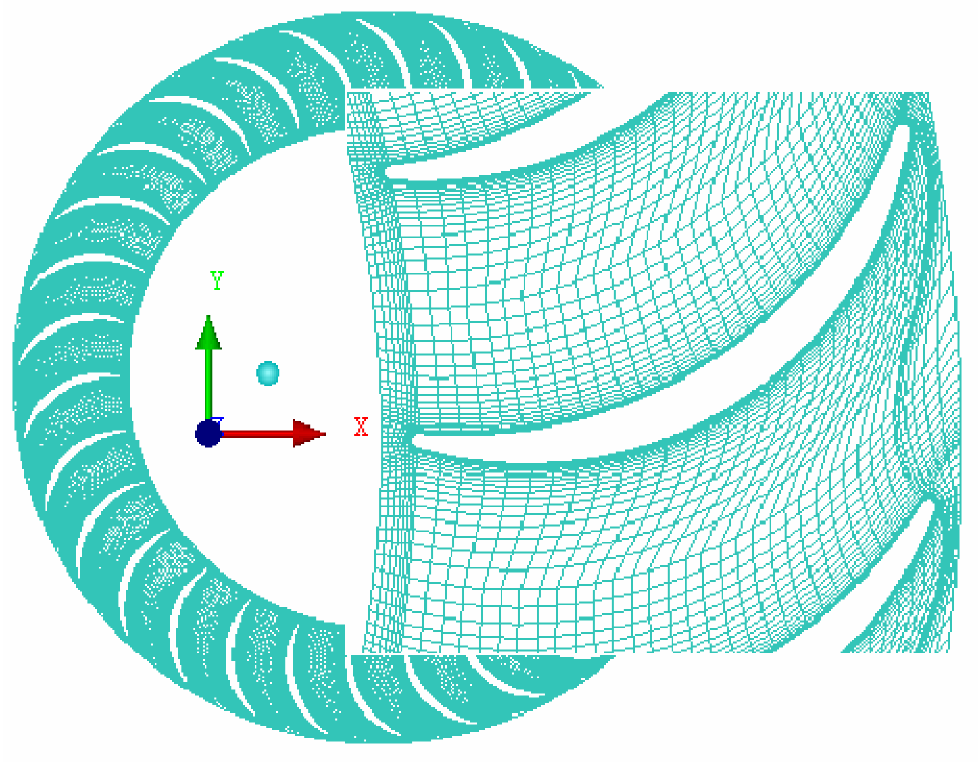

Blocking > **Create Block**  > **2D to 3D** : To open *Method* window as shown in Figure D60. Set **Method** to **Translate** and **Z Distance** to **0.1**, others are **0**, press **Apply** to create 3D block.

Figure D60: Method window

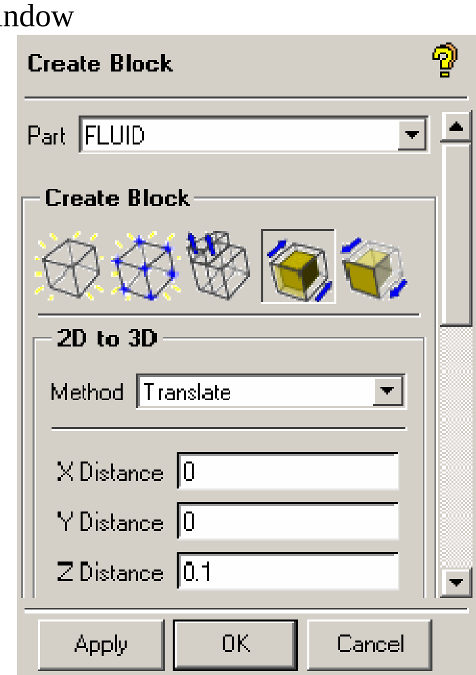

Toggle **Pre-Mesh** from *tree widget* to see the quality of the meshes, disassociate edges and associate edges to curves if required. The final look of the meshes is shown in Figure 61.

Figure D61:

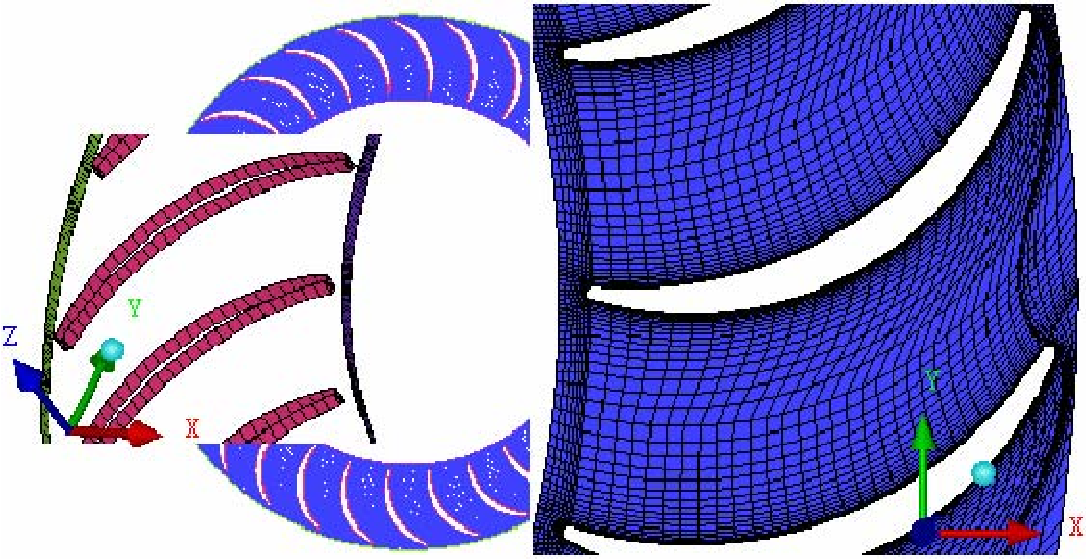

4.3 Inlet Section Mesh

Blocking > Create Block > **Initialize block** : Under **Initialize Block**, set **Type** to **3D**. And select two opposite surfaces at inlet section. Name **Part** as **FLUID** and press **Apply** to create block.

Blocking > Associate > **Associate Vertex**: Toggle **ON** Geometry > Points and Blocking > vertices > Numbers from *tree widget*. Under **Entity**, select **Point** and associate vertex to point.

Blocking > Associate > **Associate Edge to Curve** : Associate edges to curves as shown in Figure D62.

Blocking > Pre-Mesh Params >**Edge Param(s)** : Set the number of nodes on each edge as shown in Figure D63. Check **Copy to parallel edges** and **Copy absolute**. Then press **Apply** to accept.

Figure D62:

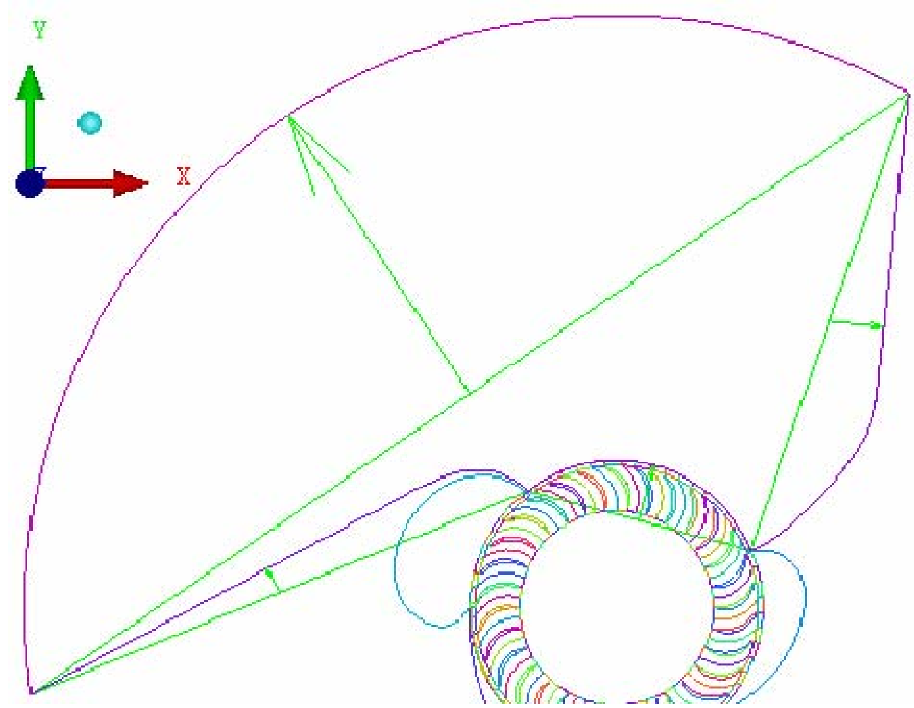

Figure D63:

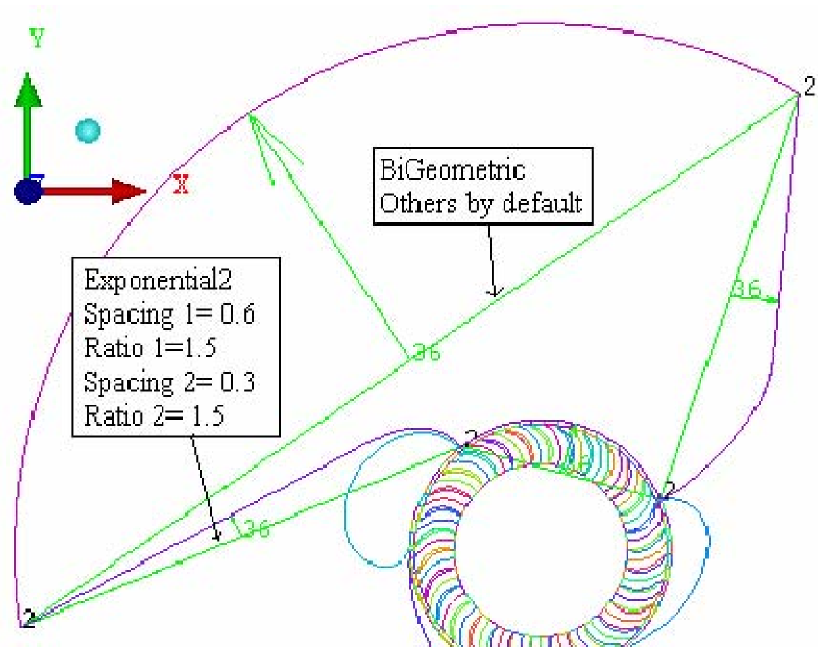

After setting up the parameters on each edge, toggle **Pre-Mesh** from *tree widget*, then the mesh is created. **Convert it to Unstruct Mesh** before saving the file: Use the **right mouse** and select **Pre-Mesh > Convert to Unstruct Mesh** in the *model Tree window*. The final mesh at inlet section is shown in Figure D64.

Figure D64:

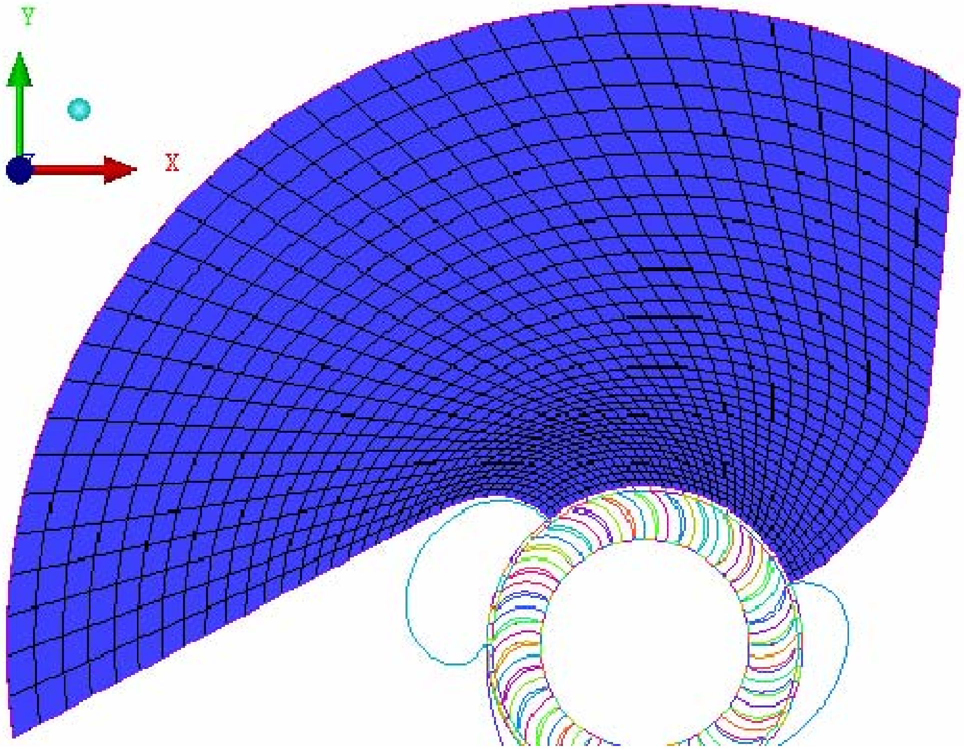

4.4 Mesh between Inlet Section and Blades

Blocking > **Create Block** > **Initialize block** : Under **Initialize Block**, set **Type** to **2D Planer.** Name **Part** as **FLUID** and press **Apply** to create a single block.

Blocking > **Associate** > **Associate Vertex** : Toggle **ON Geometry** > **Points** and **Blocking** > **vertices** > **Numbers** from *tree widget*. Under **Entity**, select **Point**. And associate vertices to appropriate points.

Blocking > **Split Block** > **Split Block** : Split the left and right edge.

Blocking > **Associate** > **Associate Vertex** : Associate vertices to appropriate points as shown in Figure D65.

Figure D65:

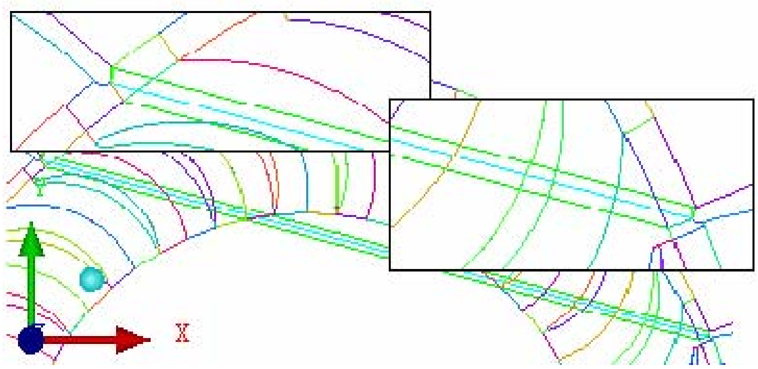

Blocking > Edit Edge **> Split Edge** : To open *Edit Edge(s)* window. Set **Split type** to **Linear**, then to split appropriate edges. Also use **Blocking > Move Vertex > Move Vertex** to move and arrange the edge as shown in Figure D66.

Figure D66:

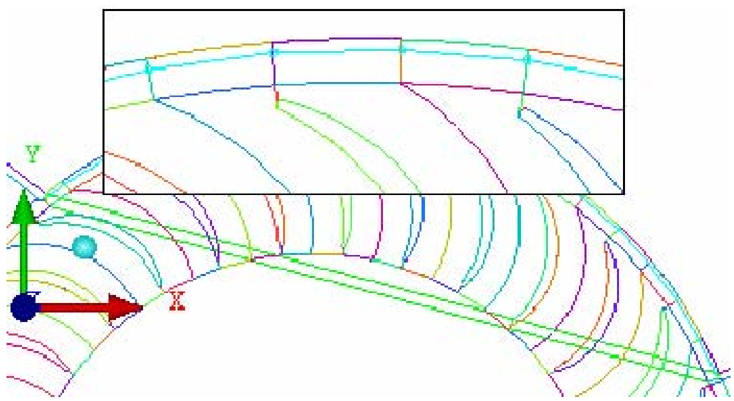

Blocking > Pre-Mesh Params  **>Edge Param(s)**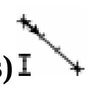: Check **Copy to parallel edges** and **Copy absolute**. Set mesh parameter at each edge as shown in Figure D67.

Figure D67:

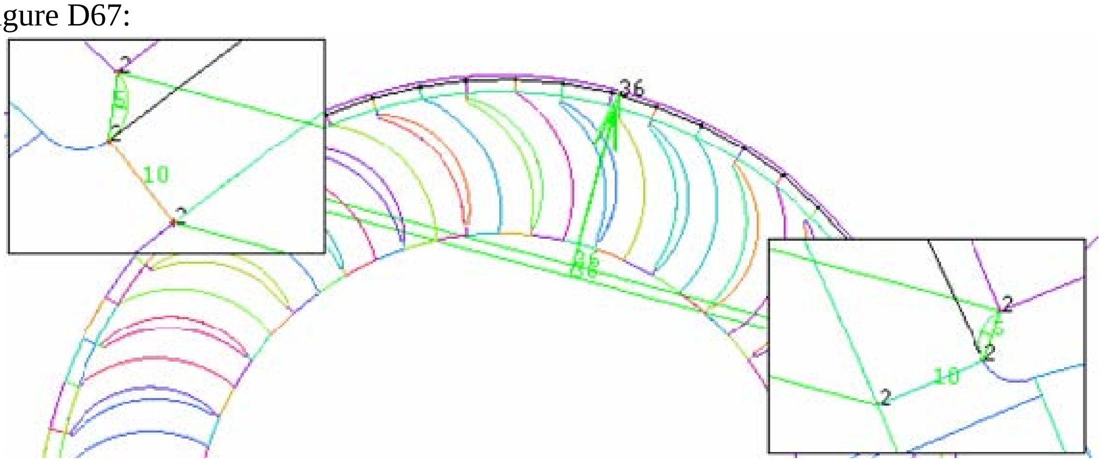

Toggle **Pre-Mesh** from *tree widget* and see mesh generated is proper or not. If it is acceptable, then follow the steps mentioned to generate meshes from 2D-3D.

Blocking > **Create Block** > **2D to 3D** : Set **Method** to **Translate** and **Z Distance** to **0.1**, others are **0**, press **Apply** to create 3D block.

Toggle **Pre-Mesh** from *tree widget* again to see the quality of the meshes. If edges are not associated properly, disassociate edges first, and then associate edges to curves.

4.4 Final Meshes

The meshes of other sections have to be generated by the previous procedure, either by 2D block to 3D block or 3D block only. It depends on the geometry. The meshes for each section are saved in different name. The final mesh was created by opening each mesh files and merging them into one mesh.

4.5 Writing Output

Output > **Select solver**: Select the (Select solver) to open the *Select* window as shown in Figure D68. Roll down to select CFX-5 solver.

Figure D68 Solver Selection Window

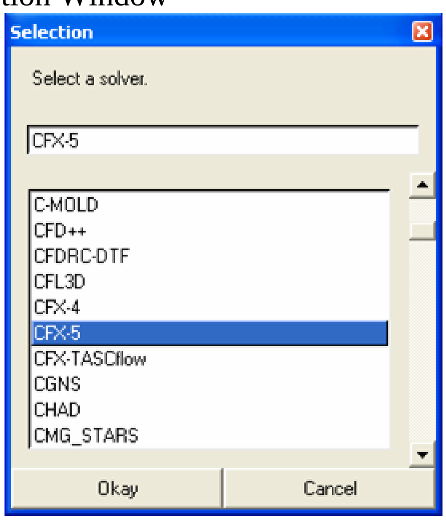

Output > **Write input:** Select the (View input) to open the output file window as shown in Figure D69. In the directory, type the expected name such as *.cfx5, then press Done.

Figure D69	Output File Window

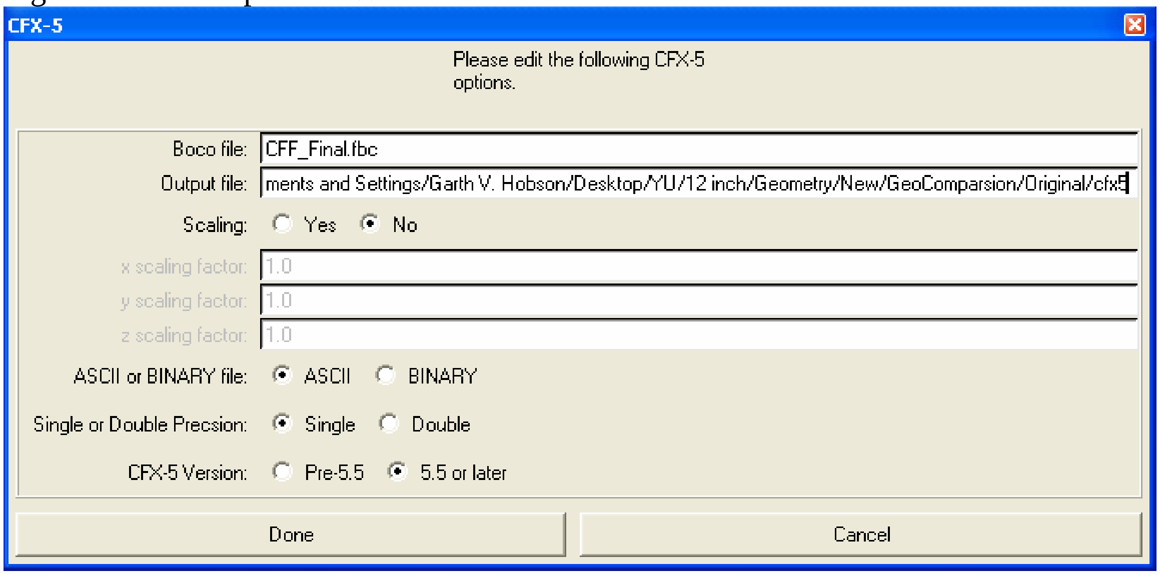

APPENDIX E. PROCEDURES OF SETUP IN CFX-PRE

I. Defining the Transient Simulation

A Creating a New Simulation

1. If required, launch CFX-Pre.
2. Select **File > New Simulation**.
3. Click **General** in the New Simulation File Window.
4. If required, set the path location to a different folder.
5. Under **File name** type *CrossFlowFan*.
6. Click **Save**.
7. The **Mesh** tab is displayed.

B Importing a Mesh

1. Select **File > Import Mesh** or click **Import Mesh**.
2. Leave **Mesh Format** set to **ICEM CFD**.
3. In the bottom left of the screen, under **File** click **Browse**.
4. From the working directory, select *CrossFlowFan.cfx5*.
5. Click **Open**.
6. Set **Mesh Units** to **in**.
7. Click **Ok**.
8. The mesh is opened.

C Define the Simulation Type

In order to check if the solver will give convergent result or not, the first revolution is suggested and is set up as follows.

1. Select **Create > Flow Objects** > **Simulation Type** from the main menu.

   Simulation Type appears
2. Set **Option** to **Transient**.
3. Under **Time Duration**, Set **Option** to **Total Time**, and **Total time** to **0.02** [s].
4. Under **Time Steps**, Set **Option** to **Timestep**, and **Timesteps** to **5.55555e-5** [s]
5. Under **Initial Time**, Set **Option** to **Automatic with Value**, and **Time**

to **0** [s]

6. Click **Ok** to save the information.

D Creating the Domain

1. To Create **Rotation Domain**

    a) Click **Create a Domain**.

    b) In **Create Domain**, set **Name** to *Rotation* and click **OK**.

    Edit Domain: **Rotation** is displayed

    c) On the **General Options** panel:

    (1) Set **Location** to **Assembly, Assembly 3**.

    (2) Leave Domain **Type** set to **Fluid Domain**.

    (3) Set Fluid **List** to **Air Ideal Gas**.

    (4) Leave **Coord Frame** set to **Coord 0**.

    (5) Set **Reference Pressure** to **1** [atm].

    (6) Under **Buoyancy**, leave **Option** set to **Non Buoyant**.

    (7) Under **Domain Motion**, leave **Option** set to **Rotating**.

    (8) Set **Angular Velocity** to **3000** [rev min^-1].

    (9) Turn on **Alternate Rotation Model**.

    (10) Under **Axis Definition**, leave **Option** set to **Coordinate Axis**.

    (11) Set **Rotation Axis** to **Global Z**.

    d) Click the **Fluid Mode**ls tab and leave all options set to their respective defaults except:

    (1) Under **Heat Transfer Model**, leave Option set to **Total Energy**.

    (2) Turn on **Include Viscous Work Term**.

    (3) Under **Turbulence Model**, leave **Option** set to **k-Epsilon**.

    (4) Click **Ok** to create the domain.

2. To Create **Stationary Domain**

    a) Click **Create a Domain**.

    b) In **Create Domain**, set **Name** to *Stationary* and click **OK**.

    Edit Domain: **Stationary** is displayed

    c) On the **General Options** panel:

(1) Set **Location** to **Assembly 2, Assembly 4, Assembly 5, Assembly 6, Assembly 7, Assembly 8, and Assembly 9, Assembly 10**.

(2) Leave **Domain Type** set to **Fluid Domain**.

(3) Set **Fluid List** to **Air Ideal Gas**.

(4) Leave **Coord Frame** set to **Coord 0**.

(5) Set **Reference Pressure** to 1 [atm].

(6) Under **Buoyancy**, leave **Option** set to **Non Buoyant**.

(7) Under **Domain Motion**, leave **Option** set to **Stationary**.

d) Click the **Fluid Models** tab and leave all options set to their respective defaults except:

(1) Under **Heat Transfer Model**, leave **Option** set to **Total Energy**.

(2) Turn on **Include Viscous Work Term**.

(3) Under **Turbulence Model**, leave option set to **k-Epsilon**.

e) Click **Ok** to create the domain.

E Creating the Boundary Conditions

1. To Create the **Inlet Boundary Condition**

a) Click **Create a Boundary Condition**  on the main toolbar.

b) Set **Name** to *Inlet* and **Domain** to **Stationary**, then **Ok**.

Edit Boundary is displayed.

c) On the **Basic Settings** panel, set:

(1) **Boundary Type** to **Opening**

(2) **Location** to **INLET**

d) Click the **Boundary Details** tab, then:

(1) Under **Flow Regime**, leave **Option** set to **Subsonic**.

(2) Under **Mass and Momentum**, set **Option** to **Pressure and Direction (Stable)**.

(3) Set **Relative Pressure** to 0 [Pa]

(4) Under **Flow Direction**, set **Option** to **Normal to Boundary Condition**.

(5) Under **Turbulence**, set **Option** to **Medium (Intensity = 5%)**.

        (6) Under **Heat Transfer**, set **Option** to **Static Temperature**.

        (7) Set **Static Temperature** to 300 [K].

    e) Click **Ok** to create the boundary.

2. To Create the **Outlet Boundary** Condition

    a) Click **Create a Boundary Condition**.

    b) Set **Name** to *Outlet* and **Domain** to **Stationary**, then **Ok**.

    Edit Boundary is displayed.

    c) On the **Basic Settings** panel, set:

        (1) **Boundary Type** to **Opening**

        (2) **Location** to **OUTLET**

    d) Click the Boundary Details tab, then:

        (1) Under **Flow Regime**, leave **Option** set to **Subsonic**.

        (2) Under **Mass and Momentum**, set **Option** to **Static Pressure**.

        (3) Set **Relative Pressure** to **0** [Pa]

        (4) Under **Flow Direction**, set **Option** to **Normal to Boundary Condition**.

        (5) Under **Turbulence**, set **Option** to **Medium (Intensity = 5%)**.

        (6) Under **Heat Transfer**, set **Option** to **Static Temperature**.

        (7) Set **Static Temperature** to 300 [K].

    e) Click **Ok** to create the boundary condition.

3. To Create the **Symmetry Boundary** Condition

    First create the symmetric boundary condition in **Stationary Domain**.

    a) Click **Create a Boundary Condition**.

    b) Set **Name** to *SYM1*and **Domain** to **Stationary**, then **Ok**.

    Edit Boundary is displayed.

    c) On the **Basic Settings** panel, set:

        (1) **Boundary Type** to **Symmetry**

        (2) **Location** to **SYM1 C, SYM1 D, SYM1 E, SYM1 F, SYM1 G, SYM1 H, SYM1 I, SYM1 J**

    d) Click **Ok** to create the boundary condition.

Similarly create the opposite symmetric boundary condition.

a) Click **Create a Boundary Condition**.

b) Set **Name** to *SYM2*and **Domain** to **Stationary**, then **Ok**.

Edit Boundary is displayed.

c) On the **Basic Settings** panel, set:

(1) **Boundary Type** to **Symmetry**

(2) **Location** to **SYM2 C, SYM2 D, SYM2 E, SYM2 F, SYM2 G, SYM2 H, SYM2 I, SYM2 J**

d) Click **Ok** to create the boundary condition.

Then create the symmetric boundary condition in **Rotation Domain**.

a) Click **Create a Boundary Condition**.

b) Set **Name** to *SYM3*and **Domain** to **Rotation**, then **Ok**.

Edit Boundary is displayed.

c) On the **Basic Settings** panel, set:

(1) **Boundary Type** to **Symmetry**

(2) **Location** to **SYM1 A, SYM1 B**

d) Click **Ok** to create the boundary condition.

Similarly create the opposite symmetric boundary condition

a) Click **Create a Boundary Condition**.

b) Set **Name** to *SYM4*and **Domain** to **Rotation**, then **Ok**.

Edit Boundary is displayed.

c) On the **Basic Settings** panel, set:

(1) **Boundary Type** to **Rotation**

(2) **Location** to **SYM2 A, SYM2 B**

d) Click **Ok** to create the boundary condition.

2. To Create the Wall Boundary Condition

a) Click **Create a Boundary Condition**.

b) Set **Name** to *Wall* and **Domain** to **Stationary**, then **Ok**.

Edit Boundary is displayed.

c) On the **Basic Settings** panel, set:

(3) **Boundary Type** to **Wall**

(4) **Location** to **Wall**

d) Click the **Boundary Details** tab, then:

(1) Under **Wall Influence On Flow**, leave **Option** set to **No Slip**.

(2) Under **Wall Roughness**, set **Option** to **Smooth Wall**.

(3) Under **Heat Transfer**, set **Option** to **Adiabatic**.

e) Click **Ok** to create the boundary.

3. To Create the Blades Boundary Condition

a) Click **Create a Boundary Condition**.

b) Set **Name** to *Blades* and **Domain** to **Rotation**, then **Ok**.

Edit Boundary is displayed.

c) On the **Basic Settings** panel, set:

(1) **Boundary Type** to **Wall**

(2) **Location** to **Blades**

d) Click the **Boundary Details** tab, then:

(1) Under **Wall Influence On Flow**, leave **Option** set to **No Slip**.

(2) Under **Wall Roughness**, set **Option** to **Smooth Wall**.

(3) Under **Heat Transfer**, set **Option** to **Adiabatic**.

e) Click **Ok** to create the boundary.

D Creating Domain Interface

1. To create **the interface** between **Rotation Domain and Stationary Domain**

a) Click **Create a Domain Interface** on the main toolbar.

b) Leave **Name** by default (Domain Interface 1), then **Ok**.

Edit Domain Interface is displayed.

c) On **Basic Setting**, set **Interface Type** to **Fluid Fluid**.

d) Under **Side 1**, set **Domain** to **Rotation**.

e) Set **Region List 1** to **OUTERCIRCLE A**.

f) Under **Side 2**, set **Domain** to **Stationary**.

g) Set **Region List 2** to **OUTERCIRCLE B, OUTERCIRCLE C, OUTERCIRCLE D, OUTERCIRCLE E**.

h) On **Interface Models**, under **Frame Change**, set **Option** to **Transient Rotor Stator**.

i) Under **Pitch Change**, set **Option** to **Automatic**.

j) Click **Ok** to create the interface.

2. To create **the interface** in **Stationary Domain**

   a) Domain Interface 2

      (1) Click **Create a Domain Interface** on the main toolbar.

      (2) Leave **Name** by default, then **Ok**.

      (3) On **Basic Setting**, set Interface Type to Fluid Fluid.

      (4) Under **Side 1**, set Domain to **All Domain**.

      (5) Set **Region List 1** to **INTERCIRCLE A**.

      (6) Under **Side 2**, set Domain to **Stationary**.

      (7) Set **Region List 2** to **INTERCIRCLE B**.

      (8) On **Interface Models**, under **Frame Change**, set **Option** to **None**.

      (9) Under **Pitch Change**, set **Option** to **Automatic**.

      (10) Click **Ok** to create the interface.

   b) Domain Interface 3

      (1) Click **Create a Domain Interface** on the main toolbar.

      (2) Leave **Name** by default, then **Ok**.

      (3) On **Basic Setting**, set Interface Type to Fluid Fluid.

      (4) Under **Side 1**, set Domain to **Stationary**.

      (5) Set **Region List 1** to **INT 1 A**.

      (6) Under **Side 2**, set Domain to **Stationary**.

      (7) Set **Region List 2** to **INT 1 B**.

      (8) On **Interface Models**, under **Frame Change**, set **Option** to **None**.

      (9) Under **Pitch Change**, set **Option** to **Automatic**.

      (10) Click **Ok** to create the interface.

   c) Domain Interface 4

      (1) Click **Create a Domain Interface** on the main toolbar.

      (2) Leave **Name** by default, then **Ok**.

      (3) On **Basic Setting**, set **Interface Type** to Fluid Fluid.

(4) Under **Side 1**, set **Domain to Stationary**.

(5) Set **Region List 1** to **INT 2 A**.

(6) Under **Side 2**, set **Domain** to **Stationary**.

(7) Set **Region List 2** to **INT 2 B**.

(8) On **Interface Models**, under **Frame Change**, set **Option** to **None**.

(9) Under **Pitch Change**, set **Option** to **Automatic**.

(10) Click **Ok** to create the interface.

d) Domain Interface 5

(1) Click **Create a Domain Interface** on the main toolbar.

(2) Leave **Name** by default, then **Ok**.

(3) On **Basic Setting**, set **Interface Type** to **Fluid Fluid**.

(4) Under **Side 1**, set **Domain** to **Stationary**.

(5) Set **Region List 1** to **INT 3 A**.

(6) Under **Side 2**, set **Domain to Stationary**.

(7) Set **Region List 2** to **INT 3 B**.

(8) On **Interface Models**, under **Frame Change**, set **Option** to **None**.

(9) Under **Pitch Change**, set **Option** to **Automatic**.

(10) Click **Ok** to create the interface.

e) Domain Interface 6

(1) Click **Create a Domain Interface** on the main toolbar.

(2) Leave **Name** by default, then **Ok**.

(3) On **Basic Setting**, set **Interface Type** to **Fluid Fluid**.

(4) Under **Side 1**, set **Domain** to **Stationary**.

(5) Set **Region List 1** to **INT 4 A**.

(6) Under **Side** 2, set **Domain** to **Stationary**.

(7) Set **Region List 2** to **INT 4 B**.

(8) On **Interface Models**, under **Frame Change**, set **Option** to **None**.

(9) Under **Pitch Change**, set **Option** to **Automatic**.

(10) Click **Ok** to create the interface.

f) Domain Interface 7

(1) Click **Create a Domain Interface** on the main toolbar.

(2) Leave **Name** by default, then **Ok**.

(3) On **Basic Setting**, set **Interface Type** to **Fluid Fluid**.

(4) Under **Side 1**, set **Domain** to **Stationary**.

(5) Set **Region List 1** to **INT 5 A**.

(6) Under **Side 2**, set Domain to Stationary.

(7) Set **Region List 2** to **INT 5 B**.

(8) On **Interface Models**, under **Frame Change**, set **Option** to **None**.

(9) Under **Pitch Change**, set **Option** to **Automatic**.

(10) Click **Ok** to create the interface.

g) Domain Interface 8

(1) Click **Create a Domain Interface** on the main toolbar.

(2) Leave **Name** by default, then **Ok**.

(3) On **Basic Setting**, set Interface Type to Fluid Fluid.

(4) Under **Side 1**, set Domain to Stationary.

(5) Set **Region List 1** to **INT 6 A**.

(6) Under **Side 2**, set Domain to Stationary.

(7) Set **Region List 2** to **INT 6 B**.

(8) On **Interface Models**, under **Frame Change**, set **Option** to **None**.

(9) Under **Pitch Change**, set **Option** to **Automatic**.

(10) Click **Ok** to create the interface.

h) Domain Interface 9

(1) Click **Create a Domain Interface** on the main toolbar.

(2) Leave **Name** by default, then **Ok**.

(3) On **Basic Setting**, set **Interface Type** to **Fluid Fluid**.

(4) Under **Side 1**, set **Domain** to **Stationary**.

(5) Set **Region List 1** to **INT 7 A**.

(6) Under **Side 2**, set Domain to Stationary.

(7) Set **Region List 2** to **INT 7 B**.

(8) On **Interface Models**, under **Frame Change**, set **Option** to **None**.

(9) Under Pitch Change, set Option to Automatic.

(10) Click **Ok** to create the interface.

i) Domain Interface 10

(1) Click **Create a** Domain **Interface** on the main toolbar.

(2) Leave **Name** by default, then **Ok**.

(3) On **Basic Setting**, set **Interface Type** to **Fluid Fluid**.

(4) Under **Side 1**, set **Domain** to **Stationary**.

(5) Set **Region List 1** to **INT 8 A**.

(6) Under **Side 2**, set **Domain** to **Stationary**.

(7) Set **Region List 2** to **INT 8 B**.

(8) On **Interface Models**, under **Frame Change**, set **Option** to **None**.

(9) Under **Pitch Change**, set **Option** to Automatic.

(10) Click **Ok** to create the interface.

E Setting Initial Values

1. Select **Create > File Objects > Global Initialisation** from the main menu bar, or click **Global Initialisation**.
2. Under **Initial Conditions**, set **Velocity Type** to **Cartesian**. Other **Options** are set to **Automatic**.
3. Turn on **Turbulence Eddy Dissipation** and leave **Option** set to **Automatic**.
4. Click Ok to set the initialisation details.

F Setting Solver Control

1. Select **Create > Flow Objects > Solver Control**, or click **Solver Control** to open **Solver Control**.
2. Under **Advection Scheme**, leave **Option** set to **Upwind**.
3. Under **Transient Scheme**, set **Option** to **Second Order Backward Euler**
4. Under **Convergence Control**, Set **Max. Iter. Per Timestep** to **3**

5. Under **Convergence Criteria**, set **Residual Type** to **RMS**.
6. Set **Residual Target** to **1e-8**.
7. Click on **Conservation Target**, set **Conservation Target** to **1e-8**.
8. Click **Ok** to set the solver parameter.

G Setting Output Control

1. Select **Create > Flow Objects > Output Control** from the main menu bar.
2. Click the **Transient Results** tab.
3. Click **Add New Item** and then click **Ok** to accept the default name for the object.
4. Under **Transient Results 1**:
   a) Set **Option** to **Full**.
   b) Leave **File Compression Level** to **Default**
   c) Turn on **Time Interval**, then set **Time Interval** to **0.001** [s]
5. Click **Ok**.

H To start without initial value for all domain

1. **Create > Expert Objects** > **Expert Parameters** from the main menu bar.
2. Click **I/O Control** tab.
3. Under **Transient Model and I/O**, Turn on **transient initialization override**, and then set **transient initialization to t**.
4. Click **Ok** to accept.

I Writing the Solver (.def) File

1. Click **Write Solver (.def) File**.

   Definition File is created.
2. **File name** *CrossFlowFan.def* is created automatically.
3. **Leave Operation** set to **Start Solver Manger**.
4. **Leave Report Summary of Interface Connections** and Quit **CFX-Pre** turned on.
5. **Click Ok**.
6. **Click Yes** when asked if you want to save the CFX file.

J Obtaining a Solution to this Transient Problem

1. When **CFX-Pre** closes and then **CFX-Solver Manager** will start, click on **Start Run** to start the run.

The residual plots for seven variables will appear: P-Mass, U-Mom, V-Mom, W-Mom, H-Energy, E-Diss.K, and K-TurbKE.

2. When **CFX-Solver** finishes, the completion message will appear. Click **Ok** to acknowledge it.
3. Click **Post-Process Results** to see the result.

II. Continuing the Transient Run

Based on the result obtained previously, more revolutions are required and are set as follows.

A Redefine the Simulation Type

1. Select **Create > Flow Objects** > **Simulation Type** from the main menu.
2. Set **Option** to **Transient**.
3. Under **Time Duration**, Set **Option** to **Total Time**, and **Total time** to **0.1** [s].

   This will provide 5 revolutions totally.
4. Under **Time Steps**, Set **Option** to **Timestep**, and **Timesteps** to **3.33333e-5** [s]
5. Under **Initial Time**, Set **Option** to **Automatic**.

   The initial time will be set automatically from the previous run.
6. Click **Ok** to save the information.

B Writing the Solver (.def) File

1. Click **Write Solver (.def) File**.

   Definition File is created.
2. Change **File name** to *CrossFlowFan1.def*

   It is happened that solver cannot run due to definition file existed already, so changing the file name somewhat is suggested.
3. Leave **Operation** set to **Start Solver Manger**.
4. Leave **Report Summary of Interface Connections** and Quit **CFX-Pre** turned on.
5. Click **Ok**.
6. Click **Yes** when asked if you want to save the CFX file.

   CFX-Solver Manager window appears after clicking **Yes**.

C Obtaining the Solution to this Transient Problem

1. On **Run Definition tab**, leave **Definition File** to *CrossFlowFan1.def*.

2. Set **Initial Values File** to **CrossFlowFan_001.res**. which is obtained from the previous run.
3. Click on **Start Run** to continue the ruin.
4. When **CFX-Solver** finishes, the completion message will appear. Click **Ok** to complete it.
5. Click **Post-Process Results** to see the result.

Note: Sometimes there is a message popping up, it says, "the memory could not be read," even there is enough memory in the computer. The procedure to ignore this problem is as follows:

1. Click on **Solver** tab
2. Under **Solver Memory**, Set **Memory Allocation Fact** to 2 or more. Hence the memory shared for CFX-Solver will be increased.

THIS PAGE INTENTIONALLY LEFT BLANK

LIST OF REFERENCES

1. Naval Air System Command contract N00019-74-C-0434, *Multi-Bypass Ratio Propulsion System Technology Development*, Vol. I-III, Vought Systems Division, LTV Aerospace Corporation, 24 July 1975.

2. Gossett D. H., " Investigation of Cross Flow Fan Propulsion for a lightweight VTOL Aircraft", Master's Thesis, Department of Aeronautics and Astronautics, Naval Postgraduate School, Monterey, California, March 2000.

3. Seaton, M. S., " Performance Measurements, Flow visualization, and Numerical Simulation of a CrossFlow Fan", Master's Thesis, Department of Aeronautics and Astronautics, Naval Postgraduate School, Monterey, California, March 2003.

4. Cheng, W. T., " Experimental and Numerical Analysis of a CrossFlow Fan", Master's Thesis, Department of Aeronautics and Astronautics, Naval Postgraduate School, Monterey, California, December 2003.

5. Kummer, J. D., Dang. T.Q., "High-Lift Propulsive Airfoil with Integrated Crossflow Fan", Journal of Aircraft Vol. 43, No.4, July-August 2006.

6. Schreiber, C. W., " Effect of Span Variation on the Performance of a Cross Flow Fan", Master's Thesis, Department of Mechanical and Astronautical Engineering, Naval Postgraduate School, Monterey, California, June 2006.

7. Shreeve, R. P., "Report of the Testing of a Hybrid (Radial to Axial) Compressor", Naval Postgraduate School, Department of Aeronautics, NPS-57Sf73112A, November 1973.

8. White, F.M., *Fluid Mechanics*, fifth edition, McGraw-Hill, San Francisco, 2003.

THIS PAGE INTENTIONALLY LEFT BLANK

INITIAL DISTRIBUTION LIST

1. Defense Technical Information Center
   Ft. Belvoir, Virginia

2. Dudley Knox Library
   Naval Postgraduate School
   Monterey, California

3. Prof. Max F. Platzer
   Department of Mechanical and Aeronautical Engineering
   Naval Postgraduate School
   Monterey, California

4. Prof. Garth V. Hobson
   Department of Mechanical and Aeronautical Engineering
   Naval Postgraduate School
   Monterey, California

5. Prof. Raymond P. Shreeve
   Department of Mechanical and Aeronautical Engineering
   Naval Postgraduate School
   Monterey, California

6. Dr. Anthony Gannon
   Department of Mechanical and Aeronautical Engineering
   Naval Postgraduate School
   Monterey, California

7. Prof. Jr-Ming Miao
   Department of Mechanical Engineering
   National Defense University
   Taiwan

8. Captain Huai-Te Yu
   Naval Postgraduate School
   Monterey, California